1994

Reliability assessment of nuclear power plant fault-diagnostic systems using artificial neural networks

Keehoon Kim
Iowa State University

Order Number 9503574

Reliability assessment of nuclear power plant fault-diagnostic systems using artificial neural networks

Kim, Keehoon, Ph.D.

Iowa State University, 1994

Reliability Assessment of Nuclear Power Plant

Fault-Diagnostic Systems Using Artificial Neural Networks

by

Keehoon Kim

A Dissertation Submitted to the

Graduate Faculty in Partial Fulfillment of the

Requirements for the Degree of

DOCTOR OF PHILOSOPHY

Department: Mechanical Engineering
Major: Nuclear Engineering

Approved:

Signature was redacted for privacy

In Charge of Major Work

Signature was redacted for privacy.

For the Major Department

Signature was redacted for privacy.

For the Graduate College

Member of the Committee:

Signature was redacted for privacy.

Signature was redacted for privacy.

Signature was redacted for privacy.

Signature was redacted for privacy.

Iowa State University
Ames, Iowa

1994

TABLE OF CONTENTS

	page
ACKNOWLEDGMENTS	iv
GENERAL INTRODUCTION	1
An Explanation of the Dissertation Organization	2
PAPER I: ERROR PREDICTION FOR A NUCLEAR POWER PLANT FAULT-DIAGNOSTIC ADVISOR USING NEURAL NETWORKS	3
ABSTRACT	5
1. INTRODUCTION	6
2. ARTIFICIAL NEURAL NETWORKS	8
2.1. ANN Models	8
2.2. Introduction to Artificial Neural Networks	8
3. ERROR PREDICTION ON A GENERALIZER	13
3.1. Stacked Generalization	13
3.2. Error Prediction with Cross Validation Partition Criterion (CVPC)	14
3.3. Error Prediction with Bootstrap Partition Criterion (BPC)	17
3.4. Error Prediction with Modified Bootstrap Partition Criterion (MBPC)	18
4. METHOD OF SOLUTIONS	20
5. RESULTS OF THE RESEARCH	26
6. CONCLUSIONS	37
ACKNOWLEDGMENTS	38
REFERENCES	39
PAPER II: ERROR ESTIMATION BY SERIES ASSOCIATION FOR ARTIFICIAL NEURAL NETWORK SYSTEMS	43
ABSTRACT	45
1. INTRODUCTION	46
2. ANN MODELING	48
3. ERROR ESTIMATION FOR ANN MODELS	50
3.1. The Original Stacking Procedure	50
3.2. Selection of Partition Criterion	50
3.3. Error Estimation by Series Association (EESA)	52
4. IMPLEMENTATIONS AND RESULTS	56
4.1. Error Estimation for a Nonlinear Mapping Problem	56
4.2. Validation of Nuclear Power Plant Fault-Diagnostic System	59
5. CONCLUSIONS	73
ACKNOWLEDGMENTS	74
REFERENCES	75

PAPER III: NUCLEAR POWER PLANT FAULT DIAGNOSIS USING NEURAL NETWORK WITH ERROR ESTIMATION BY SERIES ASSOCIATION 80

ABSTRACT 82
1. INTRODUCTION 83
2. THE NUCLEAR POWER PLANT FAULT-DIAGNOSTIC ADVISOR 85
3. ERROR ESTIMATION BY SERIES ASSOCIATION FOR NPP FAULT DIAGNOSIS 87
3.1. NPP Fault-Diagnostic Model Using ANNs 87
3.2. Modified Bootstap Partition Criterion (MBPC) 87
3.3. Error Estimation by Series Association (EESA) 89
4. METHOD OF SOLUTIONS 93
4.1. Data Description 93
4.2. Development of NPP Fault-Diagnostic Advisor F 99
4.3. Development of ANN Error Predictor P 100
4.4. Tests of F and P on Noisy Data 100
5. RESULTS OF THE RESEARCH 101
5.1. Error-Measured Diagnosis 101
5.2. Performance Test with Noise 109
5. CONCLUSIONS 114
ACKNOWLEDGMENTS 115
REFERENCES 116

GENERAL SUMMARY 121
ADDITIONAL LITERATURE 122
APPENDIX: DESCRIPTION OF TRANSIENT SCENARIOS 124

ACKNOWLEDGMENTS

First, I would like to thank my God for His endless love and grace, which have made me surmount all difficulties in my life. This Ph.D. dissertation is dedicated to God.

Special thanks to Dr. Eric Bartlett for his enthusiasm and encouragement that inspired me through this endeavor. I thank Dr. Satish Udpa, Dr. Gerald Sheble, Dr. Daniel Bullen, and Dr. Greg Leucke for being on my program committee and for their valuable suggestions and cooperation. I am grateful to the supports of the United States Department of Energy under Special Research Grant No. DE-FG-92ER75700 and the NETROLOGIC Inc. under SBIR project of the United States Nuclear Regulatory Commission. I wish to thank the Iowa Electric Light and Power Company, the Southern California Edison Co. and San Diego Gas & Electric Co. for their cooperation in providing the nuclear power plant transient simulation data.

Finally, I wish to thank my parents, my parents-in-law, my wife Gyeongsook, my daughters, Somang and Hannah, for their love and support.

GENERAL INTRODUCTION

Nuclear power plant (NPP) accidents may originate from relatively mild operational transients. When an operational transient does occur, operators must take corrective actions promptly in order to restore the abnormal plant state into a normal one or, at least, mitigate the abnormal state from developing into more severe plant conditions. Transients may develop over a short period and may not grant the operators enough time to perform a diagnosis. The potential danger in NPP transient diagnosis is in misdiagnosing a transient and therefore performing an inappropriate corrective procedure that can lead to an even more dangerous situation. A quick and accurate diagnosis is very important for prompt and safe plant controls. A computer-aided diagnostic advisor system that can perform diagnoses accurately is in demand for safety enhancement.

Artificial neural networks (ANNs) have been applied to develop the computer-aided diagnostic advisor system since they have many useful characteristics. For example, ANNs are capable of learning features by examples without explicit representation of the system dynamics (Rumelhart, McClelland & the PDP Research Group, 1986; Lippman, 1987; Blum & Li, 1991; Hecht-Nielsen, 1990; Kurkova, 1992). ANN learning is also associated with generalization. ANN generalization enables them to classify unfamiliar data based on knowledge acquired by learning. ANNs also have noise- and fault-tolerance that provides robustness. These characteristics have motivated many ANN implementations to NPP transient identification (Bartlett & Uhrig, 1992; Ohga & Seki, 1993; Cheon & Chang, 1993; Parlos, Muthusami & Atiya, 1994).

One drawback of ANN applications to real world problems is, however, that the general theories of validation and verification do not yet exist (Bartlett & Kim, 1992; Wildberger, 1994). Many ANN implementations have assumed, implicitly or explicitly, that the output of an ANN is reliable. The assumption may be inappropriate for the output obtained from an ANN presented with novel input data not included in the training data. Moreover, validation and verification of ANN outputs is crucial when the assured performance of the ANN is required for safety (Kim & Bartlett, 1993). For example, the accuracy of a diagnosis provided by a NPP fault-diagnostic advisor is essential for safe

control and operation. This is because a faulty diagnosis cannot help to assist operators to take the corrective or mitigative actions.

The objective of this study is to develop a validation and verification technique for NPP fault-diagnostic systems using ANNs. The validation and verification is realized by estimating error bounds on the advisor diagnoses. Therefore, the reliability-assessed diagnoses can assist the operators to perform their corrective or mitigative actions. Separate sets of data simulated at San Onofre Generating Station (PWR) and Duane Arnold Energy Center (BWR), respectively, were used for the development of the fault-diagnostic advisor systems using ANNs. The advisor systems were validated by the verification technique developed in this study. The error estimation technique developed here can be applied to any ANN model regardless of ANN learning paradigm.

An Explanation of the Dissertation Organization

The three sections in this dissertation are self-contained papers corresponding to three relevant phases of research. The papers are presented here in the chronological order they were written. The three papers have been submitted for publication to different technical journals. The first paper was accepted for publication in Nuclear Technology. The second paper was submitted to Neural Computation, and the third paper to IEEE Transactions on Nuclear Science. Keehoon Kim is the principal investigator and first author of the work presented here, and Dr. Eric B. Bartlett appears as second author in these papers. There are a general summary following the last paper and a list of additional references cited in the general introduction.

PAPER I: ERROR PREDICTION FOR A NUCLEAR POWER PLANT FAULT-DIAGNOSTIC ADVISOR USING NEURAL NETWORKS

Error Prediction for a Nuclear Power Plant Fault-Diagnostic Advisor Using Neural Networks

Keehoon Kim
Eric B. Bartlett

Nuclear Engineering Program
Department of Mechanical Engineering
Iowa State University
Ames, IA 50011

This manuscript has been accepted for publication in Nuclear Technology.

ABSTRACT

The objective of this research is to develop a fault-diagnostic advisor for nuclear power plant transients that is based on artificial neural networks. This paper describes a method that provides an error bound and therefore a figure of merit for the diagnosis provided by this advisor. The data used in the development of the advisor contains 10 simulated anomalies for the San Onofre Nuclear Power Generating Station (SONGS). The stacked generalization approach is used with two different partitioning schemes. The results of these partitioning schemes are compared. This work shows that the advisor is capable of recognizing all 10 anomalies while providing estimated error bounds on each of its diagnoses.

1. INTRODUCTION

The accidents at Three-Mile Island and Chernobyl have focused the demand for nuclear power plant (NPP) safety. This demand has propelled the development and implementation of innovative reactor designs(1), better safety systems(2), human factor studies(3), and stricter safety requirements(4). Even with these developments and implementations, it is still imprudent to assume that a NPP accident can never occur. Accidents may originate from many sources. For example, numerous dangerous accidents originate as relatively mild operational transients. When an operational transient does occur, a quick and accurate diagnosis is very important to plant safety since relatively simple procedures can usually be implemented to correct the situation. The major danger is in misdiagnosing a transient and therefore performing an inappropriate corrective procedure that can lead to an even more dangerous situation. Transients may, however, develop over a short period and may not grant the operators enough time to perform a diagnosis and take the appropriate corrective actions to avoid more serious plant conditions. A computer-aided diagnostic advisor system that can perform diagnoses quickly is therefore important to safety. The operators or shift technical advisors at the plant can use these quick, accurate diagnoses to help them with their own analysis of plant conditions. These diagnoses could also be used by technical support personnel for diagnostic or strategic purposes after the transient is under control, presumably to avoid future occurrences of similar difficulties.

Conventional computer-aided, fault-diagnostic advisors have used expert systems. These advisor systems can provide accurate diagnoses but have some problem areas(5,6). For example, an expert system may require significant computation time and resources to progress through the many decision levels required to formulate a diagnosis. These systems may also be subject to a combinatorial explosion of such decisions as the complexity of the monitoring system increases. Additionally, the monitored input variables can be degraded by noise, which can cause expert systems to deviate from the formulated conditions at critical decision levels.

Recent work using artificial neural networks (ANNs) to surmount some of the aforementioned shortcomings with expert systems has been published by Bartlett and

Uhrig(7,8) as well as Ohka and Seki(9). One shortcoming of ANNs is that there is a general lack of theory that allows for provision of estimated errors on ANN solutions for validation and verification purposes(5-7,10,11). Providing a figure of merit for the ANN advisor is necessary when addressing its reliability since the advisor may be presented with novel plant symptoms. The typical black box nature of ANNs is considerably reduced by assigning a figure of merit in the form of an error bound on the ANN solution. The figure of merit can also broaden the advisor users' insights about relationships between the NPP transient dynamics and the ANN advisor's solution. For example, the operators can evaluate an enigmatic diagnosis from the ANN advisor if the estimated error is large. Therefore, the error bound estimation is very important for real-world implementations. This paper describes a method that provides an error bound and therefore a figure of merit for the diagnosis provided by an ANN NPP fault-diagnostic advisor.

The next section of this paper gives background on ANNs. Section III addresses error prediction and describes the stacked generalization scheme(12) used in this work to provide error bounds on the ANN fault-diagnostic advisor. Section IV explains the methods used and the data investigated in this paper. Results and conclusions are given in sections V and VI.

2. ARTIFICIAL NEURAL NETWORKS

2.1. ANN Models

Mathematical models can be developed to characterize many physical systems. These models can be very accurate when the underlying laws are known. However, when the laws are not well understood or the system is very complex, empirical methods are employed to develop approximate mathematical models, which can be very useful if used correctly. These empirical models can be developed automatically by using methods called generalizers(12,13) because they infer parent functions from sets of data. Many generalizers provide good results if the processes they model are well behaved. For example, statistical methods work well for data that is linear and normally distributed. Unfortunately, many systems are not so well behaved because of nonlinearities in the system being modeled. Nonlinear modeling is an arduous task and is not easily accomplished with standard techniques. Recent work has demonstrated that nonlinear modeling can be accomplished by ANNs(14-17). The nonlinear modeling abilities of ANNs have served as the motivation for their use in this work because the NPP transient diagnostic problem is highly nonlinear(7,8,17,18).

2.2. Introduction to Artificial Neural Networks

ANNs are computer algorithms that are motivated by biological neural systems. ANNs consist of highly interconnected processing elements called neurons or nodes that produce output signals based on a weighted sum of the input signals they receive(19-21). The ANN in Figure 1 has four layers of neurons, referred to as the input layer, the first and second hidden layer, and the output layer. Input signals can originate from other neurons or inputs while output signals either become the input signals for other neurons or the ANN output. During training, an ANN is presented with k examples in a learning or training set of known input-output patterns, $\{(x_i, y_i) |\ y_i = f(x_i)\ ;\ i = 1 \text{ to } k\}$, each of which consists of m inputs and n outputs. When one input pattern x_i is presented to the ANN via the input layer, it is fed

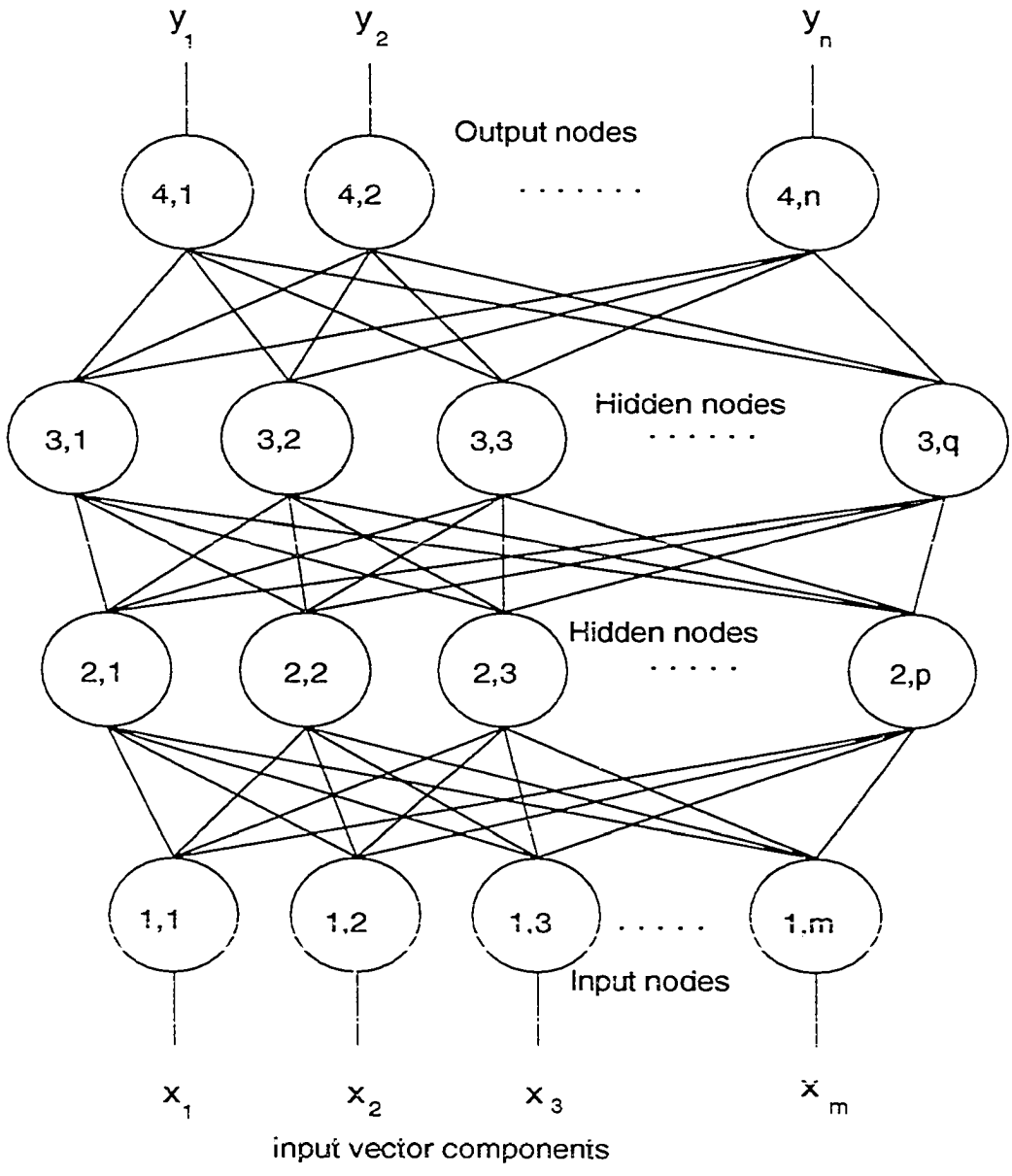

Figure 1. A feedforward neural network with four-layer architecture.

through the neurons in the hidden and output layers to generate a corresponding output pattern y_i', which is the ANN estimate of y_i. A typical general activation process in a neuron is represented in Figure 2. The weighted sum of the neuron's inputs is processed through a transfer function to produce an output signal. There are many different types of transfer functions (20,21). One of the more widely used transfer functions is the sigmoidal activation function used in this paper. The form of the sigmoidal activation function is as follows,

$$O_{pi} = 1/[\ 1+\exp(-sum)] \qquad (1)$$

where O_{pi} is the output of node i in layer p, and *sum* is the weighted sum of the outputs of the nodes in the previous layer p-1.

The ANN is trained by repetitious presentation of the training set and adjusting the inter-neural connection weights so that the output signal y_i' converges to y_i. These inter-neural weights are represented by the lines connecting the neurons in Figure 1. There are many methods for obtaining convergence, but backpropagation(19-21), which is relatively simple, straightforward and very useful, is employed widely and will be used in this paper.

A backpropagation ANN that provides a function mapping can be regarded as a generalizer if several restrictions are satisfied(12,13,22). These restrictions are as follows. Let L be a learning data set in $\mathbf{R}^m \times \mathbf{R}^n$ space where m is the dimension of the input space and n is the dimension of the output space. The first restriction requires that the order of the presentation of data be invariant, i.e., the learning of a generalizer is irrelevant to a specific order of the data presentation.

The second restriction requires that when a generalizer is asked a question from the data set L, the generalizer must reproduce the corresponding output vector from L. This restriction is subject to a training accuracy.

The third restriction requires that the domain of a generalizer must be singlevalued. In other words, two or more outputs corresponding to a single input vector cannot be allowed. For example, let (x_i, y_m) and (x_j, y_n) be input-output pairs in L. When $x_i = x_j$, the third restriction requires that $y_m = y_n$.

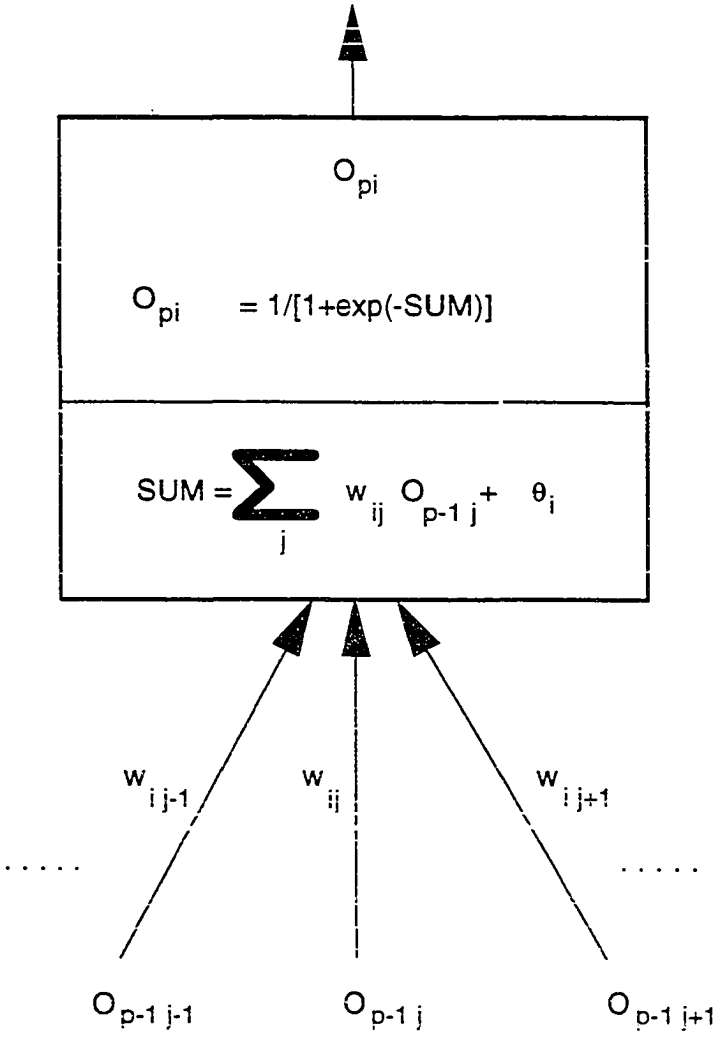

Figure 2. Forward activation in neuron O_{pi} in a neural network. θ_i is a bias for the neuron.

The fourth restriction refers to the smallest number of input-output patterns in the learning set L. In order to map the parent or desired function, a generalizer needs at least k training pairs in the learning set, such that $k > m$ where m is equal to the number of input variables. This restriction does not provide an approximate size of k for complete generalization, but only a lower limit.

The last restriction refers to the necessary dimensionality of the input vectors in L. A generalizer is not defined when the components of all the input vectors in the learning set lie on an m-1 or less dimensional hyperplane even if the generalizer has enough training patterns. For example, assume that the components of all the input vectors in a learning set lie on a hyperplane whose dimension is less than that of the generalizer. Even if the fourth restriction is fulfilled ($k > m$), the learning set would not provide sufficient information to generalize the parent function of a higher dimension. Thus, a generalizer requires the components of all the input vectors in a learning set to lie on, at least, the same dimensional hyperplane as that of the generalizer. ANNs including backpropagation are generalizers when the aforementioned restrictions are satisfied(13,22).

3. ERROR PREDICTION ON A GENERALIZER

3.1. Stacked Generalization

Stacked generalization can be thought of as an extension of cross validation(12). Cross validation is one of many methods in nonparametric statistics that have been developed to cope with difficulties associated with data that is not normally distributed(23,24). Statistical modeling by nonparametric methods can be much more accurate and appropriate for cases that depend upon non-normal data distributions or unknown distributions, such as our fault-diagnostics data(25). Cross validation can address the selection of the best model for a given non-normal experimental data set(26). Thus, cross validation can be used to pick the best generalizer among many possible generalizers by developing the generalizer with a portion of the available data and testing it on the remainder of the data(12,23,26).

Stacked generalization, unlike cross validation, can be used to improve the generalization accuracy for one or more generalizers; or when used with a single ANN generalizer, it can be used to estimate the error of a generalizer that is presented a novel input. Let $F^{(0)}$ be an ANN trained on a learning set L. Our goal is to estimate error bounds on outputs obtained by $F^{(0)}$ for novel inputs. For a chosen partition criterion, the learning set L is partitioned into two subsets. An ANN that is called the level 0 generalizer $f^{(0)}$ and has the same architecture of the $F^{(0)}$ is trained on one partitioned subset. The performance of $f^{(0)}$ is measured by testing the generalizer on the remaining partitioned subset. Since the second subset is not used in training $f^{(0)}$, the output of $f^{(0)}$ will, in general, deviate from the desired output. This deviation represents the error between the untrained input and the ANN's output. Another partition is chosen and the process of training and testing is repeated. The performance data that includes the untrained input, a vector from the untrained input to its nearest pattern in the first subset and the deviation, constitutes a new learning set L′ called the level 1 learning set. A new ANN called the level 1 generalizer $P^{(1)}$ is trained on the level 1 learning set L′. The level 1 generalizer $P^{(1)}$ learns the relationship between the inputs and the errors of $f^{(0)}$ and then can estimate a figure of merit in the form of an

error bound on outputs of the ANN $F^{(0)}$. This stacking procedure is the essence of the stacked generalization approach and is illustrated in Figure 3.

Three different partition criteria for the stacked generalization method are investigated, two of which are applied to NPP fault-diagnostics in this work. The stacking procedure is accomplished by three different partitioning criteria all of which provide a diagnostic figure of merit estimate for the NPP fault-diagnostic advisor developed in this work. They are cross validation partition criterion (CVPC), bootstrap partition criterion (BPC), and modified bootstrap partition criterion (MBPC). Each of these methods yields slightly different results and these differences are the subject of the discussion of this paper.

As a preliminary to the discussions of these methods, let us define the following concepts. Let Q be the universal set of questions (Q ={q,u}) where q is a question of interest and u is an unknown solution for the question. This situation is shown in Figure 4. The unknown solution u is provided by an ANN generalizer called $F^{(0)}$. A subset $L \subset Q$ is chosen to be a learning set used to train the generalizer. Let $L = \{(x_i,y_i) | i = 1 \text{ to } k\}$ where y_i is a known solution corresponding to x_i. The learning set L consists of k patterns of input-output vectors, $x_i \in \mathbf{R}^m$ and $y_i \in \mathbf{R}^n$. For the problem of NPP diagnostics, Q corresponds to the set of all plant transients and normal conditions. The ANN generalizer $F^{(0)}$ corresponds to an ANN NPP fault-diagnostic advisor. Asking a novel question $q \in Q\text{-}L$ of $F^{(0)}$ is equivalent to requesting the fault-diagnostic advisor to diagnose a novel transient symptom q. A diagnosis u is then obtained from the advisor $F^{(0)}$. A figure of merit ε associated with u is then provided by the level 1 ANN $P^{(i)}$ such that the resultant output from the advisor system is $u \pm \varepsilon$.

3.2. Error Prediction with Cross Validation Partition Criterion (CVPC)

Stacked generalization employs a set of t partitions chosen from the learning set L. To obtain a partition i, where i ranges from one to t, split L into two disjointed sets, L_{i1} and L_{i2}. The cross validation partition criterion (CVPC)(12) is defined such that t is equal to k where t is the number of partitions and k is the number of training patterns in L. For each i, L_{i2} consists of a single pair (x_i,y_i) in L, and the corresponding L_{i1} consists of the remainder of

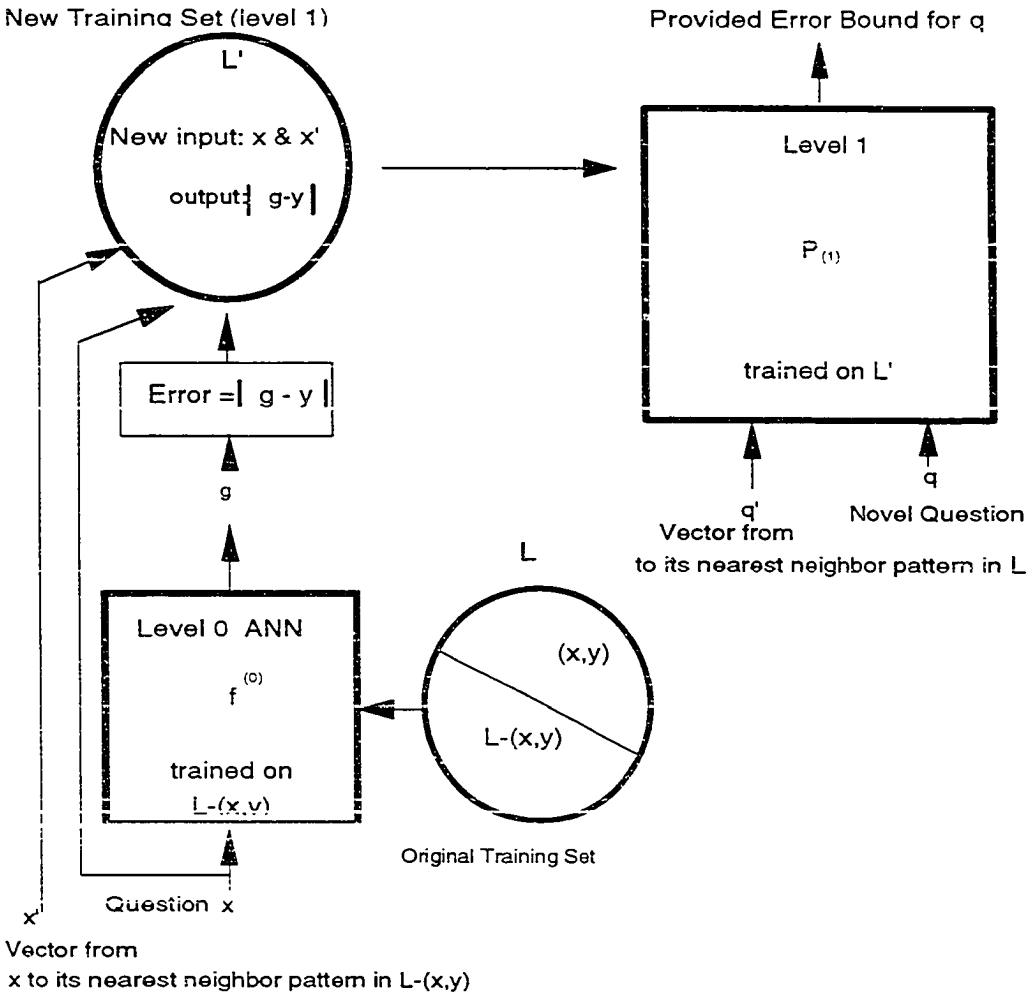

Figure 3. Illustration of the stacked generalization procedure. The level 0 generalizer $f^{(0)}$ is used in generating the level 1 learning set L' for a given partition. The level 1 generalizer $P^{(1)}$ provides a figure of merit in the form of an error bound for an output obtained by $F^{(0)}$ for the untrained question q.

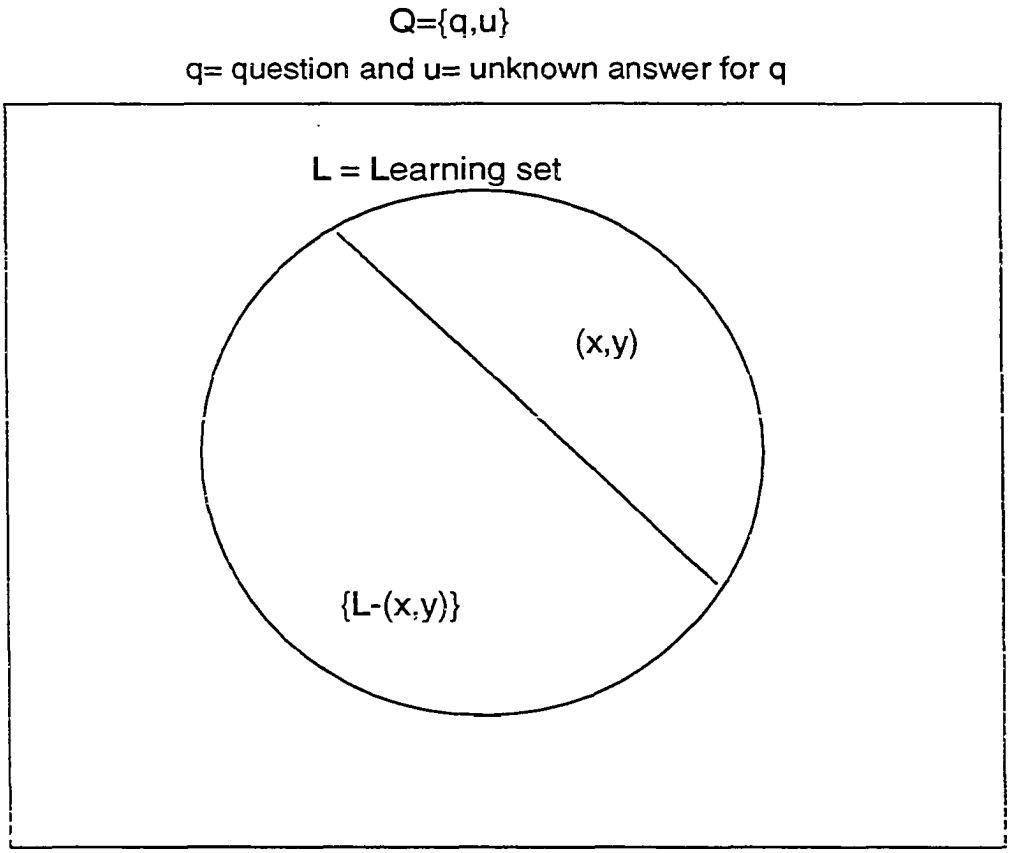

Figure 4. Illustration of a set of question and its unknown answer Q and a set of learning examples L with a partition given by cross validation partition criterion (CVPC).

L, i.e., L - (x_i,y_i). Since t is equal to k, then $\cup_{i=1}^{t} L_{i2} = L$, and $L_{i2} \cap L_{j2} = \emptyset$ for $i \neq j$. The space of the original learning set L, $\mathbf{R}^m$ x $\mathbf{R}^n$, is called the level 0 space. The level 0 generalizer $f^{(0)}$ is applied directly to the level 0 learning set L in the level 0 space. In Figures 3 and 4, a partition is shown by dividing L into two subsets, L_{i1} = L - (x,y) and L_{i2} = (x,y). Note that the subscript i for the input-output pattern is dropped for convenience in the figures. Given the partition, the generalizer $f^{(0)}$ is trained on the subset L_{i1}. The untrained question x in L_{i2} is then presented to $f^{(0)}$. The answer g given by $f^{(0)}$ for the novel question x will be, in general, different from the correct answer (output) y. In addition to this information, the vector x′ defined as difference vector from x to its nearest neighbor in L_{i1} is computed. The nearest neighbor is obtained by using Euclidean distance. Now, when the question is x, the correct answer y differs from the answer g provided by $f^{(0)}$ by $\varepsilon = |g - y|$. The error information ε along with x and x′ defines the level 1 information space for the generalizer $F^{(0)}$. This information is used to form a new learning set L′ in the level 1 space. Hence, the new level 1 learning set L′ consists of an input (x,x′) and an output |g - y| for each partition i. These pairs constitute the level 1 learning set L′. A level 1 generalizer $P^{(1)}$ is then trained on the level 1 learning set L′.

Next, we ask the ANN generalizer $F^{(0)}$ trained on the entirety of L a novel question $q \in Q - L$. The ANN generalizer $F^{(0)}$ provides a solution for the question. The level 1 generalizer $P^{(1)}$ trained on the level 1 learning set L′ is fed the question q with the vector q′ from q to its nearest neighbor in L. The output of $P^{(1)}$ then provides the figure of merit for the solution obtained from $F^{(0)}$. The results of this procedure for SONGS data are shown in Figures 6, 8 and 10.

3.3. Error Prediction with Bootstrap Partition Criterion (BPC)

Using CVPC requires that the total number of partitions t is equal to the number of training patterns k in a given learning set. The computation time for generating the level 1 learning set increases in proportion to the number of training patterns k since the level 0 ANN $f^{(0)}$ must be trained and tested k times. When k is large, which is typical of real applications, the computation time as well as human effort can be very lengthy and

impractical. The total number of partitions can be reduced by employing a method we have developed. The first method is called bootstrap partition criterion (BPC).

When applying BPC, a partitioned set L_{i2} can be chosen to have multiple elements rather than one as in CVPC. When those elements are chosen randomly from the original learning set L, we designate it as the bootstrap partition criterion (BPC) method because it is similar to the bootstrapping method in nonparametric statistics(12,27). In the original nonparametric bootstrapping method, the multiple elements are chosen randomly for each partition, however, this may allow some particular elements to appear several times. Without imposing proper conditions, the total number of partitions might increase due to the repeated selection of some patterns. The repeated selection results in a situation where the total partition number t would not be significantly reduced or the desired results are not attained. The unnecessary increase in the total partitions is avoided by adapting the constraints of Xiangdong's partition set(28). For BPC, we impose his two constraints on the partition sets with a modification as follows. First, predetermine a number of L_{i2} elements, say s. Choose at random s elements from L such that $L_{i2}= \{(x_1,y_1), (x_2,y_2), ..., (x_s,y_s)\}$ and $L_{i1} = L - L_{i2}$. Second, require $\cup_{i=1}^{t} L_{i2} = L$, and $L_{i2} \cap L_{j2} = \emptyset$ for $i \neq j$. As required by these conditions, a pattern in L_{i2} will appear only once in all of the partitions. When s is chosen such that k/s ~ 10, the total computation time will be reduced to one-tenth of that of CVPC.

3.4. Error Prediction with Modified Bootstrap Partition Criterion (MBPC)

The BPC scheme can reduce the total number of partitions t, but due to the random selection of s elements of L_{i2}, the scheme may provide varying results. In order to improve the reliability of the results for ANN NPP fault diagnostics, we propose a modified bootstrap partition criterion (MBPC) that has the advantages of BPC without the disadvantages of random selection of the elements in the partition sets. MBPC is an extension of BPC where the L_{i2} patterns are chosen systematically to model the specific problem.

For the case of NPP fault diagnostics, the ANN advisor must recognize a transient whose plant variables are dynamically changing according to plant function. In addition, the advisor needs to distinguish a particular transient from many different transients of interest.

Therefore, the learning set may consist of r separate groups pertaining to the r different transients. These r groups differ from each other such that the r patterns for L_{i2} can be selected from each transient group at the same time. This selection can minimize the loss of information related to the desired error bounds by the random selection of L_{i2} in BPC. It follows that MBPC requires two more constraints on the learning set not imposed on BPC. First, L_{i2} must be a set of r single patterns chosen from each transient group. If the number of training patterns in a specific transient group is larger than r, an additional constraint is imposed as follows. A maximum of two patterns can be selected from the particular group whose number of training patterns is larger than r. For example, assume that there are three different transients A, B and C, i.e., r = 3, and the transient groups A, B, and C have 2, 3, and 5 training patterns, respectively. If a total of 3 partitions (t = 3) are chosen, the second constraint is applied to the partitions such that two patterns from C and one pattern from A and B are selected for two partitions. For the remaining partition, one pattern is selected from A, B and C. In fact, the last partition doesn't contain any pattern from A because A has only two patterns. These modifications for NPP fault diagnostics can reduce the difficulties of using BPC while maintaining the accuracy of CVPC and speed of BPC. This can be seen by the results shown in Figures 6, 8 and 10.

4. METHOD OF SOLUTIONS

An ANN NPP fault-diagnostic advisor $F^{(0)}$ is developed to detect and classify various operational transients at San Onofre Nuclear Generating Station (SONGS). A figure of merit for $F^{(0)}$'s diagnosis is provided by a generalizer, $P^{(1)}$, called the ANN error predictor. The data used for training the ANN fault-diagnostic advisor was obtained from SONGS, owned by Southern California Edison Co. and San Diego Gas & Electric Company(29). SONGS is a pressurized water reactor (PWR) plant that provides 800 MWe. Ten transient scenarios listed in Table I are included in the data set for ANN training. The scenarios include design-basis accidents and less severe transients. Note that the stuck open pressurizer safety valve with high pressure injection inhibited is similar to the condition that occurred at the Three-Mile Island accident in 1979.

The data sets for the ten transients, each contain 33 plant variables illustrated in Table II. These variables are collected at time step intervals of one second for a period of ten minutes. Note that this time snap shot, or single time slice, of data does not include temporal information. The main advantage of the single time step approach is simplicity of training and execution(7). Thus the ANN advisor $F^{(0)}$ can diagnose transients at the very instant the plant variables are presented because the ANN does not need to observe trends or temporal variation. In each data set, normal operation conditions are followed by transient conditions. Notice that with the exception of the turbine trip from 50% power, all of the transient scenarios start from the full-power, normal operating condition. The ten transient conditions plus the normal steady-state operating conditions with a different initial power constitute the learning set with 113 patterns for the ANN advisor $F^{(0)}$. The number of the patterns in the learning set L is only about 2% out of the 6203 patterns of the entire data set Q for the ten scenarios. This learning set includes ten initial conditions due to different initial power and flux levels. The remaining 103 input-output patterns correspond to abnormal conditions of the ten transients. The learning set L of 113 input-output patterns is obtained by the procedures outlined by Bartlett and Uhrig(7). The learning set L is chosen in an iterative manner. First one pattern at the beginning and one pattern from the end of the ten simulated transients is selected to form the initial learning set. This initial learning set containing 20

Table I. List of Ten Accident Scenarios with Transient Onset Time and Desired ANN Output Layer Activation.

No.	Scenario	Transient onset time (sec.)	Desired output node activation 1	2	3	4
	Normal Operation	(before transient onset)	0	0	0	0
1.	Turbine Trip/Reactor Trip	6	1	0	0	0
2.	Loss of Main Feedwater Pumps	47	0	1	0	0
3.	Closure of Both Main Steam Isolation Valves	7	0	0	1	0
4.	Trip of All Reactor Coolant Pumps	16	0	0	0	1
5.	Trip of A Single Reactor Coolant Pump	14	1	1	0	0
6.	Turbine Trip From 50% Power	50	1	0	1	0
7.	Loss of Coolant Accident (LOCA) With Loss of Off-Site Power	7	1	0	0	1
8.	Main Steam Line Break	6	0	1	1	0
9.	Stuck Open Pressurizer Safety with High Pressure Injection Inhibited	15	0	1	0	1
10.	Single Turbine Governor Valve Closure	7	0	0	1	1

Table II. Plant Variables Used as Input to the ANN Fault-Diagnostic Adviser $F^{(0)}$.

1. Power (flux)
2. Average Temperature (Deg F)
3. Hot Leg 1 Temperature (Deg F)
4. Cold Leg 1A Temperature (Deg F)
5 Cold Leg 1B Temperature (Deg F)
6. Hot Leg 2 Temperature (Deg F)
7. Cold Leg 2A Temperature (Deg F)
8. Cold Leg 2B Temperature (Deg F)
9. Pressurizer Pressure (psia)
10. Pressurizer Level (%)
11. Pressurizer Temperature (Deg F)
12. Steam Generator 88 Narrow Range Level (%)
13. Steam Generator 88 Water Level (%)
14. Steam Generator 88 Feed Water Flow (gpm)
15. Steam Generator 88 Feed Water Flow (Lb/sec)
16. Steam Generator 88 Steam Flow (Lb/sec)
17. Steam Generator 88 Pressure (psi)
18. Steam Generator 89 Narrow Range Level (%)
19. Steam Generator 89 Water Level (%)
20. Steam Generator 89 Feed Water Flow (gpm)
21. Steam Generator 89 Feed Water Flow (Lb/sec)
22. Steam Generator 89 Steam Flow (Lb/sec)
23. Steam Generator 89 Pressure (psi)
24. Containment Pressure (psig)
25. Containment Temperature (Deg F)
26. Pressurizer Relief Steam Flow
27. Pressurizer Relief Liquid Flow
28. Core Inlet Flow
29. Saturation Margin
30. Surge Line Temperature (Deg F)
31. Source Range Counts (cps)
32. Reactor Vessel Head Level
33. Reactor Vessel Plenum Level

input-output patterns is used to train the ANN advisor. The advisor is then recalled on all the patterns over the entire time period of the simulation for each of the ten transients. The recall patterns producing the worst errors are added to the learning set. The process of training, recalling and adding patterns is repeated until most of undesirable, high recall error patterns disappear. Note that the patterns within a short period after transient onset are not added. This is because the plant variables change suddenly and dynamically for this short period such that some patterns are not uniquely defined.

The ANN advisor for SONGS is established by training $F^{(0)}$ on the learning set L. The advisor $F^{(0)}$ uses a backpropagation ANN and is trained until a training root mean square (RMS) error of 0.01 is obtained. The ANN $F^{(0)}$ has 33 input nodes each corresponding to the 33 plant variables, 22 nodes in the first hidden layer, 10 nodes in the second hidden layer, and 4 nodes in the output layer (33-22-10-4). The four output nodes are used to distinguish each of the ten transient conditions with a distinct 4-bit binary code as listed in Table I. The two-hidden-layer architecture was employed after attempting several different architectures. In this investigation, each of the three partitioning approaches outlined in the previous section is compared. The first step toward generating a level 1 learning set L′ for any of the partitioning schemes is to create t partitions of L :

i) In the CVPC case, the partition is chosen to be $t = k = 113$.
For i, where $i = 1$ to t, $L_{i2} = (x_i, y_i)$ with the conditions of $L_{m2} \cap L_{n2} = \emptyset$ for $m \neq n$ and $\cup_{i=1}^{t} L_{i2} = L$.

ii) In the BPC case, the total number of partitions, t, is chosen to be 12 with $s = 10$ the predetermined element number. For i, where $i = 1$ to t, $L_{i2} = \{(x_l, y_l) | l = 1 \text{ to } s\}$ is randomly chosen with the conditions of $L_{m2} \cap L_{n2} = \emptyset$ for $m \neq n$ and $\cup_{i=1}^{t} L_{i2} = L$. This partition scheme is not simulated in this investigation because of the disadvantage of the scheme discussed in the preceding section.

iii) In the MBPC case, r = 10 groups because L contains 10 distinct transients. For partition i, $L_{i2} = \{(x_l, y_l) | l = 1 \text{ to } r\}$ where each pattern is randomly chosen from each transient group with the conditions of $L_{m2} \cap L_{n2} = \emptyset$ for $m \neq n$ and $\cup_{i=1}^{t} L_{i2} = L$. In the learning set L for SONGS, four transient groups have training patterns larger than r where r is 10. Thus, total number of partitions, t is chosen to be 12, and the second constraint allows a maximum of two patterns to be selected from each of these four groups.

Another backpropagation ANN $f^{(0)}$ having the same architecture of the developed advisor $F^{(0)}$, is used as a level 0 ANN. For each partition, $f^{(0)}$ is trained on L_{i1} and then presented input patterns in L_{i2} as questions. The error ε of $f^{(0)}$ for a question is computed by subtracting the $f^{(0)}$ output from the desired output, as follows:

$$\varepsilon_j = | g_j - y_j |, \qquad j=1,2,3,4. \tag{2}$$

where g_j is a value of the j-th output node on $f^{(0)}$ and y_j is a j-th component of the desired output y corresponding to the question x. The next step is to calculate vector x′ from x to its nearest neighbor vector x_{nn}. The nearest neighbor vector x_{nn} from x is chosen in the L_{i1} such that x_{nn} has the smallest Euclidean distance (l_2-norm) from x. The vector x′ from x to its nearest neighbor x_{nn} is determined by the equation,

$$x'_i = ((x_i - x_{nn\,i}) + 1) / 2 \tag{3}$$

for the i-th component of the vector since negative values are not appropriate as an input to an ANN. Additionally, this transformation formula insures that all components are within the interval [0,1] required by backpropagation ANN. For all partitions given by one of two partition criteria, a total of 113 trios of x, x', and ε are acquired. Therefore, the level 1 learning set L′ consists of these 113 trios. These new input-output patterns in L′ are used to train a level 1 generalizer $P^{(1)}$ in order to provide error bounds on the results of the developed ANN fault-diagnostic advisor $F^{(0)}$. The ANN error predictor $P^{(1)}$ is a

backpropagation ANN with a 66-30-20-10-4 architecture. Again, this architecture was chosen after several attempts to find the optimal architecture.

The ANN advisor $F^{(0)}$ is designed to categorize the untaught input conditions at the plant into a normal condition or a specific transient. This classification is the diagnosis of the level 0 $F^{(0)}$ for an unknown symptom $q \in Q - L$ in the plant operational status within generalized knowledge about the ten transients. The novel input-condition that is fed into $F^{(0)}$ and the vector from the input condition to its nearest pattern in L are presented as an input condition to $P^{(1)}$. For those level 1 input conditions, the ANN error predictor $P^{(1)}$ will predict the error bounds ε on the diagnoses of the ANN fault-diagnostic advisor $F^{(0)}$.

5. RESULTS OF THE RESEARCH

Figures 5 through 11 and Table III show the results of this research. Figures 5, 7, and 9 display the advisor's true diagnostic RMS error. The true diagnostic error is the actual error as compared with the true solution. The true solutions, in this case, are obtainable because the transients were simulated by the SONGS simulation computer which is assumed to be correct. The ANN error predictor $P^{(1)}$ provides an estimated error bound associated with the advisor's diagnosis as a figure of merit estimate. The estimated error bound is shown in Figures 6, 8, and 10 corresponding to each of the odd-numbered figures, respectively. The solid line in these figures represents the estimated error bound obtained by using MBPC, the dashed line by CVPC. The figures show that the predicted errors by the MBPC method are much closer to the true diagnostic errors than those by the CVPC method. Note that MBPC reduces considerably the total number of partitions, t = 12, compared with that of CVPC, t = 113, for generating L′. Figure 11 shows an example of the classification resulting from the combination of the error bounds with the diagnoses of the advisor $F^{(0)}$ for turbine trip/reactor trip as seen in Figures 9 and 10. Note that when an error bound falls below 0.1, the diagnosis is considered to be acceptable. This error-combined classification at each instant of input data presentation can be provided as a final result to the operators or technical support staff at SONGS, or indeed this approach can be used at any other NPP or process plant where accident avoidance is paramount. Table III summarizes the results of the advisor $F^{(0)}$ and the error predictor $P^{(1)}$ developed by using MBPC. The third column shows the time when the advisor $F^{(0)}$ makes a diagnosis with the true diagnostic RMS error below 0.1 after transient onset. The fourth column displays the time when an error bound predicted by $P^{(1)}$ falls below 0.1 after transient onset.

The ANN advisor $F^{(0)}$ responds very quickly to the onset of the transients. However, since the plant input variables are dynamically and suddenly changing during the short transitory period after the onset of each abnormal condition, the advisor's diagnoses are inconclusive for this period. This transitory period for each transient is shown in the odd-numbered figures as well as in the third column of Table III. The advisor $F^{(0)}$ classifies the abnormal conditions with true diagnostic errors below 0.1 within 30 seconds after

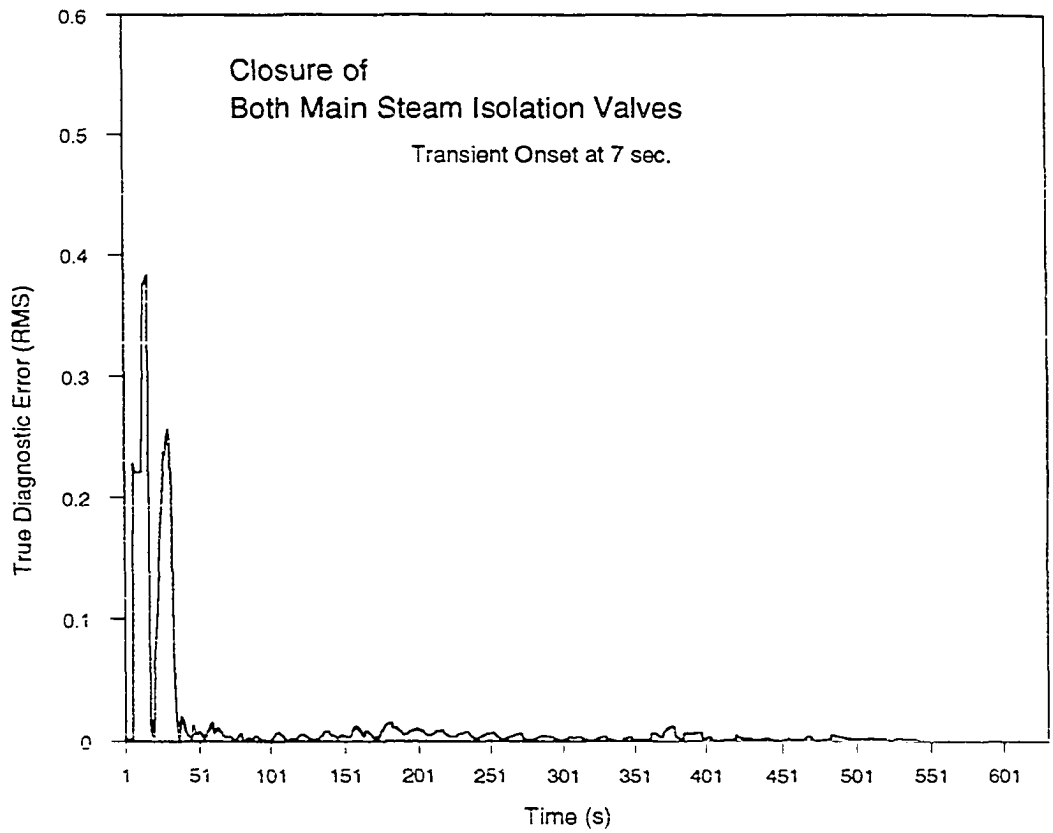

Figure 5. True diagnostic error (RMS) of $F^{(0)}$ diagnosis compared with the true solution in the case of closure of both main steam isolation valves.

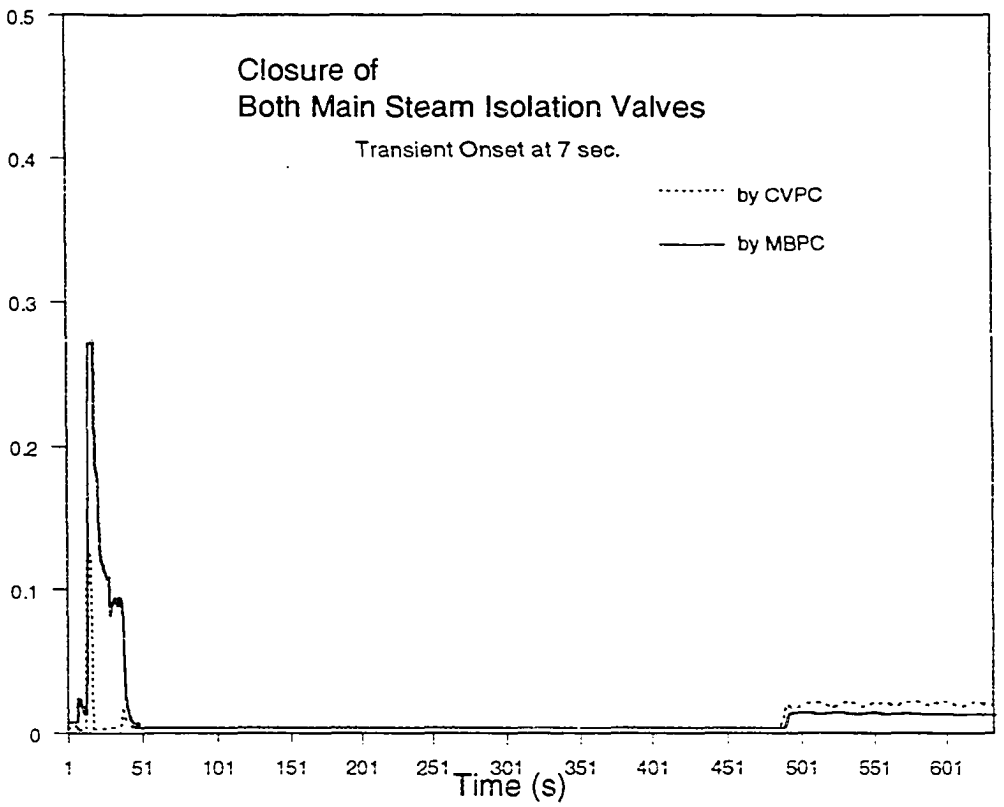

Figure 6. Estimated error bounds provided by the error predictor $P^{(1)}$ for two different partitioning schemes on the advisor $F^{(0)}$ diagnosis. Solid line represents the estimated error bounds by using modified bootstrap partition criterion (MBPC); dashed line by using cross validation partition criterion (CVPC).

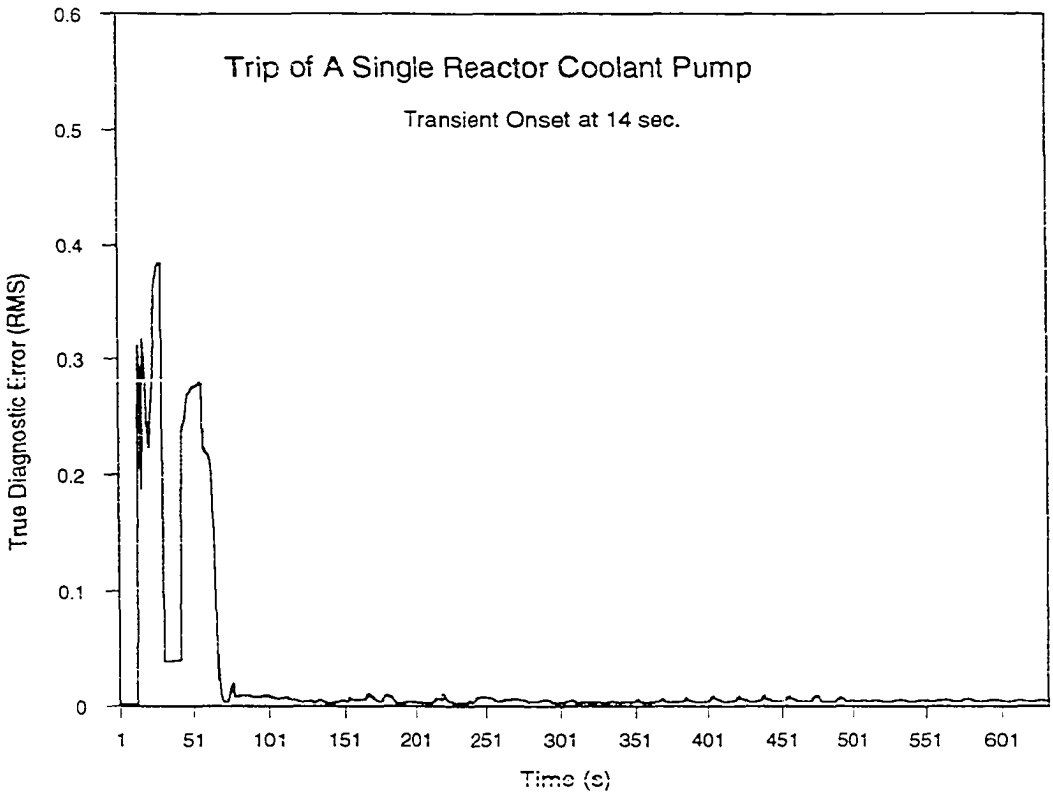

Figure 7. True diagnostic error (RMS) of $\bar{F}^{(0)}$ diagnosis compared with the true solution in the case of trip of a single reactor coolant pump.

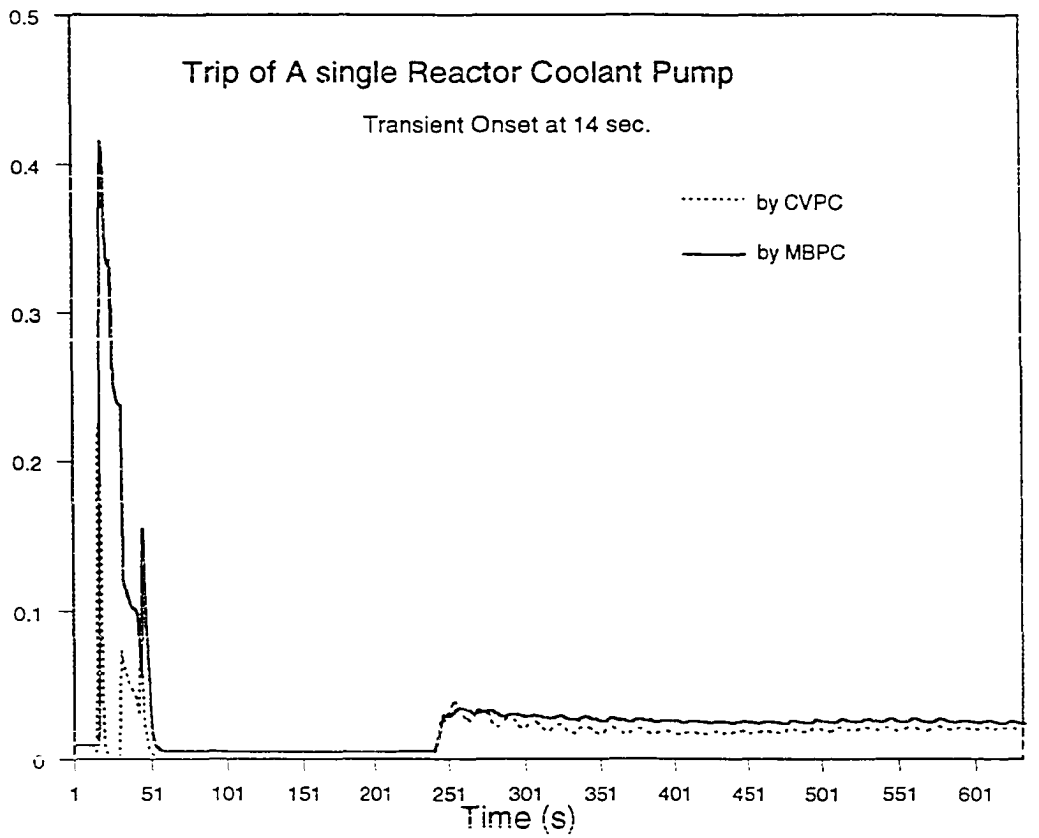

Figure 8. Estimated error bounds provided by the error predictor $P^{(1)}$ for two different partitioning schemes on the ANN advisor $F^{(0)}$ diagnosis. Solid line represents the estimated error bounds by using modified bootstrap partition criterion (MBPC); dashed line by using cross validation partition criterion (CVPC).

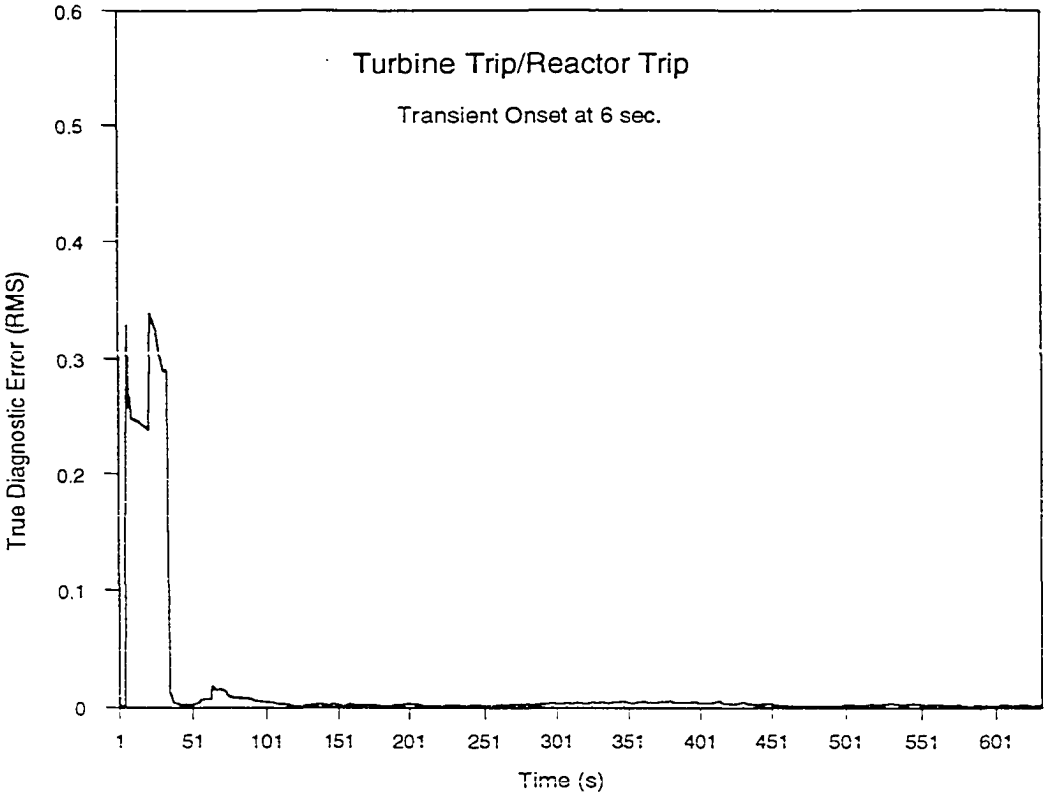

Figure 9. True diagnostic error (RMS) of $\bar{F}^{(0)}$ diagnosis compared with the true solution in the case of turbine trip/reactor trip.

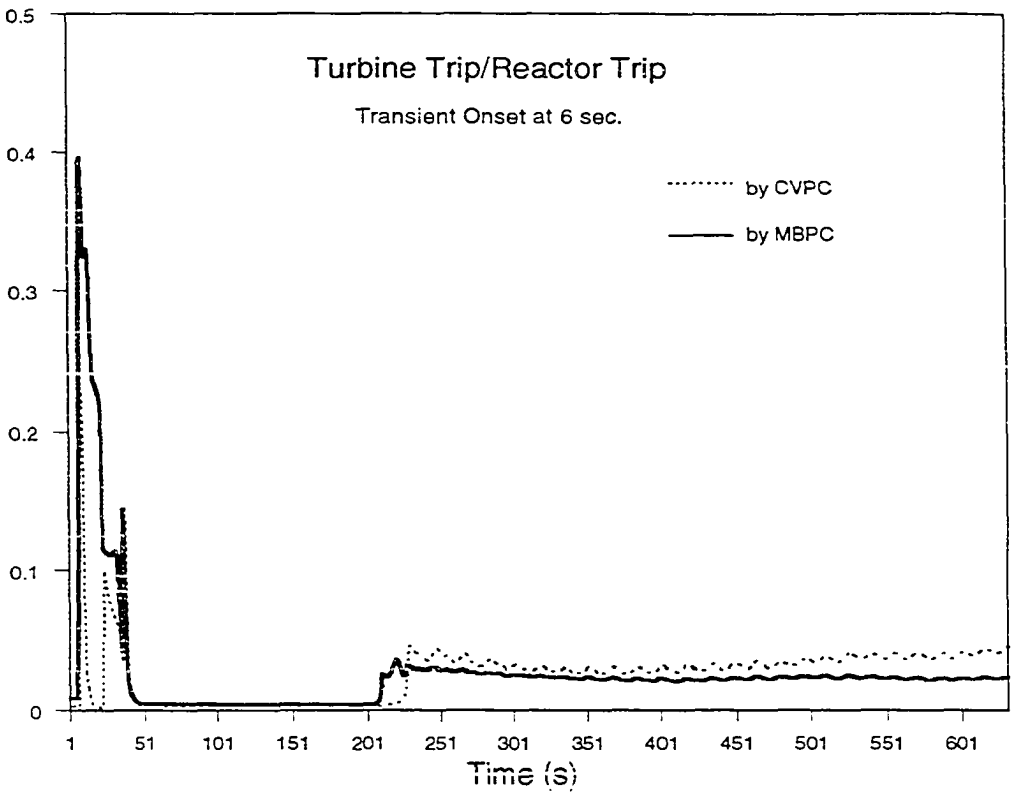

Figure 10. Estimated error bounds provided by the error predictor $P^{(1)}$ for two different partitioning schemes on the ANN advisor $F^{(0)}$ diagnosis. Solid line represents the estimated error bounds by using modified bootstrap partition criterion (MBPC); dashed line by using cross validation partition criterion (CVPC).

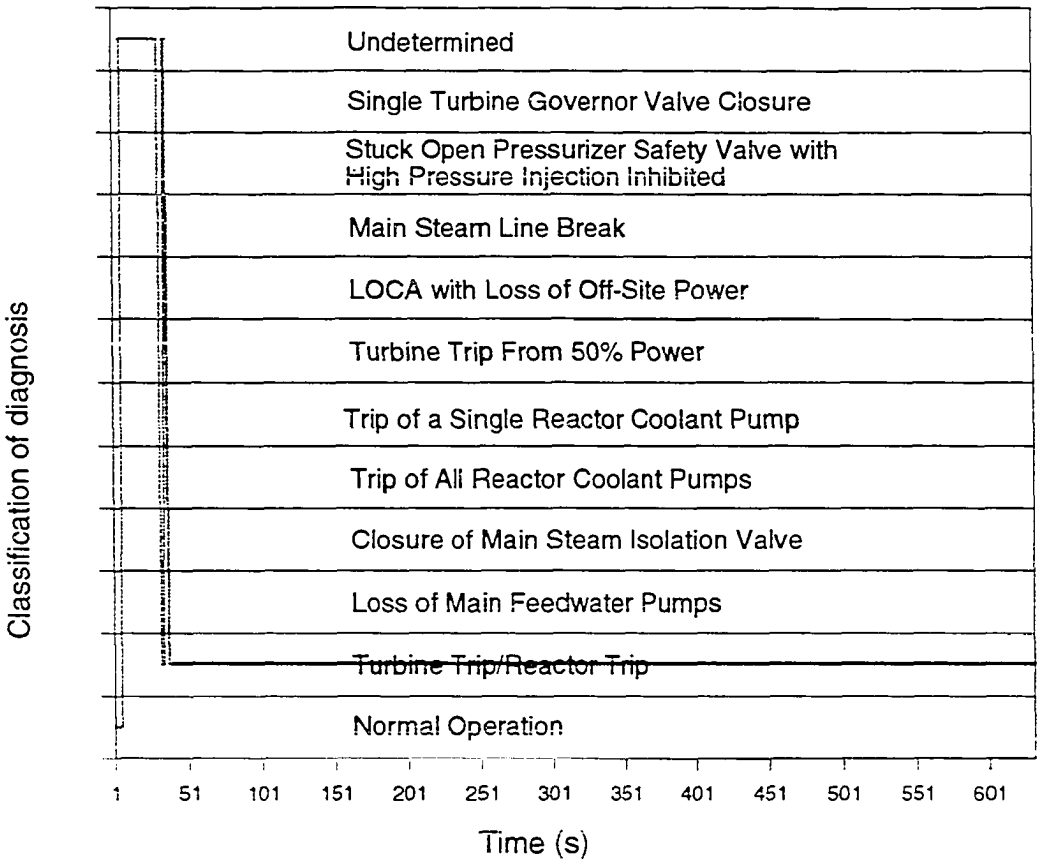

Figure 11. Classification of the advisor diagnosis combined with the predicted error bound for the turbine trip/reactor trip. This classification will be provided plant personnel as a final result of the ANN fault-diagnostic advisor system, as an transient proceeds in a NPP.

Table III. Summary of the Results of the ANN Adviser $F^{(0)}$ and the Error Predictor $P^{(1)}$.

Transient Scenario	Transient onset time (sec.)	Time after transient onset for the true diagnostic error to fall below 0.1[a] (sec.)	Time after transient onset for the error bound predicted by $P^{(1)}$ to fall below 0.1[a] (sec.)
1. Turbine Trip/Reactor Trip	6	30	32
2. Loss of Main Feedwater Pumps	47	3	36
3. Closure of Both Main Steam Isolation Valves	7	28	21
4. Trip of All Reactor Coolant Pumps	16	2	20
5. Trip of a Single Reactor Coolant Pump	14	62	31
6. Turbine Trip From 50% Power	50	1	211
7. Loss of Coolant Accident (LOCA) with Loss of Off-Site Power	7	14	4
8. Main Steam Line Break	6	4	20
9. Stuck Open Pressurizer Safety with High Pressure Injection Inhibited	15	1	46
10. Single Turbine Governor Valve Closure	7	16	1

[a] The value is arbitrarily assigned for an illumination purpose.

transient onset, and even immediately in the case of the stuck open pressurizer safety with high pressure injection inhibited. One exception is the trip of a single reactor coolant pump for which the classification takes about 62 seconds. This transient is characteristically similar to the trip of all reactor coolant pumps. It is understandable that the advisor may need more time to distinguish between these two transients. Note that the required time for diagnosing the trip of all reactor coolant pumps after the onset is only 2 seconds.

In the even numbered figures, the predicted error bounds indicate the estimated uncertainty in the $F^{(0)}$ advisor's diagnosis. For example, during the transitory period in Figure 10, in this case from 6 seconds through 37 seconds, the predicted errors are so much larger than 0.1 that the diagnosis for this period is unreliable. Hence, the classification is undetermined for this transitory period as seen in Figure 11. Since the diagnosis is undetermined, the plant personnel should not consider the output of the advisor when determining plant conditions for mitigation purposes. After the transitory period passes, the predicted error bounds are less than 0.1. The diagnosis of the advisor is then reliable and Figure 11 shows that the classification is turbine trip/reactor trip. In Table III, the predicted error of single turbine governor valve closure is below 0.1 for the entire period. But the true diagnostic error is higher than 0.1 for the transitory period of 16 seconds after the onset. This inconsistency can be eliminated by adding more data delineating the features of the transitory period. This remedy is confirmed by the fact that the training data set L used in this research contains no patterns between a period of from 2 to 29 seconds.

Another fascinating example is the turbine trip from 50% power. In Table III, the error bounds on the diagnoses are large for 211 seconds after the onset at 50 seconds, including the normal operation period. This indicates that the diagnosis is unreliable for both the normal operation and the transient condition periods. In contrast with the predicted error bounds, the true diagnostic errors falls below 0.1 in one second after the transient onset. This discrepancy looks like an undesirable result of the method used in this research. But, in fact, it justifies the method. Notice that all the data for the other transients were collected from 100% power, except for this particular transient where the data were collected from 50% power. Consequently, from the viewpoint of generalization accuracy as measured by stacked generalization, the advisor is not able to sufficiently generalize this specific scenario of the

turbine trip from 50% power from others. In other words, the confidence on the diagnoses for this transient is very low. The assuredness on the diagnoses of this transient can be increased by training the ANN advisor with more transients from this lower reactor power level. This additional training will increase the generalization accuracy for this transient as well as others at this lower power level.

As seen in the odd-numbered figures, the true diagnostic RMS error is conventionally used as a measure of a recall performance. The recall performance is typically utilized to check the generalization accuracy within a single transient. Hence, the generalization accuracy of the ANN diagnoses within a single specific transient is obtained by checking the recall performance. However, this generalization accuracy within a single transient cannot provide the generalization accuracy for the unique transient scenario being compared with other transient scenarios. For example, the error prediction result indicates that the transient of the turbine trip from 50% power needs additional training data in order to be generalized from the other transients. Hence, the generalization accuracy for a transient scenario with respect to other transient scenarios can only be obtained by applying the error prediction method investigated in this work. Similarly, the error prediction method can be used to recognize the same transients that result from different causes as the one on which the advisor was trained.

6. CONCLUSIONS

The objective of this work is to demonstrate a verification technique that provides a figure of merit for the diagnosis of an ANN fault-diagnostic advisor for NPPs. To this end, an ANN advisor is successfully developed to detect and classify ten transient scenarios and ten normal conditions in a PWR nuclear power plant. The error prediction is accomplished by applying the stacked generalization technique to the ANN advisor for providing a figure of merit for the advisor. The results demonstrate the feasibility of the error prediction method for the validation of NPP status diagnostics. The results of the proposed MBPC method show a considerable reduction in computation time and effort without any reduction in the accuracy of the predicted error. Additionally, our error prediction approach can tell us the generalization accuracy for each individual transient scenario as compared with all the other scenarios. The error prediction technique developed in this investigation can also be utilized in all ANN applications.

Fundamentally, the error prediction used in this work uses the nonparametric statistical information in a learning set. Accordingly, each example in a learning set is closely related to generalization accuracy, i.e., the more appropriate the selection of the examples in the training set, the better the generalization. Hence, we suggest that stacked generalization be applied as a more suitable method for the selection of examples for the learning set in future work. In addition, further refinement of the stacked generalization technique will be needed because the dimension of input vectors is doubled in the level 1 space. Level 1 ANN training time therefore increases considerably when the number of plant input variables is large, which is common in fault-diagnostic problems. Furthermore, the correlations of the generalization accuracy of a level 1 generalizer to its training accuracy should be investigated. For more advanced NPP fault-diagnosis, we suggest further investigations related to the robustness of the error prediction method and parametric variations of the trained transients such as, noise responses, different severities for a transient and very similar transient scenarios.

ACKNOWLEDGMENTS

This work was made possible by the generous support of the United States Department of Energy under Special Research Grant No. DEFG02-92ER75700, entitled "Neural Network Recognition of Nuclear Power Plant Transients", and the San Onofre Nuclear Generating Station who provided the simulated data. Their support does not however constitute an endorsement of the views expressed in this paper.

REFERENCES

1. J. EIBL et al., "An Improved Design Concept of the Inner Structures of Next Generation PWR Containments," 5th U.S. Nuclear Regulatory Commission Workshop on Containment Integrity, Washington D.C., May 12-14 (1992).

2. J. J. TAYLOR, "The Safety Design of Next-Generation Reactors," *ANS trans.*, **66**, 302 (1992).

3. D. D. WOODS, E. M. ROTH, L. F. HANES, "Models of Cognitive Behavior in Nuclear Power Plant Personnel, A Feasibility Study," NUREG/CR-4532, Vol. 2, U. S. Nuclear Regulatory Commission (1986).

4. "Advanced Light Water Reactor Utility Requirements Document, Vol. 1-ALWR Policy & Top-Tier Requirements," NP6780, Electric Power Research Institute (Mar. 1990).

5. E. B. BARTLETT, K. KIM, "Nuclear Power Plant Diagnostics with Artificial Neural Networks," Final Phase 1 Report to U. S. NRC Subcontract with NETROLOGIC (1992).

6. E. B. BARTLETT et al., "Neural Network Recognition of Nuclear Power Plant Transients," Annual Report to U. S. Department of Energy, DOE/ER/75700-1 (1993).

7. E. B. BARTLETT, R. E. UHRIG, "Nuclear Power Plant Status Diagnostics Using an Artificial Neural Network," *Nucl. Technol.*, **97**, 272 (1992).

8. E. B. BARTLETT, R. E. UHRIG, "Nuclear Power Plant Status Diagnostics Using Artificial Neural Networks," *Proc. of ANS Meeting on AI'91: Frontiers of Innovative Computing for the Nuclear Industry*, **2**, 644 (1991).

9. Y. OHGA, H. SEKI, "Abnormal Event Identification in Nuclear Power Plants Using a Neural Network and Knowledge Processing," *Nucl. Technol.*, **101**, 159 (1993).

10. K. KIM, T. L. ALJUNDI, E. B. BARTLETT, "Nuclear Power Plant Fault-Diagnosis Using Artificial Neural Networks," *Proc. Intelligent Engineering Systems Through Artificial Neural Networks*, Vol. 2, 751-756, ASME Press, N.Y. (1992).

11. K. KIM, T. L. ALJUNDI, E. B. BARTLETT, "Confirmation of Artificial Neural Networks: Nuclear Power Plant Fault Diagnostics," *ANS Trans.*, **66**, 112 (1992).

12. D. H. WOLPERT, "Stacked Generalization," *Neural Networks*, **5**, 241 (1992).

13. D. H. WOLPERT, "A Mathematical Theory of Generalization: Part I and Part II," *Complex Systems*, **4**, 151 (1990).

14. E. K. BLUM, L. K. LI, "Approximation Theory and Feedforward Networks," *Neural Networks*, **4**, 511 (1991).

15. K. S. NARENDRA, K. PARTHASARATHY, "Identification and Control of Dynamic Systems Using Neural Networks," *IEEE Trans. Neural Networks*, **1**, no. 1, 4 (1990).

16. E. B. BARTLETT, "Analysis of Chaotic Population Dynamics Using Artificial Neural Networks," *Chaos, Solution, and Fractals: Applications in Science and Engineering*, **1**, no. 5, 413 (1992).

17. E. B. BARTLETT, K. KIM, "Error Bounds on the Output of Artificial Neural Networks," *ANS Trans.*, 69, 197-199 (1993).

18. R. E. UHRIG, "Use of Neural Networks in Nuclear Power Plant Diagnostics," *Proc. Int. Conf. on Availability Improvements in Nuclear Power Plant*, p.310, Madrid, Spain (April, 1989).

19. R. HECHT-NIELSEN, "Theory of the Backpropagation Neural Networks," *Proc. the International Joint Conference on Neural Networks*, **1**, 593 (1989).

20. D. E. RUMELHART, J. L. McClelland, the PDP Research Group, Parallel Distributed Processing: Exploration in the Microstructure of Cognition, Vol. 1 & 2, MIT Press, Cambridge, Massachusetts (1986).

21. R. P. LIPPMANN, "An Introduction to Computing with Neural Nets," *IEEE Acoustics Speech and Signal Processing Magazine*, **4**, 4 (April 1987).

22. D. H. WOLPERT, "A Benchmark for How Well Neural Nets Generalize," *Biological Cybernetics*, **61**, 303 (1989).

23. M. STONE, "Cross-validatory Choice and Assessment of Statistical Predictions," *Journal of Royal Statistical Society Series*, Vol. B36, 111 (1974).

24. S. GEISSER, "The Predictive Sample Reuse Method with Applications," *Journal of the American Statistical Association*, Vol. 70, 320 (1975).

25. M. STONE, "Asymptotics For and Against Cross-Validation," *Biometrica*, **64**, 29 (1977).

26. K. LI, "From Stein's Unbiased Risk Estimates to the Method of Generalized Cross-Validation," *The Annals of Statistics*, **13**, 1352 (1985).

27. D. SANKOFF et al., "Supercomputing for Molecular Cladistics," *Proc. of the First Conference of the International Federation of Classification Societies*, **1**, 385 (1987).

28. XIANGDONG, ZHAOXUAN, "Nonlinear Time Series Modeling by Self-Organized Methods," Report from the Department of Mechanics, Peking University, Beijing, PRC (1990).

29. Data provided by T. James, S. Olmos, and D. Rogers of San Onofre Nuclear Generating Station, San Clemente, CA.

PAPER II: ERROR ESTIMATION BY SERIES ASSOCIATION FOR ARTIFICIAL NEURAL NETWORK SYSTEMS

Error Estimation by Series Association for Artificial Neural Network Systems

Keehoon Kim
Eric B. Bartlett

Nuclear Engineering Program
Department of Mechanical Engineering
Iowa State University
Ames, Iowa 50011

This manuscript has been submitted for publication to Neural Computation.

ABSTRACT

Validation and verification of artificial neural network (ANN) outputs is an important issue when the assured performance of an ANN system is required for safety or reliability. This paper presents a new error-bound prediction technique called error estimation by series association (EESA) that provides error bounds on the outputs obtained from an ANN in order to validate the outputs or classifications. The examples investigated in this paper include a simple nonlinear mapping and a more complicated, realistic fault diagnosis problem. The results demonstrate that EESA performs error estimation successfully and therefore validates the outputs from the ANN models. Moreover, EESA can also be used to indicate that the ANN requires training on more data in order to increase generalization.

1. INTRODUCTION

Artificial neural networks (ANNs) have gained acceptance in various disciplines because they have many useful characteristics. For example, ANNs are capable of learning features by examples without explicit representation of the system dynamics (Rumelhart, McClelland & the PDP Research Group, 1986; Lippman, 1987; Blum and Li, 1991; Hecht-Nielsen, 1990; Kurkova, 1992). In addition, ANNs are able to generalize, that is, to classify unfamiliar data on the basis of knowledge acquired through learning. Another important characteristic of ANNs is noise- and fault-tolerance, which provides robustness in the ANN response. These characteristics have motivated numerous engineering implementations of ANNs into system modeling (Lapedes & Farber, 1987; Narendra & Parthasarathy, 1990; Zhang, Mesirov & Waltz, 1992; Bartlett, 1992), process control (Bhat & McAvoy, 1990; Miller, Sutton & Werbos, 1990), plant monitoring (Uhrig, 1989; Upadhyaya & Eryurek, 1992) and fault diagnosis (Venkatasubramanian & Chan, 1989; Bartlett & Uhrig, 1992).

One drawback of applying ANNs to real world problems, however, is that general theories of validation and verification do not yet exist (Bartlett & Kim, 1992; Wildberger, 1994). Many ANN implementations have assumed, implicitly or explicitly, that the output of an ANN is reliable. This assumption may be inappropriate for the output obtained from an ANN presented with novel input data not included in the training data. Moreover, validation and verification of ANN outputs is crucial when the assured performance of the ANN system is required for safety. For example, nuclear power plant (NPP) diagnosis provided by a fault-diagnostic system for an abnormal plant condition is essential for safe control and operation (Kim & Bartlett, 1993).

Leonard, Kramer, and Ungar (1992) have investigated a radial basis function network (RBFN) architecture that provides a performance measure by estimating a confidence level on its output. Kim and Bartlett have addressed validation and verification on the diagnoses obtained from a fault-diagnostic advisor using ANNs by providing error bounds on the diagnoses (Kim, Aijundi & Bartlett, 1992a & 1992b; Kim and Bartlett, 1993; Bartlett and Kim, 1993). Unlike Leonard, Kramer, and Ungar's method that is limited to RBFNs, Kim

and Bartlett's work can be applied to any ANN paradigm. In the work by Kim and Bartlett, error-bound estimations employ a stacking procedure that originates from cross validation in nonparametric statistics (Stone, 1974, 1977; Geisser, 1975; Li, 1985). Wolpert (1992) conceptualized the stacking procedure for improving generalization accuracy in his stacked generalization scheme. The stacking procedure provides error information by training a number of ANNs on different subsets of the training data and testing them on the remainder of the data. The error information generated constitutes a new learning set, which in turn is used to train an additional ANN, called the error predictor ANN, that predicts the error bounds on the output of the ANN system trained on the entirety of the original training data. These estimated error bounds are then used to provide reliability information for the purposes of validation and verification.

There are, however, difficulties when applying Wopert's stacking procedure to actual problems. First, the computational complexity of the stacking procedure depends upon the number of partitions created. Selecting a proper partition criterion is very important in minimizing the computational requirements. Second, the dimension of the input space of the ANN error predictor is doubled when compared with that of the ANN system. The reason is that the stacking procedure used by Wolpert requires an additional input vector, which is of the same dimension as the input space of the ANN system. This doubling of the input dimension will cause training times to increase considerably when the number of the input variables of a system is large (Wilf, 1986; Judd, 1990). In this paper, we present a new stacking procedure called error estimation by series association (EESA). EESA reduces the dimension of the input space of the ANN error predictor and therefore the training complexity. This reduction in the input dimension is accomplished by feeding the output of the ANN system through the ANN error predictor. This procedure and the selection of an appropriate partition criterion are addressed in Section 3. Section 4 discusses the results of EESA applied to a nonlinear mapping problem and a nuclear power plant fault-diagnostic problem. Conclusions are given in Section 5.

2. ANN MODELING

ANNs can be regarded as generalizers because they infer parent functions from sets of data (Cybenko, 1989; Wolpert, 1990; Kurkova, 1992). Many other generalizers provide good results if the processes they model are well behaved. For example, statistical methods work well for data that is linear and normally distributed. Unfortunately, many systems are not so well behaved. Modeling of ill-behaved or nonlinear systems is an arduous task and is not easily accomplished with standard techniques. However, recent work has demonstrated that nonlinear modeling can be accomplished with ANNs (Narendra and Parthasarathy, 1990; Blum & Li, 1991; Bartlett, 1992 & 1994; Bartlett & Kim, 1993). For example, the nonlinear abilities of ANNs offer an approach to solve nuclear power plant (NPP) transient diagnostic problems (Uhrig, 1989; Bartlett & Uhrig, 1992).

As a preliminary to our discussion of EESA, we define the following concepts for a diagnostic or classification problem. Let Q be the set of all abnormal and normal conditions of a system to be monitored by an ANN; $Q = \{(\mathbf{q},\hat{\mathbf{u}}) \mid \hat{\mathbf{u}} = \Gamma(\mathbf{q})\}$, where $\mathbf{q}$ is a symptom of the system condition and $\hat{\mathbf{u}}$ is the correct classification for the condition. Here Γ is the desired system function to be modeled by an ANN fault-diagnostic advisor called F. Let ANN F provide an estimation $\mathbf{u}$ of the correct classification $\hat{\mathbf{u}}$. A symptom $\mathbf{q}$ is an input vector in $\mathbf{R}^m$ where m is the dimension of the input space. An classification $\mathbf{u}$ is an output vector in $\mathbf{R}^n$ where n is the dimension of the output space of F.

The advisor F is trained on a subset of Q; $L \subset Q$ where L is chosen to be the learning set for F. Let $L = \{(\mathbf{q}_j,\hat{\mathbf{u}}_j) \mid j = 1 \text{ to } k\}$ where $\hat{\mathbf{u}}_j$ is a known solution corresponding to an input $\mathbf{q}_j$. The learning set L consists of k patterns of input-output vectors, $\mathbf{q}_j \in \mathbf{R}^m$ and $\hat{\mathbf{u}}_j \in \mathbf{R}^n$. When presented with a novel symptom $\mathbf{q} \in Q - L$, the advisor F provides $\mathbf{u}$ for $\mathbf{q}$.

We assume that L is the only available information for modeling the ANN F. Our goal is to estimate error bounds on the classifications, or output, obtained from F in order to measure its reliability. To this end, an error bound ε associated with $\mathbf{u}$ is provided by another ANN called the error predictor network P trained on a derived learning set L′ that is

generated by EESA. The resultant output from the fault-diagnostic system, F and P, developed by EESA is $\mathbf{u} \pm \varepsilon$ for a novel symptom $\mathbf{q}$. Note that the error bound ε provided by EESA is an estimated error rather than a maximum probable error.

3. ERROR ESTIMATION FOR ANN MODELS

3.1. The Stacking Procedure

In order to generate the learning set L′, a partition criterion that creates a set of t partitions on L is required. For a particular partition i, where i = 1 to t, the learning set L is partitioned into two disjointed subsets, L_{i1} and L_{i2}. An ANN, f, that has the same architecture as F is trained on the partitioned subset L_{i1}. The performance of f is measured by testing it on the remainder of L, the subset L_{i2}. From this procedure, we obtain new information about the deviation, $\varepsilon_j = \mathbf{g}_j - \hat{\mathbf{u}}_j$, between the actual output $\mathbf{g}_j$ and desired output $\hat{\mathbf{u}}_j$. Here, $\mathbf{g}_j$ is the output of f which is trained on L_{i1} only, and $\hat{\mathbf{u}}_j$ is the desired output for the novel input $\mathbf{q}_j$ from L_{i2}. The stacking procedure of Wolpert imposes the requirement that the difference vector $\mathbf{q}_j'$ from $\mathbf{q}_j \in L_{i2}$ to its nearest neighbor in L_{i1} be appended to $\mathbf{q}_j$ making the input dimension m+m. Our new method, however, does not require this large increase in the input dimension, as will be discussed later in Section 3.3. The set of input-output pairs, $\{(\mathbf{q}_j,\mathbf{q}_j'), \varepsilon_j\}$, represents the relation between the untrained input and the ANN's error. The deviations characterize the generalized response of the ANN to the novel input. Statistically, the deviations are an unbiased error estimation obtained by nonparametric cross validation (Geisser, 1975; Li, 1985; Weiss, 1991). This unbiased error provides a measure to select a best statistical model among possible models. The process of training and testing is repeated for each of the t partitions. In Wolpert's stacking procedure, the performance data ε_j with $\mathbf{q}_j$ and $\mathbf{q}_j'$ constitute the new learning set L′ used to train an ANN error predictor P.

3.2 Selection of Partition Criterion

Partitions of the learning set can be created by several different criteria. These criteria include methods such as the cross validation partition criterion (CVPC) (Wolpert, 1992), the bootstrap partition criterion (BPC) (Kim & Bartlett, 1993) and the modified bootstrap partition criterion (MBPC) (Kim & Bartlett, 1993).

CVPC requires the total number of partitions t to be equal to the number of training patterns k in the learning set. For each partition i, where i = 1 to k, $L_{i2} = (\mathbf{q}_i, \hat{\mathbf{u}}_i)$ and $L_{i1} = L - L_{i2}$ with the additional conditions that $L_{m2} \cap L_{n2} = \emptyset$ for $m \neq n$ and $\cup_{i=1}^{t} L_{i2} = L$. The computational requirements for generating L′ increases with k since ANN f must be trained and tested k times. When k is large, which is typical of real world applications, the computation time for generating L′ can be prohibitive.

BPC reduces the total number of partitions t by selecting multiple elements, say s elements, of L_{i2} rather than one as in CVPC. The BPC method we designed for the reduction in the number of partitions is slightly different from the bootstrap resampling methods in nonparametric statistics (Efron, 1982; Sankoff et al., 1987; Welch et al., 1992). The nonparametric bootstrap resampling techniques require choosing s elements randomly for each partition with replacement. The replacement may, however, allow some particular elements to appear several times. The repeated selection results in a situation where the total partition number t would not be reduced. Therefore, we impose proper conditions for our BPC in order to eliminate the undesired increase in t due to the replacement. For each i, where i = 1 to t, let $L_{i2} = \{(\mathbf{q}_l, \hat{\mathbf{u}}_l) | \, l = 1 \text{ to s, and } s < k\}$ where the pairs $(\mathbf{q}_l, \hat{\mathbf{u}}_l)$ are randomly chosen with the conditions, $L_{m2} \cap L_{n2} = \emptyset$ for $m \neq n$ and $\cup_{i=1}^{t} L_{i2} = L$. Note that when s is chosen such that t = k/s = 10, the total computation requirements are reduced by one-tenth of that in CVPC. However, due to the random selection of multiple elements of L_{i2}, the BPC method may provide varying results when L contains insufficient training data. If L contains sufficient training data, this is not a problem. We are faced with the burden of determining what degree of sufficiency we require for a model. While the estimation of data density was performed by Parzen (1962), determining what extent of the sufficiency is suitable for a problem *a priori* has not been yet addressed.

MBPC is our new extension of BPC. In MBPC the L_{i2} patterns are chosen systematically rather than randomly. In our NPP fault diagnosis example discussed in Section 4, we seek to classify operational transients based on known patterns. An operational transient is equivalent to a set of patterns represented by m plant variables in an m-dimensional feature space. A set of patterns pertaining to a particular transient must also

be distinguished from other sets of patterns pertaining to other transients. The uniqueness of these patterns in the feature space form the basis for classifying the transients of interest. Therefore, the learning set L consists of r separate groups of patterns, each pertaining to the r different transients. The r patterns for L_{i2} can then be selected from each transient group at the same time. This simultaneous selection across the pattern classes can minimize the loss of information as well as the training time related to obtaining the training data for the ANN error predictor P. The implementation of MBPC, however, requires two constraints: First, L_{i2} must be a set of r single patterns chosen from each transient or classification group. In other words, for partition *i*, $L_{i2} = \{(\mathbf{q}_l,\hat{\mathbf{u}}_l) | \, l = 1 \text{ to } r\}$ where each pattern is randomly chosen from each classification group with the conditions $L_{m2} \cap L_{n2} = \emptyset$ for $m \neq n$ and $\cup_{i=1}^{t} L_{i2} = L$. Second, if the number of training patterns in a specific classification group is larger than r, a second constraint is imposed as follows. For a partition, a maximum of two patterns can be selected from the particular group whose number of training patterns is larger than r. The imposition of the second constraint may prevent further increases in the partition number. Another option is to apply CVPC to the excessive patterns remaining after fulfilling the first constraint. This partial CVPC application can eliminate the potential disadvantage of selecting two patterns with a trade in the increase of t.

In this paper, MBPC is applied to the real world problem discussed in Section 4 to demonstrate the creation of partitions according to the method outlined above. Moreover, our MBPC method of ANN verification can be applied to a learning set of any physical system that possesses the uniqueness of grouped patterns in the feature space of the system, such as, character recognition, on-line inspection of product quality, or other such processes.

3.3. Error Estimation by Series Association

We have developed a new stacking procedure called EESA in order to resolve the problems of the stacking procedure of Wolpert. The first problem comes from the requirement that the additional vector $\mathbf{q}_j'$ be appended to input pattern $\mathbf{q}_j$ in the learning set L′. Therefore, the dimension of the input space of L′ is doubled to m + m, i.e., $(\mathbf{q}_j,\mathbf{q}_j') \in \mathbf{R}^{m+m}$ where m is the dimension of the input space L. This expansion of the

input space of L′ may cause difficulties in developing P. These difficulties include the escalation of the training complexity of P as the number of inputs increase. When m is large, which can easily occur in real applications, training P with 2m input nodes can be very difficult. For example, in the fault-diagnostic problem discussed in Section 4.2, the dimension of the input space of L′ would increase from 97 to 97 + 97 = 194 since we have m = 97 plant variables in L.

In addition to doubling the input dimension, another problem comes from adding the difference vector to the input space, which is based on the assumption that the error of ANN F is strongly related to the difference vector from a given novel input to its nearest neighbor in L (Wolpert, 1992). This assumption can be shown to fail under certain conditions. For example, let a novel pattern $\mathbf{q}$ be very close to a training pattern $\mathbf{q}_j$. A nearest neighbor computed in L_{i1} for the training pattern $\mathbf{q}_j$ from L_{i2} might differ from a nearest neighbor computed in L for the novel pattern $\mathbf{q}$. Hence, the difference vector computed in L_{i1} for $\mathbf{q}_j$ can be substantially different from the difference vector for $\mathbf{q}$ that is very close to $\mathbf{q}_j$. This inconsistency may cause P to estimate error bounds inaccurately. These inaccuracies are likely to be larger when multiple elements are chosen for L_{i2} as in BPC or MBPC, but they can be solved by implementing EESA.

The EESA scheme is performed by feeding the output from ANN F into ANN error predictor P. This is done in place of adding the difference vectors to the input. Connecting the output of F to P by EESA allows the performances of F to be directly monitored by P. A diagram of this scheme is shown in Figure 1.

Errors in the outputs of F are caused not only by how much a given novel input differs from training data in L but also by how well F is trained. EESA can address these issues since the novel input and its corresponding output from F are fed into P. The stacking procedure without EESA, however, cannot provide such information since an estimated error of P is not dependent upon the output of F, i.e., it is only dependent on the input to F. In addition to the aforementioned advantages, EESA reduces the input space dimension of P to m + n, which is usually much smaller than m + m since the dimension of outputs, n, is usually smaller than the dimension of inputs, m. The reduction in the input dimensionality alleviates the training requirements considerably.

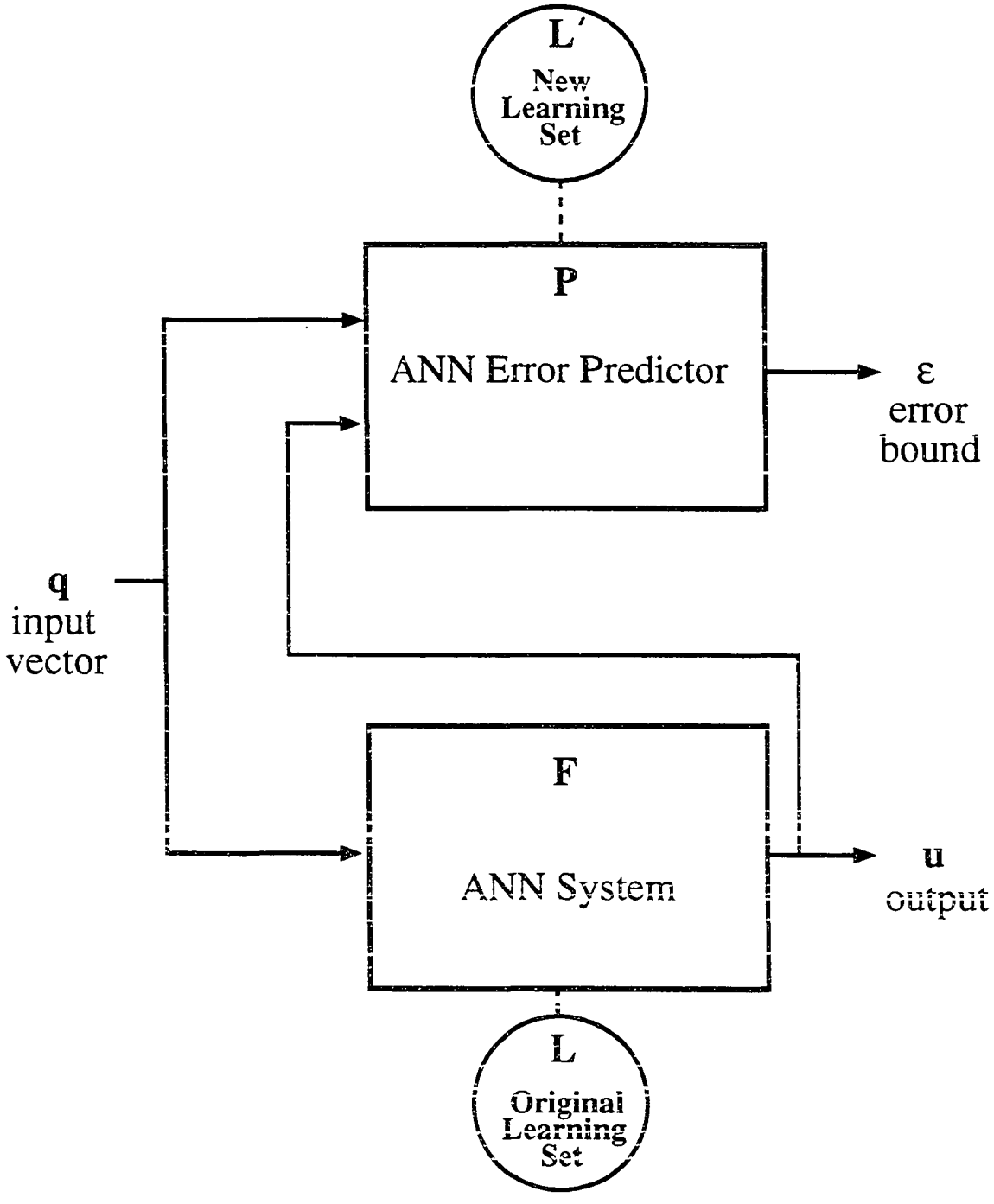

Figure 1. The structure of error estimation by series association (EESA). The ANN advisor F trained on L produces the output u, and P trained on L′ provides the error bound ε.

The following is the algorithm of EESA:

1. Create a partition i of the learning set L such that
   $L_{i2} = \{(\mathbf{x}_l, \mathbf{y}_l) \mid 1 \le l \le r,\ \mathbf{x}_l = (x_{l1}, x_{l2}, ..., x_{lm}) \in \mathbf{R}^m$ and $\mathbf{y}_l = (y_{l1}, y_{l2}, ..., y_{ln}) \in \mathbf{R}^n\}$ where r is the number of patterns for L_{i2} according to the chosen partition criterion, and $L_{i1} = L - L_{i2}$. Note that the ANN F is trained on the entirety of L.
2. Train an ANN f having the same architecture of F on L_{i1}.
3. Compute the deviations $\{\varepsilon_l\}_i$, where $\varepsilon_l = (\varepsilon_{l1}, \varepsilon_{l2}, ..., \varepsilon_{ln})$, for the partition i by testing the ANN f on the input patterns in L_{i2}. Note that $\varepsilon_{lj} = |\ f(x_l)_j - y_{lj}\ |$ where j=1 to n.
4. Compute the output $\hat{\mathbf{y}}_l$ for F for the input pattern $\mathbf{x}_l$, which is $\hat{\mathbf{y}}_l = F(\mathbf{x}_l) \in \mathbf{R}^n$.
5. Save $(\mathbf{x}_l, \hat{\mathbf{y}}_l) \in \mathbf{R}^{m+n}$ and $\varepsilon_l \in \mathbf{R}^n$, as new data patterns of the new learning set L′.
6. Repeat steps 2 through 5 for each of the partitions of L.
7. Train P on $L' = \{\ ((\mathbf{x}_v, \hat{\mathbf{y}}_v), \varepsilon_v) \mid 1 \le v \le k\}$ where k is the total number of the learning set L.

4. IMPLEMENTATIONS AND RESULTS

4.1 Error Estimation for a Nonlinear Mapping

As our first example, error estimation was performed with and without EESA on a nonlinear mapping of the function $y(x) = 0.4 \sin(\pi x) + 0.5$. A total of 15 data points for L, shown in Figure 2, were chosen from 201 data patterns generated for this experiment. The learning set L was used to train ANN F. Assume that the only data available to us is L and the goal is to estimate error bounds on the ANN's output for novel data points. Note that set L does not contain sufficient data for a perfect generalization. We selected these 15 data points of L as a learning set for this example because in real world applications it is not always possible to assure an abundance of training data. The resulting ANN F is a 2-hidden-layer network with one input node, 6 hidden nodes in the first hidden layer, 4 hidden nodes in the second hidden layer, and one output node (1-6-4-1).

The ANN F trained on L was recalled on the untrained data in order to calculate the true errors of the ANN mapping and to be able to compare the true error to our estimated errors. In order to compare the performance of EESA to that of the stacking procedure without EESA, two single-hidden-layer ANNs, P_1 and P_2 (2-5-1), were trained on the new training sets L_1' and L_2' that were generated by using EESA and the stacking procedure without EESA, respectively. CVPC was used for both cases.

The results for the sine function mapping problem are displayed in Figure 3. The true error is the absolute difference between the output of F and y(x). The P_1 and P_2 networks estimate the error bounds on the output produced by F for the 186 untrained data points. The error bound estimated by EESA is much closer to the true error than that obtained by the stacking procedure without EESA. It is also much smoother. The discontinuous jumps on the error bounds generated by P_2 are caused by the abrupt change in the difference vector for the untrained patterns as discussed earlier. High error bounds on the interval [0.35, 0.55] show that the output of F on this interval is relatively unreliable and F should be trained on data in this range. This illustrates the additional advantage of using EESA, i.e., the adequacy

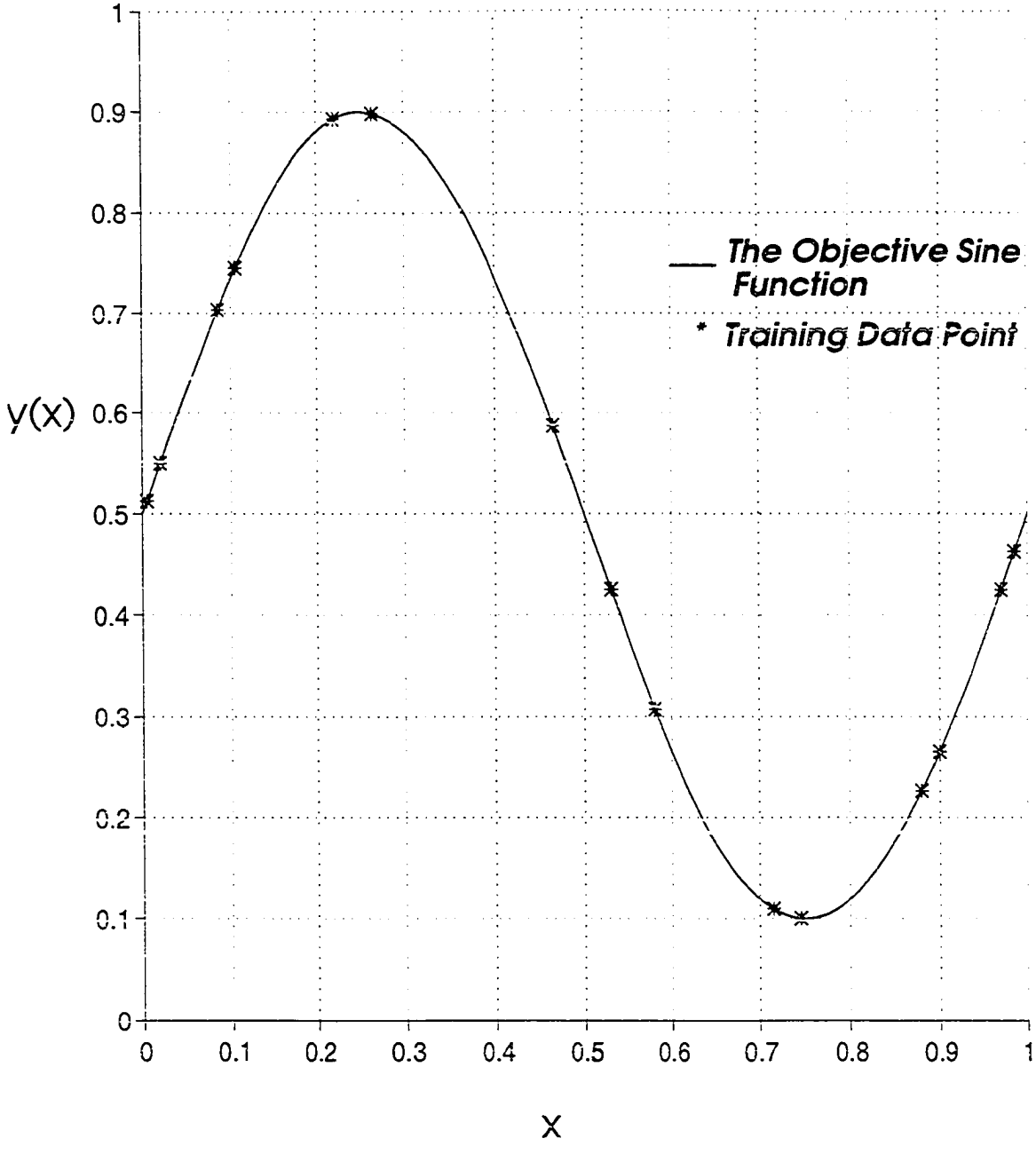

Figure 2. A nonlinear mapping problem of the sine function $y(x)=0.4\sin(\pi x)+0.5$. The learning set L containing a total of 15 data points is chosen from 201 total data points.

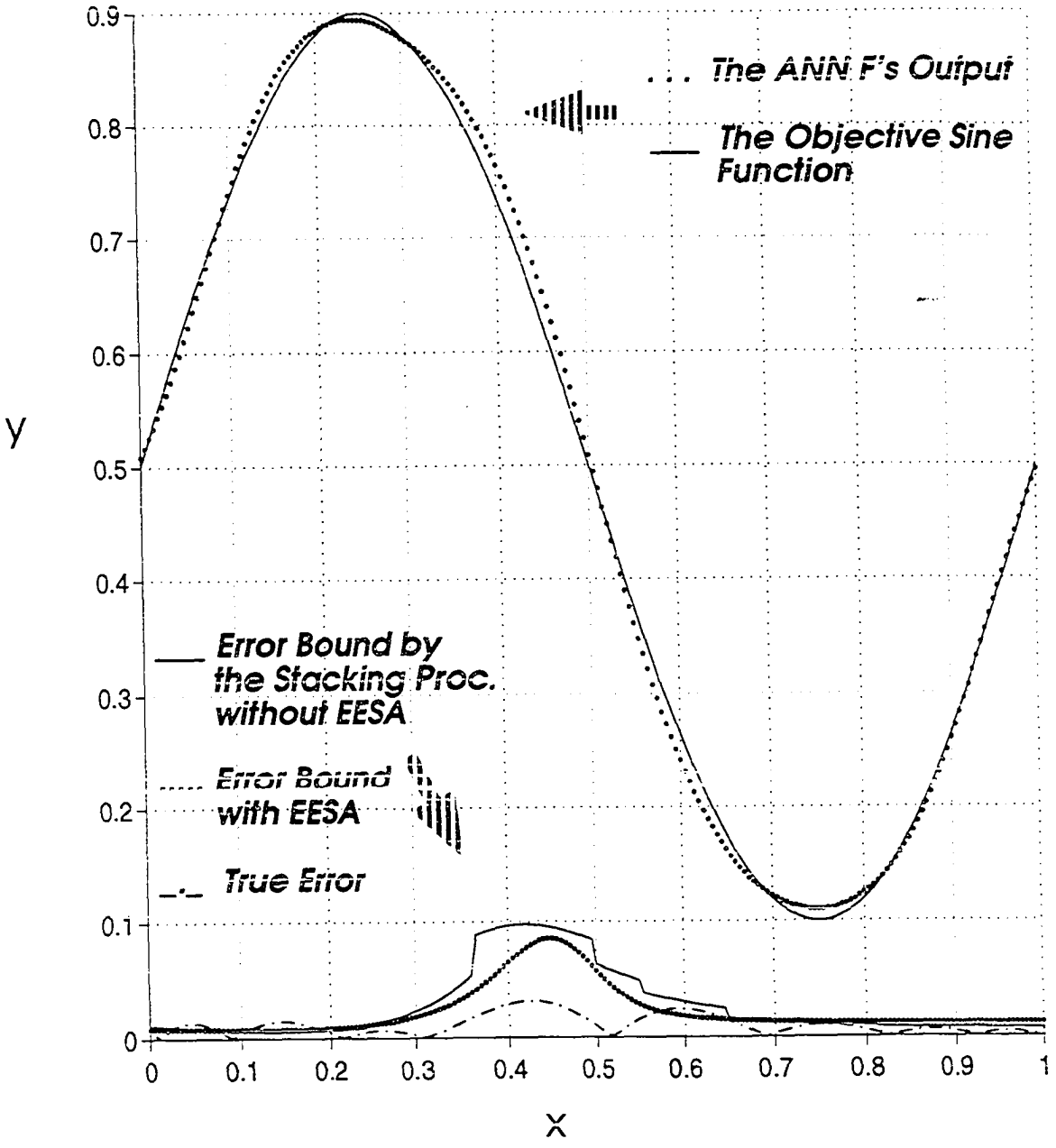

Figure 3. The estimated error bounds obtained from the error predictors for novel data points. The ANN error predictor P_1 is trained on L_1' generated by implementing EESA, and P_2 on L_2' by the stacking procedure without EESA. These estimated error bounds are compared to the true errors.

of the training data can be evaluated, and more data can be added where the estimated errors are high.

4.2 Validation of a NPP Fault-Diagnostic System

As a second illustration, EESA was applied to an NPP transient diagnostics problem to establish the ANN error predictor P and validate the output of the NPP fault-diagnostic advisor F. This work is part of an ongoing research project at Iowa State University (Bartlett, 1993). Data were obtained from the Duane Arnold Energy Center (DAEC) training simulator, owned by Iowa Electric Light and Power Company (Vest et al., 1991). A total of 25 distinct transients were simulated for this work. Note that the term transient in nuclear engineering means an abnormal operational condition that might develop into a potentially dangerous accident if appropriate corrective actions are not taken. Diagnosing the causes of a transient is, therefore, very important to the safe control and operation of a NPP. Some of the transients were simulated at different severities so that the NPP fault-diagnostic advisor F can be trained to classify the transients independent of their severities. Because the simulations were performed at various severities, the data include a total of 33 different transient scenarios as listed in Table I. For example, the transient ms04a, a main steam line rupture outside primary containment, was simulated at three different severities, 100%, 60%, and 30%. The severity of this transient specifies the size of the sheared portion of the main steam line at the turbine inlet header.

Each data set contains input patterns with 97 plant variables at intervals of one second for a period of three to ten minutes. The plant variables used as input to the ANNs, as well as the ANN outputs, were normalized from 0.1 to 0.9. The associated output used to distinguish each of the 25 transient conditions is a unique 5-bit binary code. This normalization allows for quicker training without driving the output nodes into the saturation region of the nodal sigmoid transfer function (Hecht-Nielsen, 1992). The output codes are listed in Table I. Note that this time snap shot, or single time slice, of data does not include temporal information. The main advantage of the single time step approach is simplicity of training and execution regardless of temporal trends of a transient. Advisor F is trained to diagnose transients at the very instant a plant operational symptom is presented because the

Table I. List of the 25 transients with the scenario codes and designated output codes.

No	Scenario Code	Transient Description	Output Code
1	ad05	Spurious automatic depressurization system actuation	0.9 0.1 0.1 0.1 0.1
2	cu10	Reactor water clean-up coolant leakage	0.1 0.1 0.1 0.9 0.1
3	cu10gp5	Reactor water clean-up coolant leakage with failure of Group 5 isolation valves	0.1 0.1 0.9 0.9 0.9
4	fw02a	Main condensate pump trip	0.1 0.9 0.9 0.1 0.9
5	fw08-6	Feedback heater tube leak	0.1 0.1 0.1 0.1 0.9
6	fw09a	Reactor feedwater pump trip	0.9 0.9 0.1 0.1 0.1
7	fw12c0	Feedwater regulator valve controller stuck closed	0.9 0.1 0.9 0.1 0.1
8	fw12c1	Feedwater regulator valve controller stuck open	0.9 0.1 0.1 0.9 0.1
9	fw17a	Main feedwater line break inside primary containment	0.9 0.1 0.1 0.1 0.9
10	fw18a	Main feedwater line break outside primary containment	0.1 0.9 0.9 0.1 0.1
11	ia01	Complete loss of instrumentation air	0.1 0.9 0.1 0.1 0.9
12	ic14scra	Spurious reactor trip	0.1 0.1 0.9 0.9 0.1
13	mc01a	Main circulating water pump trip	0.1 0.1 0.9 0.1 0.9
14	mc04a mc04a_2 mc04a_3	Main condenser air inleakage - 100% severity - 60% severity - 30% severity	0.1 0.1 0.1 0.9 0.9
15	ms02	RCIC line break inside primary containment	0.9 0.9 0.9 0.1 0.1
16	ms04a ms04a_2 ms04a_3	Main steam line rupture outside primary containment - 100% severity: 100% double ended shear - 60% severity: 60% double ended shear - 30% severity: 30% double ended shear	0.9 0.9 0.1 0.9 0.1
17	ms14-6	Loss of extraction steam	0.9 0.9 0.1 0.1 0.9

Table I. (continued)

No	Scenario Code	Transient Description	Output Code
18	rd13 rd13_2	Loss of air pressure to control rod drive (CRD) hydraulic control units (HCU) - 100 % severity - 60 % severity	0.9 0.1 0.9 0.9 0.1
19	rp05tc01	Main turbine trip followed by reactor protection system circuit failure	0.9 0.1 0.9 0.1 0.9
20	rp05act1	Main turbine trip followed by reactor protection system circuit failure together with failure of ARI (alternate rod insertion)	0.9 0.1 0.1 0.9 0.9
21	rr05	Recirculation pump shaft seizure	0.1 0.9 0.9 0.9 0.1
22	rr10	Recirculation pump speed feedback signal failure	0.1 0.9 0.1 0.9 0.9
23	rr15a rr15a_3	Recirculation loop rupture – 100% double ended shear (Design basis LOCA) - 30% double ended shear	0.1 0.1 0.9 0.1 0.1
24	rr30 rr30_2 rr30_3	Coolant leakage inside primary containment - 100% double ended shear - 60% double ended shear - 30% double ended shear	0.1 0.9 0.1 0.1 0.1
25	rx01	Fuel cladding (30%) failure	0.9 0.9 0.9 0.9 0.1
Normal Operation (before transient onset)			0.1 0.1 0.1 0.1 0.1

advisor does not need to observe trends or temporal variation. The disadvantage of the single time step is that F loses the temporal information that may improve the accuracy of diagnosis. The data set for each transient is divided into two parts: one for a normal operating state, and the other for an abnormal transient state after a transient onset. The 97 plant variables used in this example are tabulated in Table II.

The 25 transient conditions plus the normal steady-state operating conditions constitute learning set L for advisor F. Learning set L contains 241 input-output patterns obtained by the procedures outlined by Bartlett and Uhrig (1992). Learning set L is chosen in an iterative manner. Each pattern at the beginning and end of the ten simulated transients is selected to form the learning set. This initial learning set containing the 50 input-output patterns is used to train the ANN advisor until a predetermined training error is obtained. The trained advisor is then recalled on all the patterns over the entire data of the 33 transients. The patterns producing the worst recall errors are added to the learning set. The process of training, recalling and adding patterns is repeated until most of the undesirable, high recall errors disappear. However, some patterns showing high recall errors are not added in order to observe the response of the error estimation system to the patterns. Note that the number of patterns in L is only about 3% out of the 8,782 patterns in the entire data set Q for the 25 transients based on the simulated 33 scenarios. Learning set L includes 25 initial normal conditions to account for the many normal operating modes of the plant. The remaining 216 input-output patterns correspond to abnormal conditions from the 33 scenarios. Advisor F is a backpropagation ANN (97-45-30-10-5) and is trained on L until a training root mean square (RMS) error of 0.05 is obtained. The particular three-hidden-layer architectures used were employed after attempting several different architectures.

In this investigation, MBPC was used to create the partitions of L. Because L contains 25 distinct transients, there are 25 classification groups, each one pertaining to a specific transient, i.e., r = 25. No transient group contains a number of training patterns larger than r where r is 25. Thus, MBPC yields a total of 19 partitions, i.e., t = 19. Note that MBPC has significantly reduced the computational requirements as compared to that of CVPC where we would obtain t = 241. Hence, the process of training and testing ANN f was repeated 19 times rather than 241 times. A new learning set L′ was generated by employing EESA. An

Table II. The 97 plant variables used to trend the 25 transients used in the second example. Note that there are 33 scenarios and that the data was collected at intervals of one second for three to six minutes. The 97 variables are used as inputs to the ANN advisor F.

No.	Variable designation	Description	Min. value	Max. value	Unit
1	A041	Local power range monitor 16-25 flux level B	0.0	125.0	% power
2	A091	Source range monitor channel B	0.0	100.0	%
3	B000	Average power range monitor A Flux level	0.0	125.0	% power
4	B012	Reactor total core flow	0.0	60.0	Mlb/hr
5	B013	Reactor core pressure-differential	0.0	30.0	psid
6	B014	Control rod drive system flow	0.0	0.025	Mlb/hr
7	B015	Reactor feedwater loop A flow	0.0	4.0	Mlb/hr
8	B016	Reactor feedwater loop B flow	0.0	4.0	Mlb/hr
9	B017	Cleanup system flow	0.0	0.07691	Mlb/hr
10	B022	Total steam flow	0.0	8.0	Mlb/hr
11	B023	Cleanup system inlet temperature	0.0	755.0	Deg F
12	B024	Cleanup system outlet temperature	0.0	600.0	Deg F
13	B026	Recirculation loop A1 drive flow	0.0	15.1	Mlb/hr
14	B028	Recirculation loop B1 drive flow	0.0	15.1	Mlb/hr
15	B030	Reactor feedwater channel A1 temperature	280.0	430.0	Deg F
16	B032	Reactor feedwater channel B1 temperature	280.0	430.0	Deg F
17	B034	Recirculation loop A1 inlet temperature	260.0	580.0	Deg F
18	B036	Recirculation loop B1 inlet temperature	260.0	580.0	Deg F
19	B038	Recirculation A wide range temperature	50.4	789.6	Deg F
20	B039	Recirculation B wide range temperature	50.4	789.6	Deg F
21	B061	Reactor coolant total jet pumps 1-8 flow B	0.0	36.7	Mlb/hr
22	B062	Reactor coolant total jet pumps 9-16 flow A	0.0	36.7	Mlb/hr
23	B063	Reactor coolant total outlet steam flow A	0.0	2.0	Mlb/hr
24	B064	Reactor coolant total outlet steam flow B	0.0	2.0	Mlb/hr
25	B065	Reactor coolant total outlet steam flow C	0.0	2.0	Mlb/hr
26	B066	Reactor coolant total outlet steam flow D	0.0	2.0	Mlb/hr
27	B079	Reactor recirculation pump A motor vibration	0.0	10.0	MILS
28	B080	Reactor recirculation pump B motor vibration	0.0	10.0	MILS
29	B083	Control rod drive cooling-water differential pressure	0.0	500.0	dpsi
30	B084	Control rod drive cooling-water differential pressure	0.0	60.0	dpsi
31	B085	Torus air temperature #1	0.0	500.0	Deg F
32	B086	Torus air temperature #2	0.0	500.0	Deg F
33	B087	Torus air temperature #3	0.0	500.0	Deg F
34	B088	Torus air temperature #4	0.0	500.0	Deg F
35	B089	Drywell temperature azimuth 0 elevation 750	0.0	500.0	Deg F
36	B090	Drywell temperature azimuth 245 elevation 750	0.0	500.0	Deg F
37	B091	Drywell temperature azimuth 90 elevation 765	0.0	500.0	Deg F
38	B092	Drywell temperature azimuth 270 elevation 765	0.0	500.0	Deg F
39	B093	Drywell temperature azimuth 270 elevation 765	0.0	500.0	Deg F

Table II. (continued)

40	B094	Drywell temperature azimuth 180 elevation 780	0.0	500.0	Deg F
41	B095	Drywell temperature azimuth 270 elevation 830	0.0	500.0	Deg F
42	B096	Drywell temperature center elevation 750	0.0	500.0	Deg F
43	B098	Torus water temperature	0.0	752.0	Deg F
44	B099	Torus water temperature	0.0	752.0	Deg F
45	B103	Drywell pressure	0.0	100.0	psia
46	B104	Torus pressure	0.0	100.0	psia
47	B105	Torus water level	-10.0	10.0	inch
48	B120	Torus radiation monitor A	-1.0	100.0	%
49	B121	Torus radiation monitor B	-1.0	100.0	%
50	B122	Reactor water level	158.0	218.0	inch
51	B124	Reactor water level	158.0	218.0	inch
52	B1257	Fuel zone level indication	-153.0	218.0	inch
53	B126	Reactor water level	158.0	458.0	inch
54	B127	Reactor vessel pressure	0.0	1200.0	psig
55	B128	Reactor vessel pressure	0.0	1200.0	psig
56	B129	Reactor vessel pressure	0.0	1500.0	psig
57	B130	Reactor vessel pressure	0.0	1500.0	psig
58	B137	Torus water level	1.5	16.0	ft
59	B138	Torus water level	1.5	16.0	ft
60	B150	Core spray A flow	-1767.8	5000.0	gpm
61	B151	Core spray B flow	-1767.8	5000.0	gpm
62	B160	Reactor core isolation cooling flow	-62.5	500.0	gpm
63	B161	High-pressure core injection flow	-437.5	3500.0	gpm
64	B162	Residual heat removal A flow	-75.0	15000.0	gpm
65	B163	Residual heat removal B flow	-75.0	150.0	gpm
66	B164	Drywell radiation monitor A	-1.0	100.0	%
67	B165	Drywell radiation monitor B	0.0	100.0	%
68	B166	Post-treat activity	0.0	100.0	%
69	B168	Pretreat activity	0.0	100.0	%
70	B171	Analyzer A - O_2 concentration	-1.25	10.0	%
71	B172	Analyzer A - H_2 concentration	-1.25	10.0	%
72	B173	Analyzer B - O_2 concentration	-1.25	10.0	%
73	B174	Analyzer B - H_2 concentration	-1.25	10.0	%
74	B180	Clean-up system flow	0.0	200.0	gpm
75	B196	Reactor water level-fuel zone A	-153.0	218.0	inch
76	B197	Reactor water level-fuel zone B	-153.0	218.0	inch
77	B247	Turbine steam bypass	0.0	500.0	Deg F
78	B248	Turbine steam bypass	0.0	500.0	Deg F
79	E000	4160 V switch gear bus 1A1 A-B	0.0	5.25	KV
80	F004	Condensate pump A & B discharge pressure	0.0	600.0	psig
81	F005	Low-pressure condenser circulating water inlet temperature A	0.0	200.0	Deg F
82	F010	High-pressure condenser circulating water outlet temperature A	0.0	200.0	Deg F

Table II. (continued)

83	F011	Low-pressure condenser circulating water pressure differential A	0.0	10.0	dpsi
84	F015	Circulating water pump A & B discharge pressure	0.0	100.0	psig
85	F018	Cooling tower A discharge water temperature	0.0	752.0	Deg F
86	F019	Cooling tower B discharge water temperature	0.0	752.0	Deg F
87	F040	1P-1A reactor feed pump suction pressure	0.0	600.0	psig
88	F041	1P-1B reactor feed pump suction pressure	0.0	600.0	psig
89	F042	1P-1A reactor feed pump discharge pressure	0.0	2000.0	psig
90	F043	1P-1B reactor feed pump discharge pressure	0.0	2000.0	psig
91	F044	Condensate total flow	0.0	8.0	Mlb/hr
92	F045	Condensate makeup flow	-10.0	100.0	Klb/H
93	F046	Condensate rejection flow	0.0	50.0	Klb/H
94	F094	Feedwater final pressure	0.0	2000.0	psig
95	G001	Generator gross watts	0.0	720.0	MWE
96	T039	Low-pressure condenser pressure	0.0	30.0	inHg
97	T040	High-pressure condenser pressure	0.0	30.0	inHg

ANN error predictor P was trained on L′ by using backpropagation. The ANN error predictor P was chosen to have the architecture of 102-30-10-5. The advantages of EESA can be appreciated in that the input space dimension of P has increased only by 5 not 97. Advisor F provides its diagnosis u for an unknown symptom $q \in Q - L$. Corresponding to u, the ANN error predictor P estimates an error bound ε on the diagnosis u. The resultant output of the fault-diagnostic system is $u \pm \varepsilon$. Thus, the diagnosis and its error estimation allow the control room personnel to validate the advisor's diagnosis by interpreting its upper and lower error bound.

The results obtained from the NPP fault-diagnostic system F and P are shown in Figures 4 to 6 and Table III. The dot-dashed line in the figures represents the values of an output node of the fault-diagnostic advisor F. The solid lines above and below the dot-dashed line represent the upper- and the lower-error bound estimated by P. All combining five outputs with the error bounds provides reliability information on a diagnosis given by F at each instant of transient symptom presentation. Table III summarizes the results of the fault-diagnostic system for all 33 scenarios. The fourth and fifth columns show transient onset time and the automatic reactor safety trip time, respectively. The sixth column displays the time when the fault-diagnostic system detects an abnormal condition in the plant status. The last column shows the time when a diagnosis is validated to be reliable.

The fault-diagnostic system detects an abnormal status of the plant very promptly after the onset of the transients. However, the system outputs are indefinite for a short period after the transient has been detected because the plant input variables vary abruptly and dynamically and the relations among the input variables are not uniquely coupled for this period. After this inconclusive period passes, the fluctuations in the system outputs disappear and are followed by the unassured period during which time the error bounds on the diagnoses are large. This unassured period continues momentarily, and then the estimated error bounds become small. Hence, after the unassured period, the diagnoses are validated. For example, Figure 4 of the recirculation loop rupture at 100% severity (rr15a) shows the inconclusive period from 6 seconds to 18 seconds for which the outputs are indefinite, i.e., the values of fifth node are between 0.3 and 0.7. The inconclusive period is followed by the unassured period from 19 seconds 47 seconds for which error bounds are

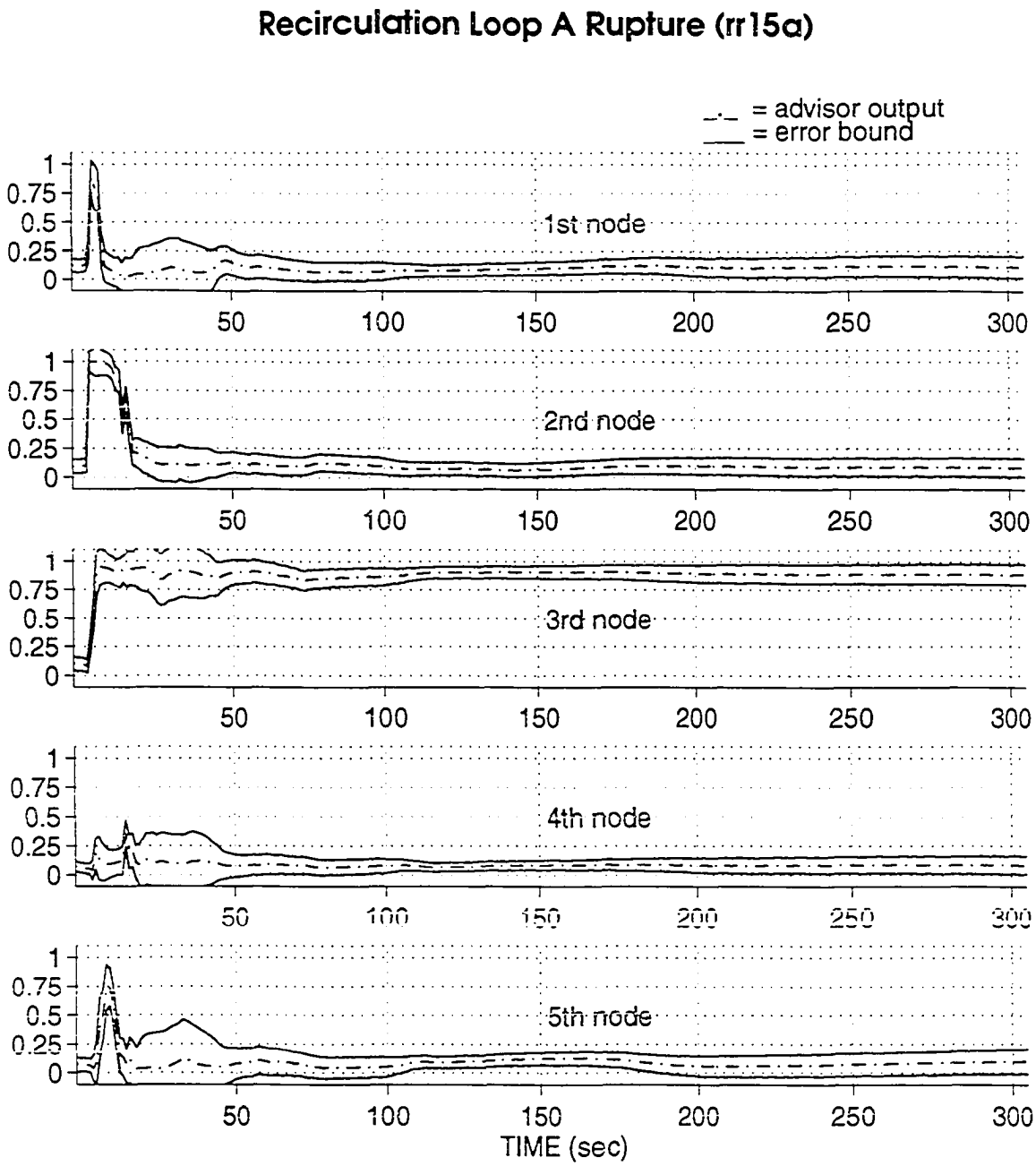

Figure 4. Diagnosis with the estimated error bounds for the recirculation loop rupture (rr15a) transient.

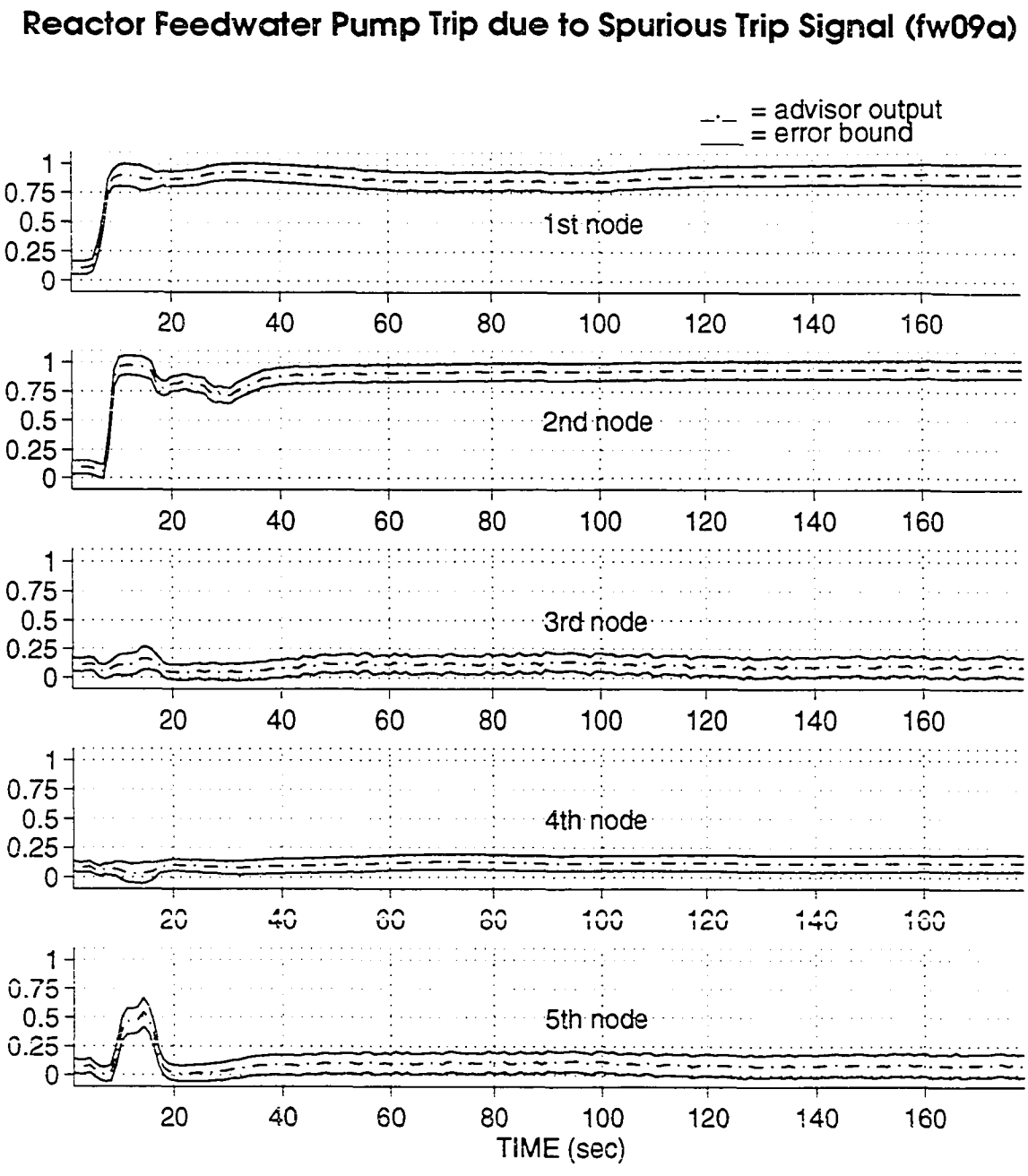

Figure 5. Diagnosis with estimated error bounds for the reactor feedwater pump trip due to spurious trip signal (fw09a) transient.

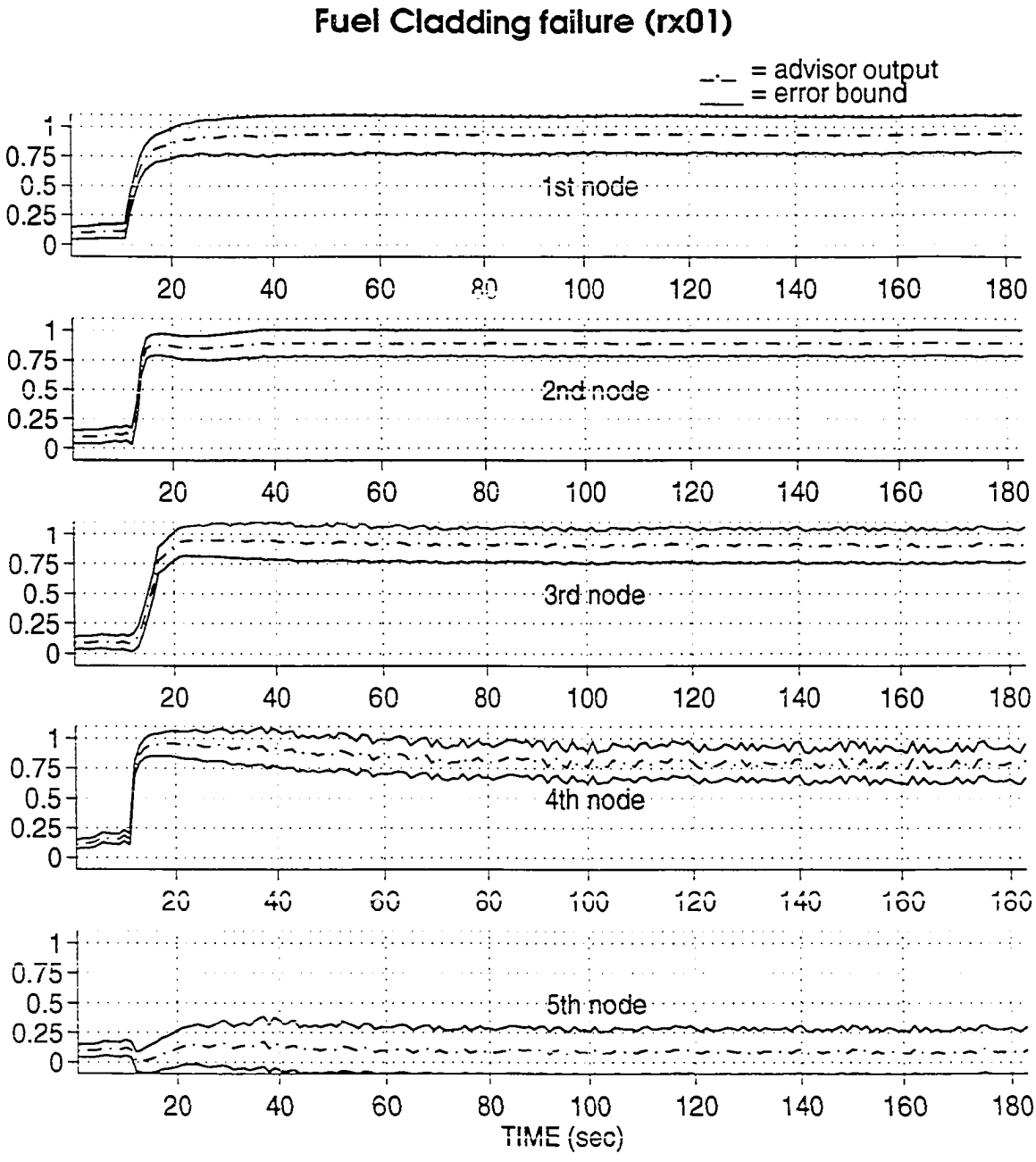

Figure 6. Diagnosis with estimated error bounds for the fuel cladding failure (rx01) transient.

Table III. Summary of the results of the fault-diagnostic system, the advisor F and the ANN error predictor P.

No	Scenario Code	Transient Description	Onset time (sec)	Safety trip time (sec)	Time of detecting abnormal plant status	Time of providing assured diagnosis
1	ad05	Spurious automatic depressurization system actuation	10	13	10	49
2	cu10	Reactor water clean-up coolant leakage	5	no trip	24	24
3	cu10gp5	Reactor water clean-up coolant leakage with failure of Group 5 isolation valves	6	51	7	48
4	fw02a	Main condensate pump trip	6	504	10	28
5	fw08-6	Feedback heater tube leak	10	33	10	35
6	fw09a	Reactor feedwater pump trip	5	no trip	6	17
7	fw12c0	Feedwater regulator valve controller stuck closed	5	16	7	47
8	fw12c1	Feedwater regulator valve controller stuck open	5	96	17	63
9	fw17a	Main feedwater line break inside primary containment	10	12	10	82
10	fw18a	Main feedwater line break outside primary containment	7	16	7	31
11	ia01	Complete loss of instrumentation air	10	no trip	23	37
12	ic14scra	Spurious reactor trip	5	7	6	64
13	mc01a	Main circulating water pump trip	6	281	10	114
14	mc04a	Main condenser air inleakage - 100% severity	10	46	17	44
	mc04a_2	- 60% severity	10	57	21	55
	mc04a_3	- 30% severity	10	69	21	63
15	ms02	RCIC line break inside primary containment	5	9	5	34

Table III. (continued)

No	Scenario Code	Transient Description	Onset time (sec)	Safety trip time (sec)	Time of detecting abnormal plant status	Time of obtaining assured diagnosis
16		Main steam line rupture outside primary containment				
	ms04a	- 100% double ended shear	5	8	6	26
	ms04a_2	- 60% double ended shear	5	8	5	23
	ms04a_3	- 30% double ended shear	5	8	5	24
17	ms14-6	Loss of extraction steam to feedwater heaters	10	no trip	20	unassured
18		Loss of air pressure to control rod drive hydraulic control units				
	rd13	- 100 % severity	10	12	12	33
	rd13_2	- 60 % severity	10	14	14	89
19	rp05tc01	Main turbine trip followed by reactor protection system circuit failure	6	27	7	57
20	rp05ac1	Main turbine trip followed by reactor protection system failure of alternative rod insertion	6	49	8	63
21	rr05	Recirculation pump shaft seizure	10	no trip	12	29
22	rr10	Recirculation pump speed feedback signal failure	5	no trip	17	unassured
23		Recirculation loop rupture				
	rr15a	- 100% severity (LOCA)	5	8	6	48
	rr15a_3	- 30% severity	5	7	6	62
24		Coolant leakage inside primary containment				
	rr30	- 100% severity	5	24	23	31
	rr30_2	- 60% severity	5	36	25	36
	rr30_3	- 30% severity	5	65	21	65
25	rx01	Fuel cladding (30%) failure	10	no trip	12	unassured

large, i.e., $\varepsilon_i > 0.15$ for all i, but the diagnosis is correct. After 48 seconds, the error-measured outputs indicate that the abnormal condition detected is assured to be the indicated transient since the error bound is small. In some cases, for example in Figure 5 of the transient fw09a, the outputs are validated immediately after the inconclusive period, without passing through the unassured period.

An additional advantage of EESA can be seen in transients ms14-6, rr10, and rx01 listed in Table III. For example, Figure 6 shows that the estimated error bounds except for the second node are too large to validate the diagnoses for the transient condition period after the normal operation period. As discussed in the case of the sine function mapping, the high error bounds mean that advisor F was not able to distinguish this particular transient from other transients for sure. This explanation is confirmed by the fact that the numbers of the training patterns pertaining to the transients ms14-6, rr10, and rx01 in L are only 4, 3, and 3 patterns, respectively. In other words, the advisor was not trained on sufficient data to have the necessary confidence in its diagnosis. Note that a typical recall root mean square (RMS) error cannot provide this information.

5. CONCLUSIONS

This paper presents a new error-bound prediction scheme called EESA that provides error bounds on the output obtained from an ANN in order to validate the ANN output. The experimental results discussed demonstrate that EESA provides useful error estimations that can be used to validate the outputs from ANN models. Our EESA scheme can be applied to a wide variety of applications. In addition, high error bounds estimated by EESA indicate that the ANN system needs more training data.

ACKNOWLEDGMENTS

This work was made possible by the generous support of the United States Department of Energy under Special Research Grant No. DEFG02-92ER75700, entitled "Neural Network Recognition of Nuclear Power Plant Transients," and the Iowa Electric Light and Power Company who provided the simulated data. Their support does not however constitute an endorsement of the views expressed in this paper.

REFERENCES

Bartlett, E. B. 1994. Dynamic node architecture learning: an information theoretic approach. *Neural Networks* 7, 129-140.

Bartlett, E. B., and Kim, K. 1993. Error bounds on the output of artificial neural networks. *Transactions of American Nuclear Society* 69, 197-199.

Bartlett, E. B. 1993. *Neural Network Recognition of Nuclear Power Plant Transients.* Annual Report to U. S. Department of Energy, DOE/ER/75700-1.

Bartlett, E. B. 1992. Analysis of chaotic population dynamics using artificial neural networks. *Chaos, Solution, and Fractals: Applications in Science and Engineering* 1 (5), 413-421.

Bartlett, E. B., and Kim, K. 1992. *Nuclear power plant diagnostics with artificial neural networks.* Final Phase 1 Report to U. S. Nuclear Regulatory Commission. Subcontracted with NETROLOGIC.

Bartlett, E. B., and Uhrig, R. E. 1992. Nuclear power plant status diagnostics using an artificial neural network. *Nuclear Technology* 97, 272-281.

Bhat, N., and McAvoy, T. J. 1990. Use of neural nets for dynamic modeling and control of chemical process systems. *Computers Chem. Engng.* 14, 573-583.

Blum, E. K., and Li, L. K. 1991. Approximation theory and feedforward networks. *Neural Networks* 4, 511-515.

Cybenko, G. 1989. Approximation by superposition of a sigmoidal function. *Mathematics of Control, Signals, and Systems* 2, 303-314.

Efron, B. 1982. The jacknife, the bootstrap, and other resampling plans, *CBMS-NSF Regional Conference Series in Applied Mathematics* 38, Society for Industrial and Applied Mathematics, Phildelphia, Pa.

Geisser, S. 1975. The predictive sample reuse method with applications. *Journal of the American Statistical Association* 70, 320.

Hecht-Nielsen, R. 1990. *Neurocomputing*. Addison-Wesley, Reading, Mass.

Judd, J. S. 1990. *Neural network design and the complexity of learning*. The MIT Press, Cambridge, Mass.

Kim, K., and Bartlett, E. B. 1993. Error prediction for a nuclear power plant fault-diagnostic advisor using neural networks. *Nuclear Technology,* in press.

Kim, K., Aljundi, T. L., and Bartlett, E. B. 1992a. Nuclear power plant fault-diagnosis using artificial neural networks. In *Proceedings Intelligent Engineering Systems Through Artificial Neural Networks*, 2, 751-756, C. I. Dagli et al. (Eds.), ASME Press, New York.

Kim, K., Aljundi, T. L., and Bartlett, E. B. 1992b. Confirmation of artificial neural networks: Nuclear power plant fault diagnostics. *Transactions of American Nuclear Society* 66, 112-114.

Kurkova, V. 1992. Kolmogorov's theorem and multilayer neural networks. *Neural Networks* 5, 501-506.

Lapades, A., and Farber, R. 1987. *Nonlinear signal processing using neural networks: prediction and system modeling.* Los Alamos National Laboratory Technical Report LA-UR-87-2662.

Leonard, J. A., Kramer, M. A., and Ungar, L. H. 1992. A neural network architecture that computes its own reliability. *Computers Chem. Engng.* 16, 819-835.

Li, K. 1985. From Stein's unbiased risk estimates to the method of generalized cross-validation. *The Annals of Statistics* 13, 1352.

Lippmann, L. P. 1987. An introduction to computing with neural nets. *IEEE Acoustics Speech and Signal Processing Magazine* 4, 4-22.

Miller, W. T., Sutton, R. S., and Werbos, P. J. (Eds.) 1990. *Neural Networks for Control.* MIT Press. Cambridge, Mass.

Narendra, K. S., and Parthasarathy, K. 1990. Identification and control of dynamic systems using neural networks. *IEEE Transaction on Neural Networks* 1 (1), 4-26.

Parzen. E. 1962. On estimation of a probability density function and mode. *Ann. Math. Statist.* 33, 1065-1076.

Rumelhart, D. E., McClelland, J. L., and the PDP Research Group. 1986. *Parallel distributed processing: Exploration in the microstructure of cognition.* Vols. 1 & 2, MIT Press, Cambridge, Mass.

Sankoff, D., Abel, Y., Cenergren, R. J., and Gray, M. W. 1987. Supercomputing for molecular cladistics. *Proceedings of the First Conference of the International Federation of Classification Societies* 1, 385-394.

Stone, M. 1974. Cross-validatory choice and assessment of statistical predictions. *Journal of Royal Statistical Society Series* B36, 111-147.

Stone, M. 1977. Asymptotics for and against cross-validation. *Biometrica* 64 , 29-35.

Upadhyaya, B. R., and Eryurek, E. 1992. Application of neural networks for sensor validation and plant monitoring. *Nuclear Technology* 97, 170-176.

Uhrig, R. E. 1989. Use of neural networks in nuclear power plant diagnostics. *Proc. Int. Conf. on Availability Improvements in Nuclear Power Plant*, 310-315 Madrid, Spain.

Venkatasubramanian, V., and Chan, K. 1989. A neural network methodology for process fault diagnosis. *American Institute of Chemical Engineers Journal* 35(12), 1993-2002.

Vest, D., Hunt, C., and Berchenbriter, D. 1991-1994. Personal discussion, data collection and correspondence with Duane Arnold Energy Center simulator complex employees, Iowa Electric Light and Power Company, Palo, Ia.

Weiss, S. M., and Kulikowski, C. A. 1991. *Computer Systems that Learn.* Morgan Kaufmann, San Mateo, Calif.

Welch, R. M., Sengupta, S. K., Goroch, A. K., Rabindra, P, Rangaraj, N., and Navar, M. S. 1992. Polar cloud and surface classification using AVHRR imagery: An intercomparison of methods. *Journal of Applied Meteorology* 31, 405-420.

Wildberger, A. M. 1994. Alleviating the opacity of neural networks. To be presented at the *IEEE World congress on Computational Intelligence*, June 26- July 2, 1994, Orlando, Fla.

Wolpert, D. H. 1992. Stacked generalization. *Neural Networks* 5, 241-259.

Wolpert, D. H. 1990. A mathematical theory of generalization: Part I and part II. *Complex Systems* 4, 151-249.

Wilf, H. S. 1986. *Algorithms and complexity.* Prentice Hall, Englewood Cliffs, NJ.

Zhang, X., Mesirov, J. P., and Waltz, D. L. 1992. Hybrid system for prediction for protein secondary structure prediction. *Journal of Molecular Biology* 225, 1049-1063.

PAPER III: NUCLEAR POWER PLANT FAULT DIAGNOSIS USING NEURAL NETWORKS WITH ERROR ESTIMATION BY SERIES ASSOCIATION

Nuclear Power Plant Fault Diagnosis Using Neural Networks with Error Estimation by Series Association

Keehoon Kim
Eric B. Bartlett

Nuclear Engineering Program
Department of Mechanical Engineering
Iowa State University
Ames, Iowa 50011

This manuscript has been submitted for publication to IEEE Transactions on Nuclear Science.

ABSTRACT

This paper presents a new error estimation scheme called error estimation by series association (EESA) for the reliability assessment of nuclear power plant (NPP) fault-diagnostics using artificial neural networks (ANNs). The EESA scheme provides estimated errors on the diagnosis obtained from an ANN NPP fault-diagnostic advisor in order to help validate its diagnosis. The data used in this work contains 25 simulated transients for the Duane Arnold Energy Center nuclear power station ranging from a main steam line break to an anticipated transient without scram (ATWS) condition. The results of the EESA implementation of the data demonstrate its capability to help validate and verify the fault-diagnostic advisor. EESA can also help to reduce the computational difficulties of the error estimation procedure. This work has shown that the fault diagnostic advisor developed by using ANNs with EESA is effective at providing proper diagnoses with predicted errors for all 25 transients analyzed at various severity levels even when the transients are degraded by noise.

1. INTRODUCTION

Artificial neural networks (ANNs) are being developed to monitor and control nuclear power plant (NPP) systems. ANN applications to NPP systems have been investigated in such areas as sensor validation [1], plant component monitoring [2-4], reactor parameter prediction [5-7], system control [8], and fault-diagnostics [9-12]. In these applications, however, the output of the ANNs used is implicitly assumed to be reliable. This assumption may be inappropriate for the output produced by an ANN presented with novel input data. Moreover, validation and verification of ANN outputs is crucial when the appropriate performance of the ANN is required for the safe operation of the plant. For example, the diagnosis provided by an ANN fault-diagnostic advisor must be assured because a faulty diagnosis could mislead plant personnel into taking incorrect or inappropriate corrective actions.

Kim, Aljundi and Bartlett [13,14] and Kim and Bartlett [15] have addressed validation and verification of the diagnoses obtained from an ANN NPP fault-diagnostic advisor by estimating error bounds on the diagnoses. The error-bound estimation discussed in our earlier papers applied a stacking procedure that originates from cross validation in nonparametric statistics [16-19]. Wolpert [20] conceptualized the stacked generalization technique in order to improve the accuracy of ANN generalization. The stacking procedure provides error information by repeatedly training an ANN on different subsets of the available training data and then testing it on the remainder of the data. The error information obtained by tabulating the responses of the ANN to the novel data constitutes new information, and this new information is used to train another ANN. This ANN, called the error predictor network, estimates the errors on the ANN advisor that is trained on the entirety of the training data. These estimated errors are then used to provide reliability information about the fault-diagnostic advisor's diagnosis.

There are, however, difficulties in the implementation of the stacking procedure to NPP fault-diagnostics [21]. First, the computational complexity of the stacking procedure increases with the number of partitions in the learning set. Minimizing the number of partitions is therefore an important part of applying the stacking procedure. Kim and

Bartlett [15] have developed a modified bootstrap partition criterion (MBPC) and a bootstrap partition criterion (BPC) that reduce the computational complexity of the procedure by reducing the number of partitions. These criteria have advantages over the cross validation partition criterion (CVPC) [20]. Second, the dimension of the input space of the ANN error predictor is doubled in comparison to that of the ANN advisor. The reason is that the stacking procedure of Wolpert requires an additional input vector, which is of the same dimension as the input space of the advisor. The doubling of the input dimension may cause considerable training difficulties when the number of the input variables of a system is large [22,23]. We have developed a new stacking procedure called error estimation by series association (EESA) that reduces the input dimensionality of the ANN error predictor. EESA is performed by feeding the output of the ANN advisor into the ANN error predictor. In this paper, an NPP fault-diagnostic system that provides error-measured diagnoses for novel symptoms is developed by implementing EESA. Data used for this research were collected at Duane Arnold Energy Center (DAEC) training simulator [24].

In addition, we investigate the noise tolerance of our ANN advisor and error prediction system. Noise or corrupted signals can originate from many sources in an NPP. We show that this degraded data can be fed directly into the fault-diagnostic system. The degraded information causes the fault-diagnostic system to deviate only slightly from its desired behavior. In this paper, various forms of artificially generated noise are used for the performance test of the system developed.

2. THE NUCLEAR POWER PLANT FAULT-DIAGNOSTIC ADVISOR

Artificial neural networks are computer algorithms that are motivated by biological neural systems. ANNs consist of highly interconnected processing elements called neurons or nodes that produce output signals on the basis of weighted sums of the input signals they receive [25,26]. Figure 1 shows a typical ANN that has three layers of neurons: the input layer, the hidden layer, and the output layer. Input signals can originate from other neurons or inputs. Output signals either become the input signals for other neurons or the ANN output. During training, an ANN is presented with k examples from a learning or training set called L of known input-output patterns, $\{(x_j, y_j) \mid y_j = f(x_j) ; 1 \le j \le k\}$. Here f is the desired function to be modeled by the ANN. Each of these input-output patterns consists of m inputs and n outputs, i.e., $x_i \in \mathbf{R}^m$ and $y_i \in \mathbf{R}^n$. When one input pattern such as x_j is presented to the ANN via the input layer, the input pattern is fed through the neurons in the hidden and output layers to generate a corresponding output pattern y_j', which is the ANN estimate of y_j. The weighted sum of the neuron's inputs is processed through a transfer function to produce an output signal. This general activation process in a neuron is also represented in Figure 1. The ANN is trained by repetitious presentation of the training set L and adjustment of the interneural connection weights so that the output signal y_j' converges to y_j [27]. These interneural weights are represented by the lines connecting the neurons in Figure 1. Although there are many methods for obtaining convergence, backpropagation [25,27], which is relatively simple, straightforward, and very useful, is employed in this paper.

ANNs are mathematical generalizers since they infer parent functions from sets of data [28-30]. Many other generalizers, such as memory-based reasoning schemes [31] and regularization theory [32], provide good results if the processes they model are well behaved. Unfortunately, many physical systems are not so well behaved because of their inherent nonlinearity. For example, NPP transient diagnosis is not easily accomplished with standard analytical methods. Recent work, however, has demonstrated that nonlinear modeling can be easily accomplished by ANNs [33-37]. The nonlinear abilities of ANNs offer a promising new approach to solving the NPP transient diagnostic problem [9,38,39].

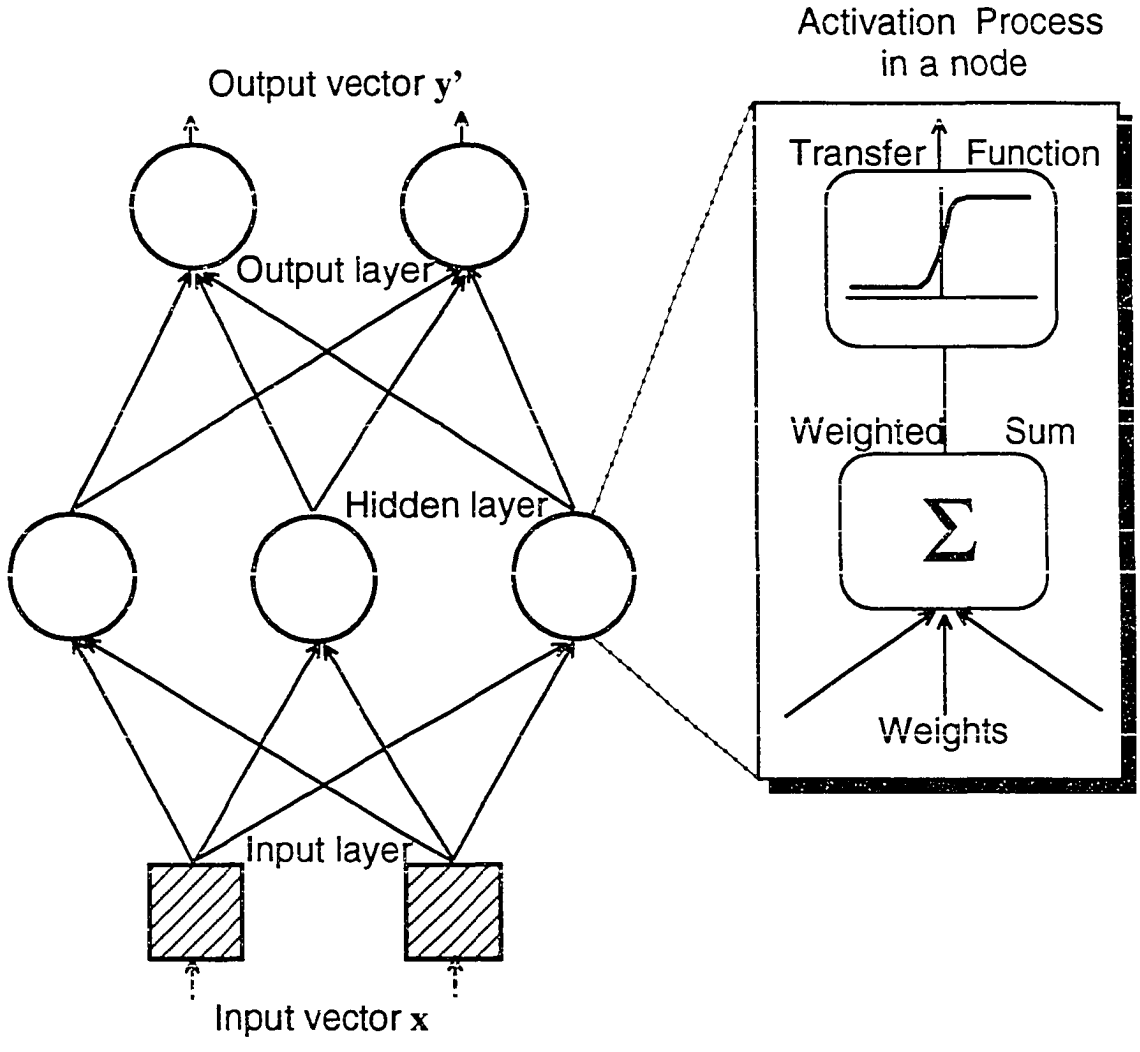

Figure 1. A typical architecture of a multi-layered feedforward ANN. The general activation process in a neuron is shown in the box.

3. ERROR ESTIMATION BY SERIES ASSOCIATION FOR NPP FAULT DIAGNOSIS

3.1. NPP Fault-Diagnostic Model Using ANNs

As a preliminary to our discussion of EESA, we define the following concepts. Let Q be the set of all NPP transients and normal symptoms and conditions to be identified by the fault-diagnostic advisor; Q ={q,u}, where q is a symptom of the plant condition and u is the correct diagnosis for the condition. An estimate û of the diagnosis u is provided by the advisor using an ANN called F. A symptom q is an input vector in $\mathbf{R}^m$ where m is the dimension of the input space or the number of monitored plant variables. An estimated diagnosis û is an output vector in $\mathbf{R}^n$ where n is the dimension of the output space of the advisor. The fault-diagnostic advisor F is trained on a subset of Q; $L \subset Q$ where L is chosen to be the learning set for F. Let $L = \{(x_j, y_j) \mid 1 \le j \le k\}$ where y_j is a known correct output corresponding to an input x_j. The learning set L consists of k patterns of input-output vectors, $x_j \in \mathbf{R}^m$ and $y_j \in \mathbf{R}^n$. When presented with a novel transient symptom $q \in Q - L$, the advisor F provides a diagnosis û for the symptom. Our goal is to estimate the error associated with the novel diagnosis û obtained from F in order to measure its reliability. An error bound ε associated with û is provided by another ANN called the error predictor network P trained on L'. EESA generates the new learning set L' for the ANN error predictor P. Designing the system F and P for an NPP diagnostic advisor is discussed in Section 4. The resultant output from the fault-diagnostic system is an output û plus or minus some predicted error, $\hat{u} \pm \varepsilon$, for a novel plant symptom q.

3.2. Modified Bootstrap Partition Criterion (MBPC)

The generation of the new learning set L' for P involves a stacking procedure that requires the learning set L be partitioned according to some partition criterion. For each partition i, L is divided into two disjoint subsets L_{i1} and L_{i2}. An ANN, designated as f, that has the same architecture as F is trained on the subset L_{i1} and then is tested on the subset

L_{i2}. The performance of f is measured in terms of the deviation, $\varepsilon = | g - y |$, between the actual and desired output where g is the output of f and y is the desired output for the input x in L_{i2}. The performance data set $\{\varepsilon\}$ contains new information about the relation between the untrained inputs and a generalized response of ANN f to those inputs. Wolpert [20] also appends the difference vector x′ from x to its nearest neighbor in L_{i1} to become additional input to the ANN error predictor P. For each partition, the performance data $\{(x,x'), \varepsilon\}$ constitute a new learning set L′ that is used to train the ANN error predictor P. Difficulties caused by adding the difference vector, $x' \in \mathbf{R}^m$, are resolved by us by employing EESA which adds the output vector $\hat{u}$ of the advisor F, $\hat{u} = F(x) \in \mathbf{R}^n$. The details of the discussion are given in Section 3.3.

Several different partition criteria can be used to generate L_{i1} and L_{i2}. These include the cross validation partition criterion (CVPC) [20], the bootstrap partition criterion (BPC) [15] and the modified bootstrap partition criterion (MBPC) [15]. In this paper, MBPC is applied to the NPP fault diagnostics to demonstrate the advantages of creating the partitions over the other criteria. Our MBPC reduces the computational requirements of the original stacking procedure without any trade off in the accuracy of the error estimation. For example, CVPC requires that the total number of partitions t is equal to the number of training patterns k in the learning set L. The computational burden of the process of training and testing ANN f increases with k since the process must be repeated k times in order to develop the learning set L′. When k is large, which is typical of NPP applications, the computational difficulty therefore increases dramatically. The total number of partitions t can be reduced by employing BPC, which reduces the number of partitions by selecting multiple elements for L_{i2} rather than one at a time as in CVPC. However, BPC may provide varying results since the multiple elements are randomly chosen. If L contains sufficient training data, this is not a problem. However, a sufficient training set may not always be available in every engineering application.

MBPC is a new extension of BPC where the L_{i2} elements are chosen systematically rather than randomly. In our fault-diagnostic problem, an operational transient is equivalent to a set of patterns represented by m plant variables in an m-dimensional feature space over time. This transient can be represented by distinct patterns in the subspace of the transient.

Moreover, a set of the patterns pertaining to the particular transient is also distinguished from other sets pertaining to other transients in each different subspace. The distinctness of patterns in each feature subspace forms a basis for classifying transients in the NPP diagnosis. Therefore, the learning set L consists of r separate groups pertaining to the r different transients. These r groups differ from each other such that the r patterns for L_{i2} can be selected from each transient group at the same time. This simultaneous selection can minimize the loss of information as well as the computational time required to estimate the errors.

MBPC requires two constraints. First, L_{i2} must be a set of r single patterns chosen from each transient group. In other words, for partition *i*, $L_{i2} = \{(x_l, y_l) \mid 1 \le l \le r\}$ where each pattern is randomly chosen from each group with the conditions $L_{m2} \cap L_{n2} = \emptyset$ for $m \neq n$ and $\cup_{i=1}^{t} L_{i2} = L$. Hence, the number of total partitions t can be reduced to $t \sim k/r$. Second, if the number of training patterns in a specific transient group is larger than r, a second constraint is imposed as follows. For a partition, a maximum of two patterns can be selected from the particular transient group whose number of training patterns is larger than r. The imposition of the second constraint may prevent a further increase in the size of the partition number. Another option for the second constraint is to apply CVPC to the excess patterns remaining after fulfilling the first constraint. This partial CVPC application can eliminate a potential disadvantage of the selection of two patterns with a trade in the slight increase of the number of total partitions. In this paper, MBPC is used for the NPP fault-diagnostic problem to demonstrate its advantages in creating partitions. MBPC can be applied to a learning set of any physical system that possesses the distinctness of grouped patterns in the feature space of the system.

3.3. Error Estimation by Series Association (EESA)

We have developed a new stacking procedure called EESA in order to resolve some of the difficulties that occur when employing the original stacking procedure of Wolpert. The first difficulty comes from the requirement that the additional input vector x′ must be appended to the input vector x in order to make L′. In other words, L′ requires each input

pattern to be comprised of a pair (x, x′) where x is an input pattern in the subset L_{i2} and x′ is a difference vector from the input x to its nearest pattern in the subset L_{i1}. Therefore, the dimension of the input space L′ is doubled to m + m, thus, $(x,x') \in \mathbf{R}^{m+m}$ where m is the dimension of the input space L. This expansion of the input dimension of L′ may cause difficulties when developing P. These difficulties include the escalation of the training requirements for P as the number of inputs increase [22,23]. For example, in the NPP fault-diagnostic problem we described herein, the dimension of the input space L′ will be 97 + 97 = 194 since we have m = 97 plant variables in L. When m is large, training P with 2m input nodes can be very difficult.

In addition to the doubling of the input dimension, a second problem arises due to the questionable appropriateness of adding the difference vector x′ to the input of F. The usefulness of the difference vector is based on the assumption that the error in F is strongly related to the difference vector from a given novel input to its nearest neighbor in L [20]. This assumption can be easily shown to be baseless as follows. Let a novel pattern q be very close to a training pattern x. A nearest neighbor computed in L_{i1} for the training pattern x from L_{i2} might differ from a nearest neighbor computed in L for the novel pattern q. Hence, the difference vector computed in L_{i1} for x can be substantially different from the difference vector for q despite the fact that it is very close to x. This inconsistency in the difference vector measurements may cause P to estimate the error bounds inaccurately. These inaccuracies are likely to be larger when multiple elements are chosen for L_{i2} as in BPC or MBPC. These aforementioned difficulties can be solved by implementing EESA as we will discuss below.

Error estimation by series association (EESA) is performed by feeding the output from the advisor F into the ANN error predictor P. This is done in place of using the input difference vector. The connection of the output of F to P by EESA allows the performances of F to be directly monitored by P. Figure 2 illustrates the structure of EESA.

The true errors in the outputs of F are caused not only by how much a given novel input differs from training data in L but also by how well F is trained. The stacking procedure of Wolpert cannot provide such information since the estimated error in this case is not dependent upon the output of F, i.e., it is only dependent on the input to F. On the other

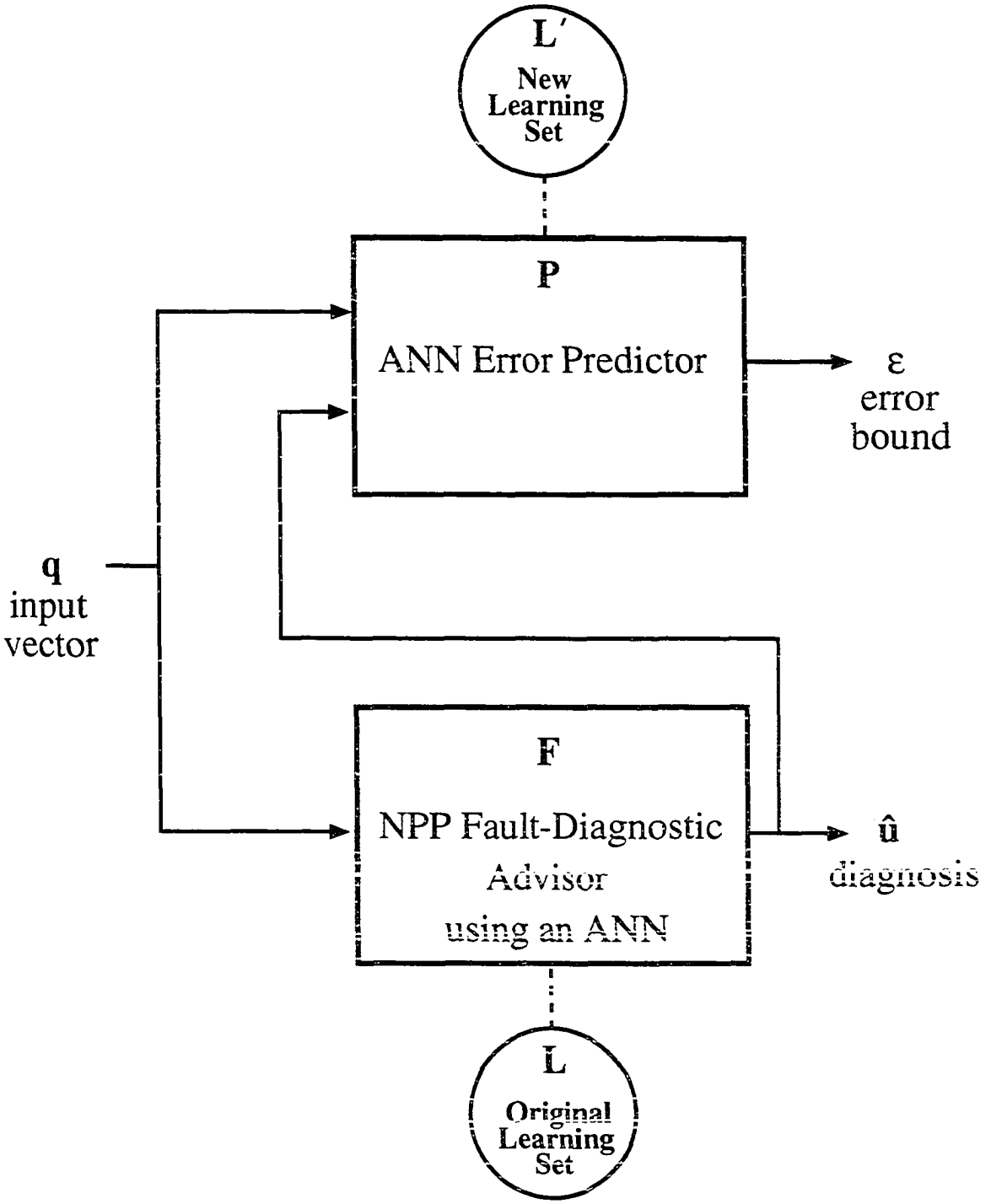

Figure 2. The structure of error estimation by series association (EESA). The ANN advisor F trained on L produces the output u, and P trained on L′ provides the error bound ε.

hand, EESA can address these issues since a novel input and its corresponding output from F are fed into P. In addition to the aforementioned advantages, EESA reduces the input space dimension of P to m + n. This is much smaller than m + m since the number of inputs is typically much greater than the number of outputs. The reduction in the input dimensionality of P reduces the training requirements considerably.

The following is the algorithm of EESA:

1. Create a partition i of the learning set L such that $L_{i2} = \{(\mathbf{x}_l, \mathbf{y}_l) \mid 1 \le l \le r,\ \mathbf{x}_l = (x_{l1}, x_{l2}, ..., x_{lm}) \in \mathbf{R}^m$ and $\mathbf{y}_l = (y_{l1}, y_{l2}, ..., y_{ln}) \in \mathbf{R}^n\}$ where r is the number of patterns for L_{i2} according to the chosen partition criterion, and $L_{i1} = L - L_{i2}$. Note that the ANN F is trained on the entirety of L.
2. Train ANN f having the same architecture of F on L_{i1}.
3. Compute the deviations $\{\varepsilon_l\}_i$, where $\varepsilon_l = (\varepsilon_{l1}, \varepsilon_{l2}, ..., \varepsilon_{ln})$, for the partition i by testing ANN f on the input patterns in L_{i2}. Note that $\varepsilon_{lj} = | f(x_l)_j - y_{lj} |$ where j=1 to n.
4. Compute the output $\hat{\mathbf{u}}_l$ for F for the input pattern $\mathbf{x}_l$, which is $\hat{\mathbf{u}}_l = F(\mathbf{x}_l) \in \mathbf{R}^n$.
5. Save $(\mathbf{x}_l, \hat{\mathbf{u}}_l) \in \mathbf{R}^{m+n}$ and $\varepsilon_l \in \mathbf{R}^n$, as new data patterns of the new learning set L'.
6. Repeat steps 2 through 5 for each of the partitions of L.
7. Train P on $L' = \{ (\mathbf{x}_v, \hat{\mathbf{u}}_v), \varepsilon_v) \mid 1 \le v \le k\}$ where k is the total number of the learning set L.

4. METHOD OF SOLUTIONS

4.1. Data Description

In this paper EESA is applied to an NPP transient diagnostics problem. The data was obtained from the Duane Arnold Energy Center (DAEC) training simulator, owned by Iowa Electric Light and Power Company [24]. DAEC is a boiling water reactor (BWR) plant that provides 540 MWe. The simulated data contains no noise.

A total of 25 distinct transients were simulated for this work. Some of the transients were collected at different severities so that the NPP fault-diagnostic advisor F can be designed to diagnose the transients independent of their severities. Because the simulations were performed at various severities, the transients collected include a total of 33 different scenarios. these scenarios are listed in Table I. The data include, for example, the transient "ms04a", main steam line rupture outside primary containment. This transient was simulated at three different severities, 100%, 60%, and 30%. The severity of this transient specifies the size of the sheared portion of the main steam line at the turbine inlet header.

Each data pattern used in developing the ANN NPP diagnostic advisor contains an input vector of 97 plant variables. These vectors were collected at intervals of one second for a period of three to ten minutes. Note that this time snap shot, or single time slice, of data does not include temporal information. The main advantage of the single time step approach is simplicity of training and execution irrespective of the temporal trends of a transient. The advisor F can therefore diagnose transients at the very instant a plant operational symptom is presented to it because F does not need to observe trends or temporal variation. The disadvantage of the single time step is that F loses temporal information that may improve the diagnose accuracy. This temporal information however was not needed for our work. The 97 plant variables used are tabulated in Table II. The data for each transient is divided into two parts; The first part is the normal operating data, followed by the second part for the abnormal transient state after the transient onset.

The 25 transient conditions including the normal steady-state operating conditions and their associated outputs constitute the learning set L for advisor F. This learning set L

Table I. List of the 25 transients with the scenario codes and designated output codes.

No	Scenario Code	Transient Description	Output Code
1	ad05	Spurious automatic depressurization system actuation	0.9 0.1 0.1 0.1 0.1
2	cu10	Reactor water clean-up coolant leakage	0.1 0.1 0.1 0.9 0.1
3	cu10gp5	Reactor water clean-up coolant leakage with failure of Group 5 isolation valves	0.1 0.1 0.9 0.9 0.9
4	fw02a	Main condensate pump A trip	0.1 0.9 0.9 0.1 0.9
5	fw08-6	Feedback heater tube leak	0.1 0.1 0.1 0.1 0.9
6	fw09a	Reactor feedwater pump trip due to spurious trip signal	0.9 0.9 0.1 0.1 0.1
7	fw12c0	Feedwater regulator valve controller stuck closed	0.9 0.1 0.9 0.1 0.1
8	fw12c1	Feedwater regulator valve controller stuck open	0.9 0.1 0.1 0.9 0.1
9	fw17a	Main feedwater line break inside primary containment	0.9 0.1 0.1 0.1 0.9
10	fw18a	Main feedwater line break outside primary containment	0.1 0.9 0.9 0.1 0.1
11	ia01	Complete loss of instrumentation air from air receiver	0.1 0.9 0.1 0.1 0.9
12	ic14scra	Spurious reactor trip without operator action	0.1 0.1 0.9 0.9 0.1
13	mc01a	Main circulating water pump trip	0.1 0.1 0.9 0.1 0.9
14	mc04a mc04a_2 mc04a_3	Main condenser air inleakage - 100% severity - 60% severity - 30% severity	0.1 0.1 0.1 0.9 0.9
15	ms02	RCIC line break inside primary containment	0.9 0.9 0.9 0.1 0.1
16	ms04a ms04a_2 ms04a_3	Main steam line (MSL) rupture outside primary containment - 100% severity: 100% double ended shear - 60% severity: 60% double ended shear - 30% severity: 30% double ended shear	0.9 0.9 0.1 0.9 0.1
17	ms14-6	Loss of extraction steam to feedwater heaters	0.9 0.9 0.1 0.1 0.9

Table I. (continued)

No	Scenario Code	Transient Description	Output Code
18	rd13 rd13_2	Loss of air pressure to control rod drive (CRD) hydraulic control units (HCU) - 100 % severity - 60 % severity	0.9 0.1 0.9 0.9 0.1
19	rp05tc01	Main turbine trip followed by reactor protection system circuit failure	0.9 0.1 0.9 0.1 0.9
20	rp05act1	Main turbine trip followed by reactor protection system circuit failure together with failure of ARI (alternate rod insertion)	0.9 0.1 0.1 0.9 0.9
21	rr05	Recirculation pump shaft seizure	0.1 0.9 0.9 0.9 0.1
22	rr10	Recirculation pump speed feedback signal failure caused by speed circuit control failure	0.1 0.9 0.1 0.9 0.9
23	rr15a rr15a_3	Recirculation loop A rupture – 100% double ended shear (Design basis LOCA) - 30% double ended shear	0.1 0.1 0.9 0.1 0.1
24	rr30 rr30_2 rr30_3	Coolant leakage inside primary containment - 100% double ended shear - 60% double ended shear - 30% double ended shear	0.1 0.9 0.1 0.1 0.1
25	rx01	Fuel cladding (30%) failure	0.9 0.9 0.9 0.9 0.1
Normal Operation (before transient onset)			0.1 0.1 0.1 0.1 0.1

Table II. The 97 plant variables used to trend the 25 transients used in the second example. Note that there are 33 scenarios and that the data was collected at intervals of one second for three to six minutes. The 97 variables are used as inputs to the ANN advisor F.

No	Variable Designation	Description	Min. value	Max. value	Unit
1	A041	Local power range monitor 16-25 flux level B	0.0	125.0	% power
2	A091	Source range monitor channel B	0.0	100.0	%
3	B000	Average power range monitor A Flux level	0.0	125.0	% power
4	B012	Reactor total core flow	0.0	60.0	Mlb/hr
5	B013	Reactor core pressure-differential	0.0	30.0	psid
6	B014	Control rod drive system flow	0.0	0.025	Mlb/hr
7	B015	Reactor feedwater loop A flow	0.0	4.0	Mlb/hr
8	B016	Reactor feedwater loop B flow	0.0	4.0	Mlb/hr
9	B017	Cleanup system flow	0.0	0.07691	Mlb/hr
10	B022	Total steam flow	0.0	8.0	Mlb/hr
11	B023	Cleanup system inlet temperature	0.0	755.0	Deg F
12	B024	Cleanup system outlet temperature	0.0	600.0	Deg F
13	B026	Recirculation loop A1 drive flow	0.0	15.1	Mlb/hr
14	B028	Recirculation loop B1 drive flow	0.0	15.1	Mlb/hr
15	B030	Reactor feedwater channel A1 temperature	280.0	430.0	Deg F
16	B032	Reactor feedwater channel B1 temperature	280.0	430.0	Deg F
17	B034	Recirculation loop A1 inlet temperature	260.0	580.0	Deg F
18	B036	Recirculation loop B1 inlet temperature	260.0	580.0	Deg F
19	B038	Recirculation A wide range temperature	50.4	789.6	Deg F
20	B039	Recirculation B wide range temperature	50.4	789.6	Deg F
21	B061	Reactor coolant total jet pumps 1-8 flow B	0.0	36.7	Mlb/hr
22	B062	Reactor coolant total jet pumps 9-16 flow A	0.0	36.7	Mlb/hr
23	B063	Reactor coolant total outlet steam flow A	0.0	2.0	Mlb/hr
24	B064	Reactor coolant total outlet steam flow B	0.0	2.0	Mlb/hr
25	B065	Reactor coolant total outlet steam flow C	0.0	2.0	Mlb/hr
26	B066	Reactor coolant total outlet steam flow D	0.0	2.0	Mlb/hr
27	B079	Reactor recirculation pump A motor vibration	0.0	10.0	MILS
28	B080	Reactor recirculation pump B motor vibration	0.0	10.0	MILS
29	B083	Control rod drive cooling-water differential pressure	0.0	500.0	dpsi
30	B084	Control rod drive cooling-water differential pressure	0.0	60.0	dpsi
31	B085	Torus air temperature #1	0.0	500.0	Deg F
32	B086	Torus air temperature #2	0.0	500.0	Deg F
33	B087	Torus air temperature #3	0.0	500.0	Deg F
34	B088	Torus air temperature #4	0.0	500.0	Deg F

Table II. (continued)

No	Variable Designation	Description	Min. value	Max. value	Unit
35	B089	Drywell temperature azimuth 0 elevation 750	0.0	500.0	Deg F
36	B090	Drywell temperature azimuth 245 elevation 750	0.0	500.0	Deg F
37	B091	Drywell temperature azimuth 90 elevation 765	0.0	500.0	Deg F
38	B092	Drywell temperature azimuth 270 elevation 765	0.0	500.0	Deg F
39	B093	Drywell temperature azimuth 270 elevation 765	0.0	500.0	Deg F
40	B094	Drywell temperature azimuth 180 elevation 780	0.0	500.0	Deg F
41	B095	Drywell temperature azimuth 270 elevation 830	0.0	500.0	Deg F
42	B096	Drywell temperature center elevation 750	0.0	500.0	Deg F
43	B098	Torus water temperature	0.0	752.0	Deg F
44	B099	Torus water temperature	0.0	752.0	Deg F
45	B103	Drywell pressure	0.0	100.0	psia
46	B104	Torus pressure	0.0	100.0	psia
47	B105	Torus water level	-10.0	10.0	inch
48	B120	Torus radiation monitor A	-1.0	100.0	%
49	B121	Torus radiation monitor B	-1.0	100.0	%
50	B122	Reactor water level	158.0	218.0	inch
51	B124	Reactor water level	158.0	218.0	inch
52	B1257	Fuel zone level indication	-153.0	218.0	inch
53	B126	Reactor water level	158.0	458.0	inch
54	B127	Reactor vessel pressure	0.0	1200.0	psig
55	B128	Reactor vessel pressure	0.0	1200.0	psig
56	B129	Reactor vessel pressure	0.0	1500.0	psig
57	B130	Reactor vessel pressure	0.0	1500.0	psig
58	B137	Torus water level	1.5	16.0	ft
59	B138	Torus water level	1.5	16.0	ft
60	B150	Core spray A flow	-1767.8	5000.0	gpm
61	B151	Core spray B flow	-1767.8	5000.0	gpm
62	B160	Reactor core isolation cooling flow	-62.5	500.0	gpm
63	B161	High-pressure core injection flow	-437.5	3500.0	gpm
64	B162	Residual heat removal A flow	-75.0	15000.0	gpm
65	B163	Residual heat removal B flow	-75.0	150.0	gpm
66	B164	Drywell radiation monitor A	-1.0	100.0	%
67	B165	Drywell radiation monitor B	0.0	100.0	%
68	B166	Post-treat activity	0.0	100.0	%
69	B168	Pretreat activity	0.0	100.0	%
70	B171	Analyzer A - O_2 concentration	-1.25	10.0	%

Table II. (continued)

No	Variable Designation	Description	Min. value	Max. value	Unit
71	B172	Analyzer A - H_2 concentration	-1.25	10.0	%
72	B173	Analyzer B - O_2 concentration	-1.25	10.0	%
73	B174	Analyzer B - H_2 concentration	-1.25	10.0	%
74	B180	Clean-up system flow	0.0	200.0	gpm
75	B196	Reactor water level-fuel zone A	-153.0	218.0	inch
76	B197	Reactor water level-fuel zone B	-153.0	218.0	inch
77	B247	Turbine steam bypass	0.0	500.0	Deg F
78	B248	Turbine steam bypass	0.0	500.0	Deg F
79	E000	4160 V switch gear bus 1A1 A-B	0.0	5.25	KV
80	F004	Condensate pump A & B discharge pressure	0.0	600.0	psig
81	F005	Low-pressure condenser circulating water inlet temperature A	0.0	200.0	Deg F
82	F010	High-pressure condenser circulating water outlet temperature A	0.0	200.0	Deg F
83	F011	Low-pressure condenser circulating water pressure differential A	0.0	10.0	dpsi
84	F015	Circulating water pump A & B discharge pressure	0.0	100.0	psig
85	F018	Cooling tower A discharge water temperature	0.0	752.0	Deg F
86	F019	Cooling tower B discharge water temperature	0.0	752.0	Deg F
87	F040	1P-1A reactor feed pump suction pressure	0.0	600.0	psig
88	F041	1P-1B reactor feed pump suction pressure	0.0	600.0	psig
89	F042	1P-1A reactor feed pump discharge pressure	0.0	2000.0	psig
90	F043	1P-1B reactor feed pump discharge pressure	0.0	2000.0	psig
91	F044	Condensate total flow	0.0	8.0	Mlb/hr
92	F045	Condensate makeup flow	-10.0	100.0	Klb/H
93	F046	Condensate rejection flow	0.0	50.0	Klb/H
94	F064	Feedwater final pressure	0.0	2000.0	psig
95	G001	Generator gross watts	0.0	720.0	MWE
96	T039	Low-pressure condenser pressure	0.0	30.0	inHg
97	T040	High-pressure condenser pressure	0.0	30.0	inHg

contains 241 input-output patterns obtained by the procedures outlined by Bartlett and Uhrig [9]. Note that the number of the patterns in L is only about 3% out of the 8,782 patterns of the entire data set Q for the 25 transients based on the simulated 33 scenarios. The set L includes 25 initial conditions to account for the many normal operating modes of the plant. The remaining 216 input-output patterns correspond to abnormal conditions of the 33 scenarios. The learning set L is chosen in an iterative manner. First one pattern at the beginning and one pattern from the end of the ten simulated transients is selected to form the initial learning set. This initial learning set containing 50 input-output patterns is used to train the ANN advisor. The advisor is then recalled on all the patterns over the entire time period of the simulation for each of the 33 transients. The recall patterns producing the worst errors are added to the learning set. The process of training, recalling and adding patterns is repeated until most of undesirable, high recall error patterns disappear. Note that the patterns within a short period after transient onset are not added. This is because the plant variables change suddenly and dynamically for this short period such that some patterns are not uniquely defined.

4.2. Development of NPP Fault-Diagnostic Advisor F

The NPP fault-diagnostic advisor F for DAEC is established by training an ANN on the learning set L described in the previous section. The advisor F is a backpropagation ANN and is trained until a training root mean square (RMS) error of 0.05 is obtained. The ANN F has 97 input nodes each corresponding to the 97 plant variables, 45 nodes in the first hidden layer, 30 nodes in the second hidden layer, 10 nodes in the third hidden layer, and 5 nodes in the output layer (97-45-30-10-5). The five output nodes are used to distinguish each of the 25 transient conditions with a distinct 5-bit binary code as shown in Table I. Note that for a faster convergence, 0.1 was substituted for 0, and 0.9 was substituted for 1 in the binary codes. This substitution allows for quicker training without driving the output nodes into the saturation region of the nodal sigmoid transfer function [27]. The particular three-hidden-layer architecture was employed after attempting several different architectures.

4.3. Development of ANN Error Predictor P

In this investigation, MBPC was used for creating the partitions of L. Because L contains 25 distinct transients, there are 25 classification groups each one pertaining to a specific transient, i.e., r = 25. No transient group has the number of training patterns larger than r where r is 25. MBPC yields a total of 19 partitions, i.e., t = 19. Note that MBPC has significantly reduced the computational requirements when compared to that of CVPC where we would obtain t = 241. Another backpropagation ANN f having the same architecture (97-45-30-10-5) of the developed advisor F, was used in generating L′. For all 19 partitions, a total of 241 trios of x, û, and ε are acquired. Hence, L′ consists of these 241 trios. The ANN error predictor P using backpropagation was trained on L′ with the architecture of 102-30-10-5. This architecture was selected after several attempts to find the optimal architecture. The advantages of EESA can be appreciated in that the input space dimension of P has increased only by 5 not 97. This increase is considerably less than that of the stacking procedure without EESA.

4.4. Tests of F and P on Noisy Data

The fault-diagnostic system F and P, trained on computer-generated data with no noise, were tested by adding the artificially generated noise to Q and recalling the system on the noise-added Q. Gaussian and uniform noise were generated with different random seeds at different standard deviations for each distribution, for example, σ = 1%, 2%, 3%, and 4%. Results of this part of our investigation are discussed in Section 5.2.

5. RESULTS OF THE RESEARCH

5.1. Error-Measured Diagnosis

The results obtained from the NPP fault-diagnostic system by implementing EESA with MBPC are shown in Figures 3 to 6 and Table III. In the figures, the dot-dashed line represents the values of an output node of the advisor F. The solid lines above and below the dot-dashed line represent, respectively, the upper- and the lower- error bound estimated by P on each output of F. All the five outputs combined with the error bounds provide reliability information on a diagnosis given by F at the instant the transient symptom was presentation. The error-measured diagnosis is shown in Figures 3 and 6. Table III summarizes the results of F and P for all 33 scenarios. The fourth and fifth columns show transient onset time and the automatic reactor safety trip time, respectively. Note that the automatic reactor safety trip is based on many more monitored variables and is actuated when a certain variable goes out of range. No root cause diagnosis is given. The sixth column displays the time when the fault-diagnostic system detects an abnormal status of the plant with a deviation, ± 0.1, from the normal output values, 0.1 or 0.9. The last column shows the time when a diagnosis is validated with $\hat{u}_i - \varepsilon_i > 0.7$ for the designated output 0.9 or $\hat{u}_i + \varepsilon_i < 0.3$ for the output 0.1, for all i.

The ANN fault-diagnostic system detects an abnormal status of the plant very promptly after the onset of the transients so that operator can immediately recognize the deviations from a plant normal condition. However, the system's diagnosis is indefinite for a short period after the transient detection. This is because the plant input variables fluctuate abruptly and dynamically for this inconclusive period. The input patterns during the period do not form a basis for classifying transients because of the abrupt variations of the plant variables in the feature space, i.e., the input patterns are not coupled to the transient characteristics. Hence, L was selected to contain none of these data. After the inconclusive period passes, the fluctuations in the advisor F's outputs disappear and are followed by the unassured period during which time the error bounds on the diagnoses are large. During this time the diagnosis maybe correct. But, since the estimated errors are large, the diagnosis is

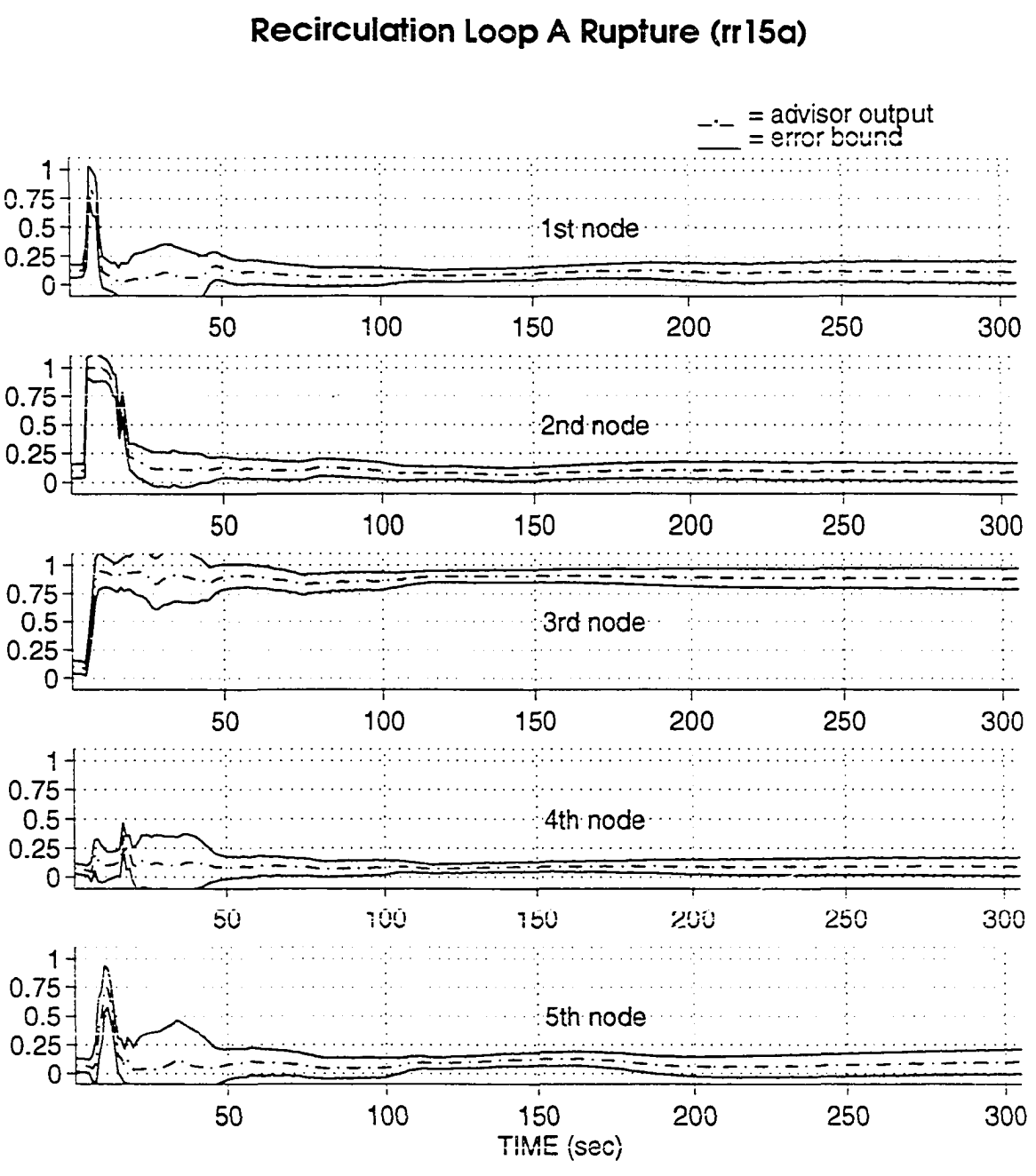

Figure 3. Diagnosis with the estimated error bounds for the recirculation loop rupture (rr15a) transient.

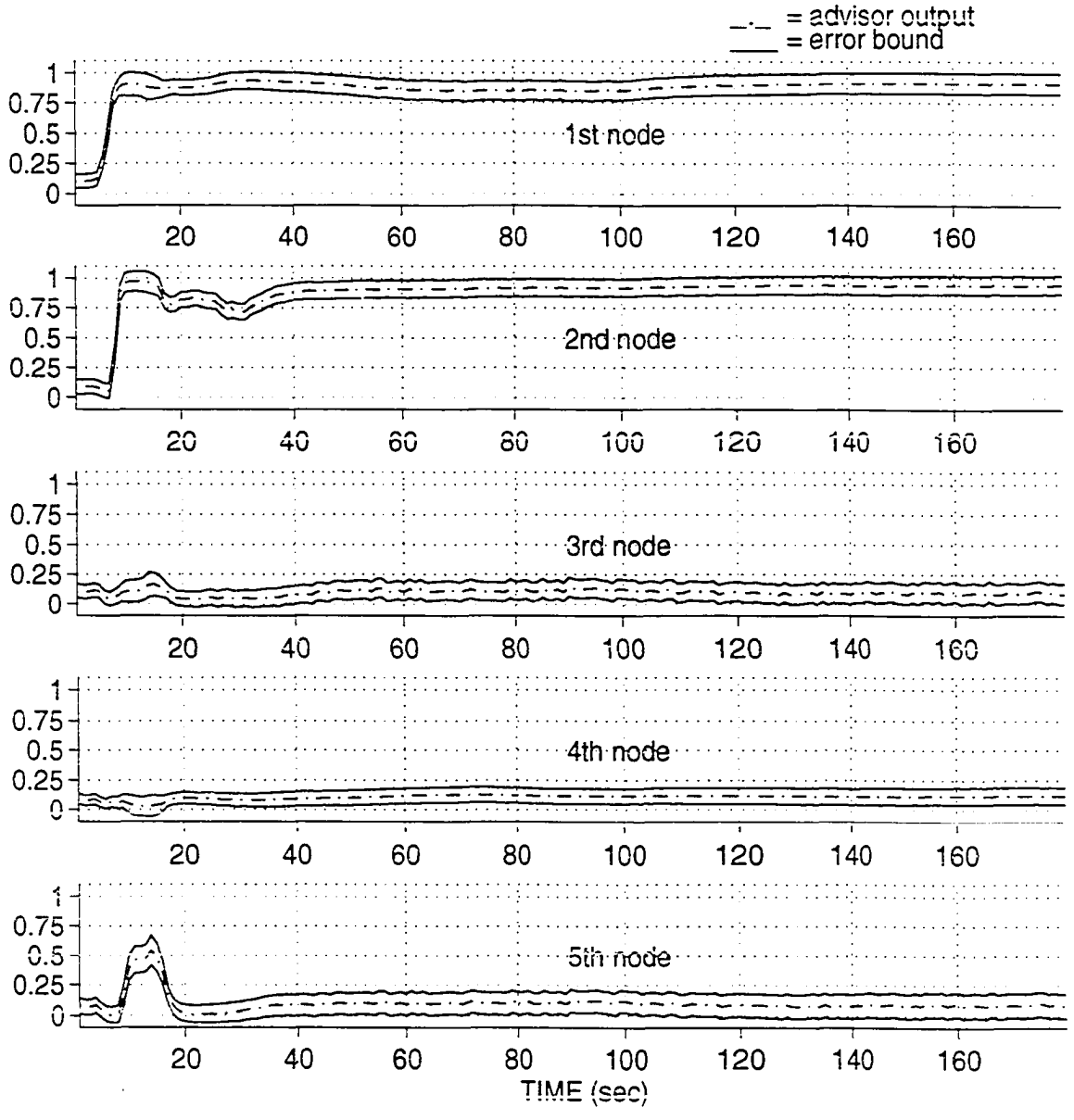

Figure 4. Diagnosis with estimated error bounds for the reactor feedwater pump trip due to spurious trip signal (fw09a) transient.

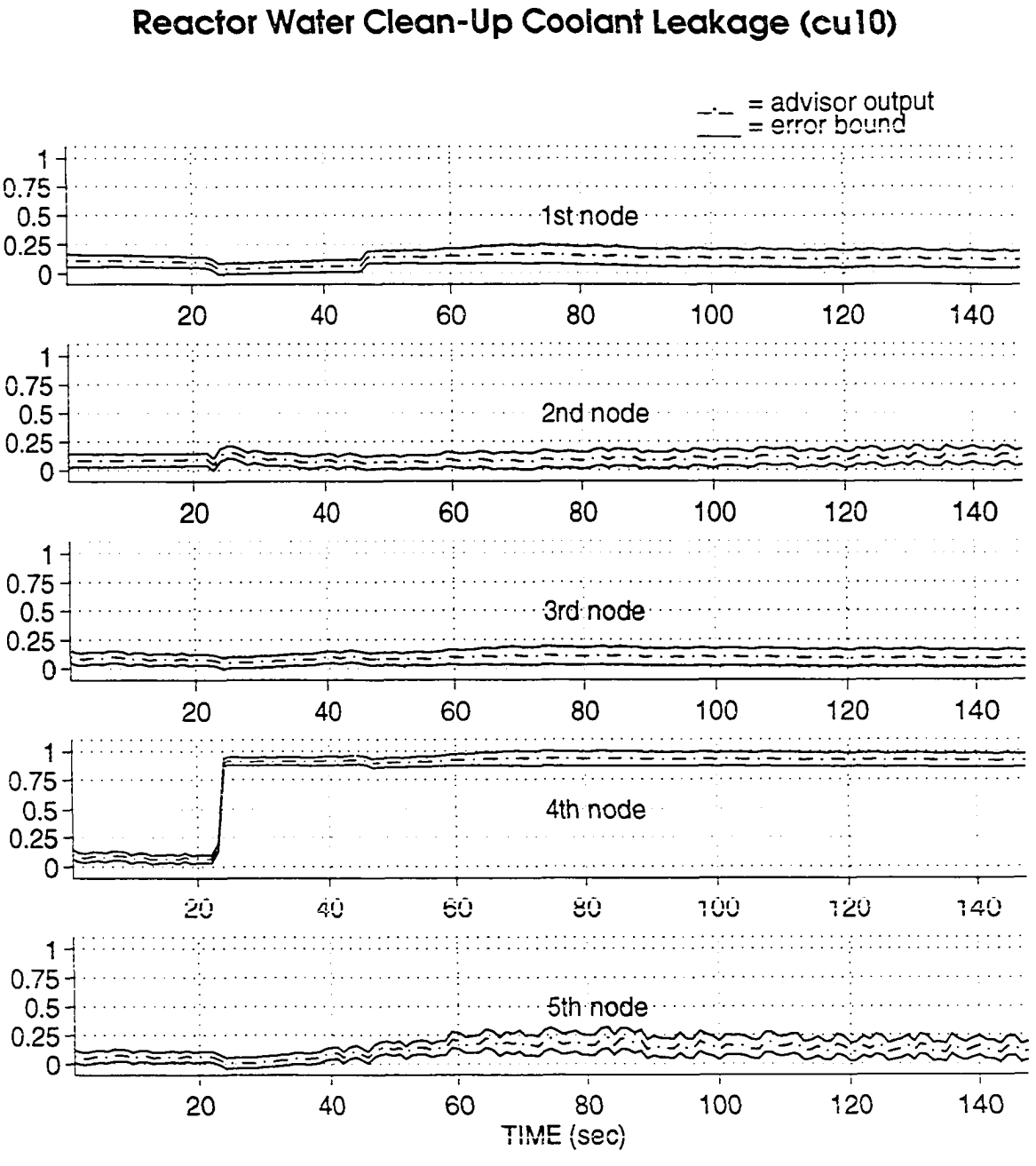

Figure 5. Diagnosis with estimated error bounds for the reactor water clean-up coolant leakage (cu10) transient.

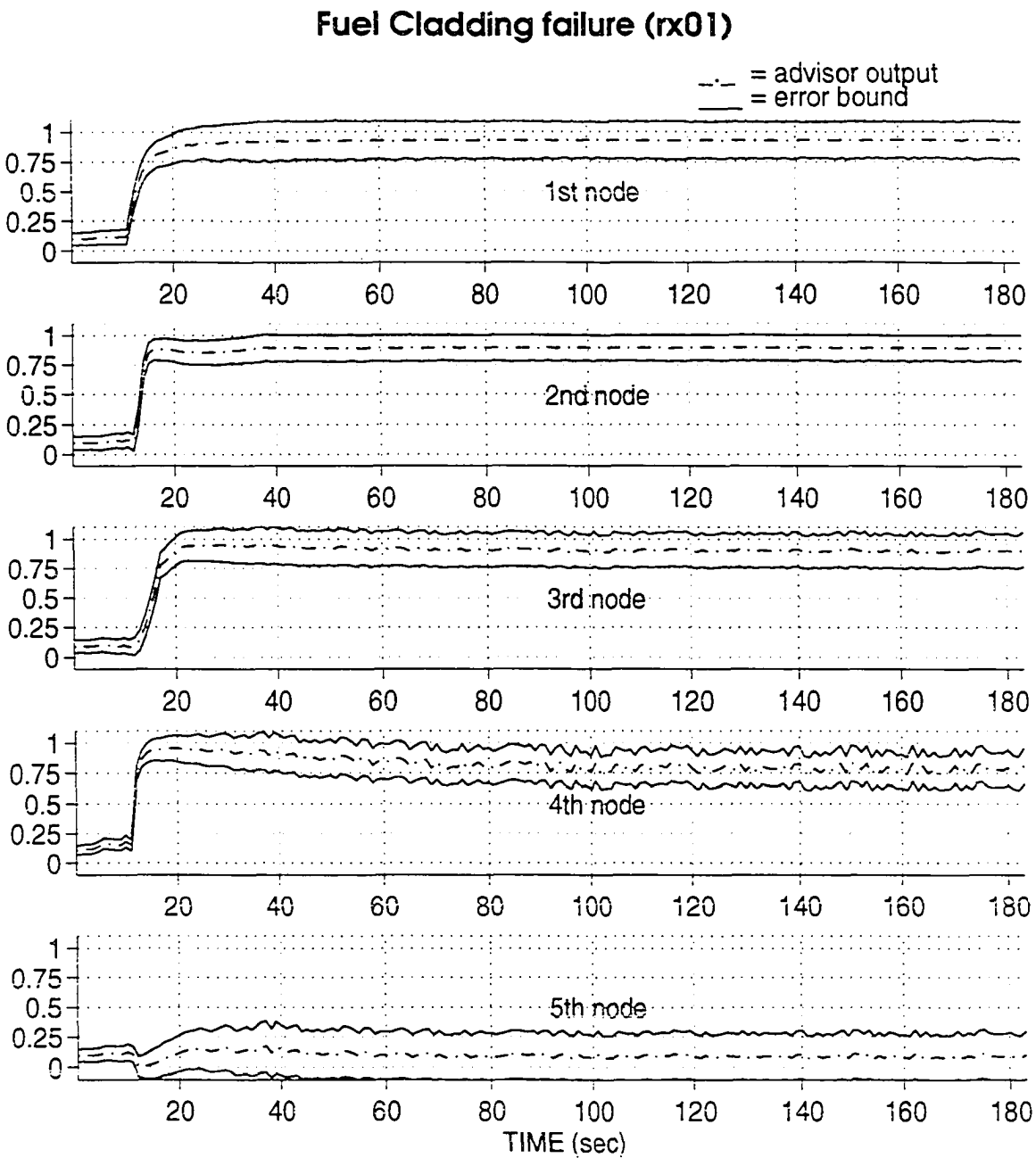

Figure 6. Diagnosis with estimated error bounds for the fuel cladding failure (rx01) transient.

Table III. Summary of the results of the fault-diagnostic system, the advisor F and the ANN error predictor P.

No	Scenario Code	Transient Description	Onset time (sec)	Safety trip time (sec)	Time of detecting abnormal plant status	Time of providing assured diagnosis
1	ad05	Spurious automatic depressurization system actuation	10	13	10	49
2	cu10	Reactor water clean-up coolant leakage	5	no trip	24	24
3	cu10gp5	Reactor water clean-up coolant leakage with failure of Group 5 isolation valves	6	51	7	48
4	fw02a	Main condensate pump A trip	6	504	10	28
5	fw08-6	Feedback heater tube leak	10	33	10	35
6	fw09a	Reactor feedwater pump trip due to spurious trip signal	5	no trip	6	17
7	fw12c0	Feedwater regulator valve controller stuck closed	5	16	7	47
8	fw12c1	Feedwater regulator valve controller stuck open	5	96	17	63
9	fw17a	Main feedwater line break inside primary containment	10	12	10	82
10	fw18a	Main feedwater line break outside primary containment	7	16	7	31
11	ia01	Complete loss of instrumentation air from air receiver	10	no trip	23	37
12	ic14scra	Spurious reactor trip without operator action	5	7	6	64
13	mc01a	Main circulating water pump trip	6	281	10	114
14		Main condenser air inleakage				
	mc04a	- 100% severity	10	46	17	44
	mc04a_2	- 60% severity	10	57	21	55
	mc04a_3	- 30% severity	10	69	21	63
15	ms02	RCIC line break inside primary containment	5	9	5	34

Table III. (continued)

No	Scenario Code	Transient Description	Onset time (sec)	Safety trip time (sec)	Time of detecting abnormal plant status	Time of obtaining assured diagnosis
16		Main steam line (MSL) rupture outside primary containment				
	ms04a	- 100% double ended shear	5	8	6	26
	ms04a_2	- 60% double ended shear	5	8	5	23
	ms04a_3	- 30% double ended shear	5	8	5	24
17	ms14-6	Loss of extraction steam to feedwater heaters	10	no trip	20	unassured
18		Loss of air pressure to control rod drive hydraulic control units				
	rd13	- 100 % severity	10	12	12	33
	rd13_2	- 60 % severity	10	14	14	89
19	rp05tc01	Main turbine trip followed by reactor protection system circuit failure	6	27	7	57
20	rp05ac1	Main turbine trip followed by reactor protection system failure of alternative rod insertion	6	49	8	63
21	rr05	Recirculation pump shaft seizure	10	no trip	12	29
22	rr10	Recirculation pump speed feedback signal failure	5	no trip	17	unassured
23		Recirculation loop A rupture				
	rr15a	- 100% severity (LOCA)	5	8	6	48
	rr15a_3	- 30% severity	5	7	6	62
24		Coolant leakage inside primary containment				
	rr30	- 100% severity	5	24	23	31
	rr30_2	- 60% severity	5	36	25	36
	rr30_3	- 30% severity	5	65	21	65
25	rx01	Fuel cladding (30%) failure	10	no trip	12	unassured

unreliable. This unassured period continues momently, and then the estimated error bounds become small and the diagnoses are then validated. For example, Figure 3 of the recirculation loop rupture at 100% severity (rr15a) shows the inconclusive period from 6 seconds to 18 seconds for which the outputs are indefinite, i.e., the values of fifth node are between 0.3 and 0.7. Note that we used 0.3 and 0.7 here as cutoff points and that other cutoff points such as 0.25 and 0.75 would yield slightly different results. The inconclusive period is followed by the unassured period from 19 seconds 47 seconds for which error bounds are large, i.e., $\varepsilon_i > 0.15$. Again, 0.15 is somewhat arbitrary. After 48 seconds, the error-measured outputs indicate that the abnormal condition detected is assured to be the indicated transient since the error bound is small. In some cases, for example in Figure 4, the outputs are validated immediately after the inconclusive period, without passing through the unassured period.

Another interesting example is shown in Figure 5, the reactor water clean-up leakage (cu10) scenario. The transient onset begins at 5 seconds. The error-measured diagnosis, however, indicates that the plant is in normal operational status from 6 seconds to 23 seconds even after the transient onset. This inconsistency can be explained by inspecting the input data for the period. The plant input variables seldom deviate from normal operational data except for the condensate rejection flow variable (variable no. 93). This variable changes only slightly until 23 seconds. Since the variations of this variable during the period are very small, the diagnosis displays a normal operational status for the period. The transient is detected and classified correctly at 24 seconds. Transients that show similar behaviors to the above example include ia01, mc04a, mc04a_2, mc04a_3, rr30, rr30_2, and rr30_3.

An additional advantage of EESA can be seen in transients ms14-6, rr10, and rx01 listed in Table III. For example, Figure 6 (rx01) shows that the estimated error bound for the fifth node is too large to validate the diagnoses for the transient condition period after the normal operation period. The high error bounds mean that the advisor was not able to distinguish this particular transient from other transients. This explanation is confirmed by the fact that the numbers of the training patterns pertaining to the transients ms14-6, rr10, and rx01 in L, are only 4 patterns, 3 patterns, and 3 patterns, respectively. In other words, the

advisor was not trained on sufficient data to have the necessary confidence in its diagnosis. The confidence in the transient diagnoses in these cases will be improved by adding more patterns delineating the features of the transients.

5.2. Performance Test With Noise

The fault-diagnostic system shows two kinds of responses to the added noise. First, the performance of the system for some transients is very robust and stable against noisy inputs. For example, Figures 7 to 9 of transient ad05 show that the performance is almost not affected by noise regardless of noise distributions and standard deviations. Other transients showing similar behavior include cu10gp, fw02a, fw08-6, fw12c0, fw18a, mc04a, mc04a_2, mc04a_3, ms02, rd13, rp05tc01, rr15a, and rr15a_3. Second, there are transients whose performance is degraded proportionally to the standard deviation of the added noise. Figure 10 of rx01 that was tested with Gaussian noise with a standard deviation of 3% of the normalized signal displays the substantial degradation of system performance. The 3% Gaussian noise to the inputs might be too large to be realistic because of the long tails of the Gaussian distribution. Noise sensitivity of the system in these transients can be greatly reduced by adding noise to L and then training F on the noisy L.

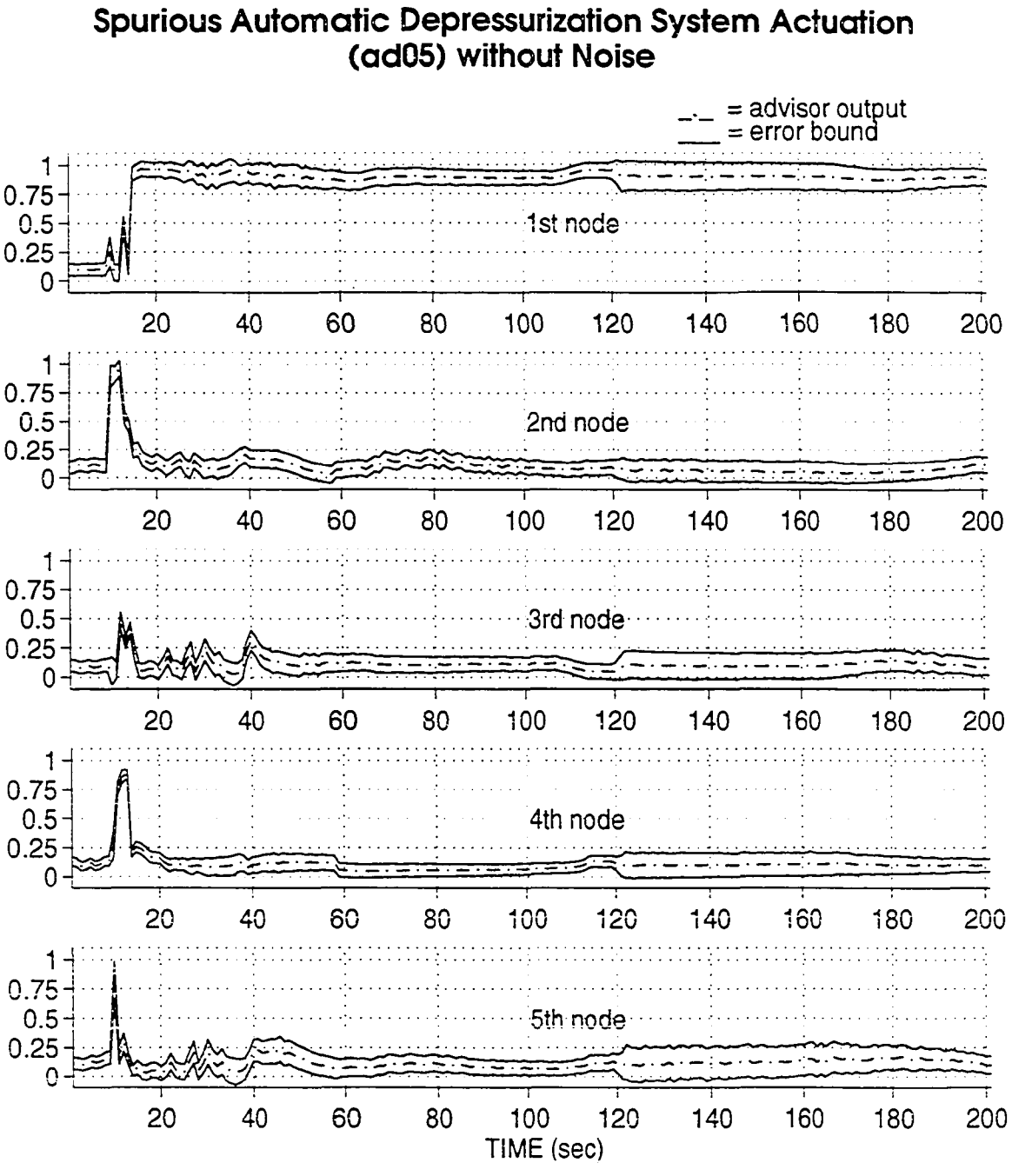

Figure 7. Diagnosis with estimated error bounds for the spurious automatic system actuation transient without added noise to the input data.

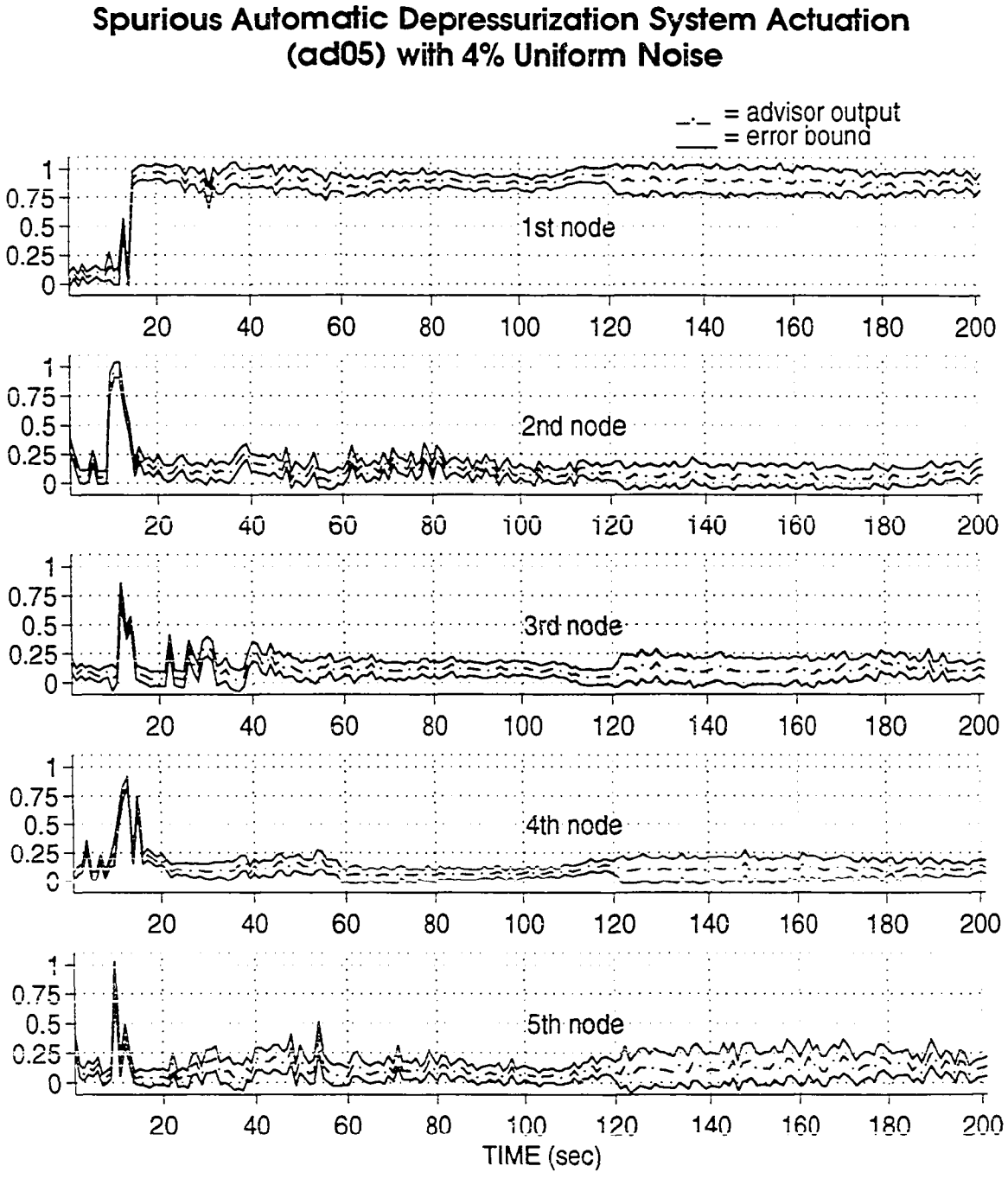

Figure 8. Diagnosis with estimated error bounds for the spurious automatic system actuation (ad05) transient with 4% uniform noise to the input data.

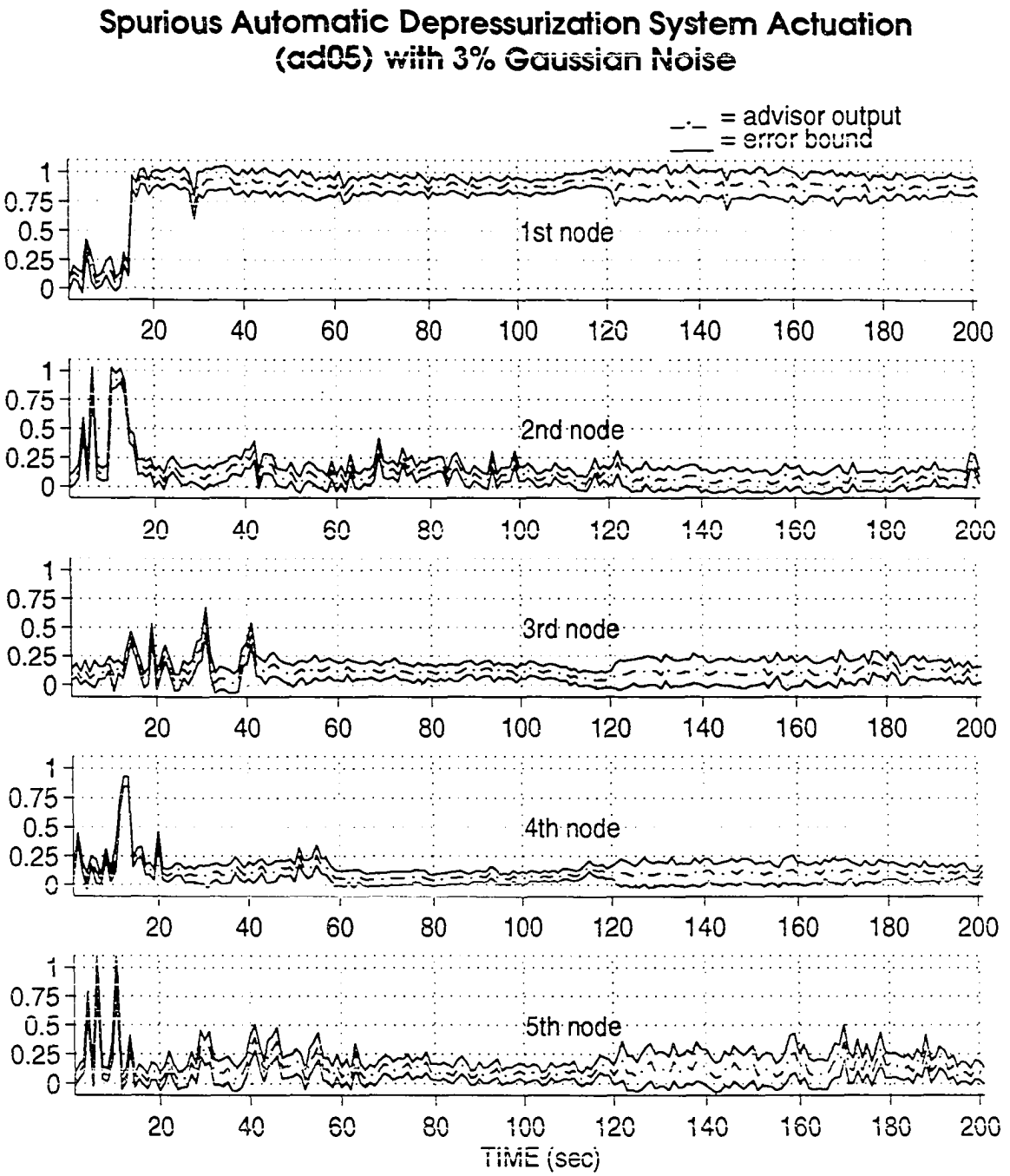

Figure 9. Diagnosis with estimated error bounds for the spurious automatic system actuation (ad05) transient with 3% Gaussian noise to the input data.

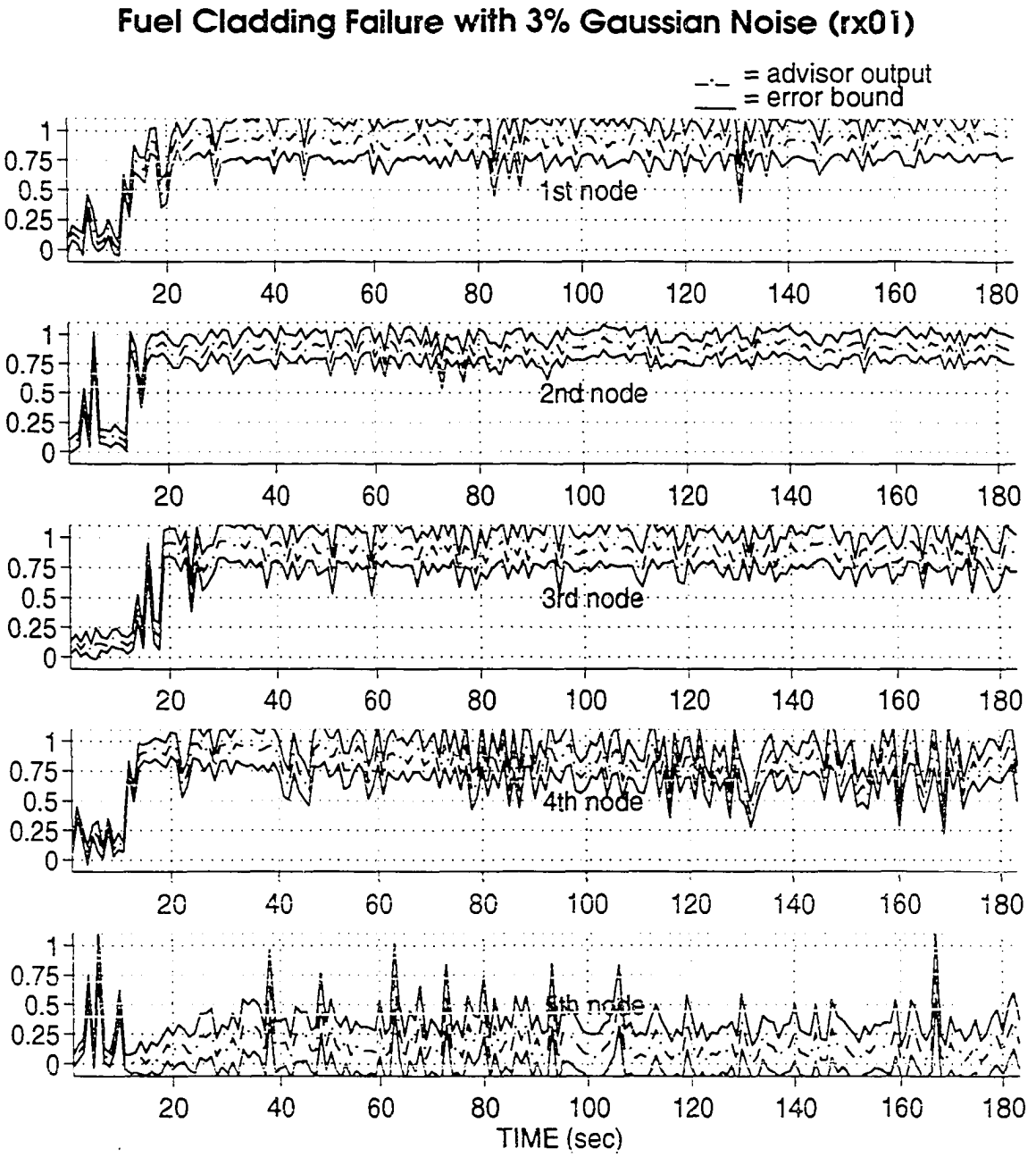

Figure 10. Diagnosis with estimated error bounds for the fuel cladding failure (rx01) transient with 3% Gaussian noise to the input data.

6. CONCLUSIONS

The objective of this research is to develop a new error-bound prediction scheme that provides error bounds on the output obtained from a NPP fault-diagnostic advisor using an ANN in order to validate the advisor output. We have developed the EESA scheme that can be used to help validate and verify the ANN fault-diagnostic advisor's output. Furthermore, EESA can resolve the complexity and difficulty of previous verification procedures. The results of the EESA implementation of the DAEC data demonstrate that EESA can validate the advisor's diagnosis with the significant reduction of the computational requirements. When noise is added to the fault-diagnostic system, the performance test shows relative robustness in the process of transients as well as the expected degradation in the validity of the diagnosis as shown by the increased predicted error for those cases effected by noise. In general, high error bounds estimated by EESA indicate that an ANN system needs more training for a complete generalization. The EESA scheme developed in this study can be implemented to any system irrespective of ANN learning paradigms.

ACKNOWLEDGMENTS

This work was made possible by the generous support of the United States Department of Energy under Special Research Grant No. DEFG02-92ER75700, entitled "Neural Network Recognition of Nuclear Power Plant Transients," and the Iowa Electric Light and Power Company who provided the simulated data. Their support does not however constitute an endorsement of the views expressed in this paper.

REFERENCES

[1] B. R. Upadhyaya and E. Eryurek, "Application of neural networks for sensor validation and plant monitoring," *Nuclear Technology*, vol. 97, pp. 170-176, 1992.

[2] A. Ikonomopoulos, L. H. Tsoukalas and R. E. Uhrig, "Monitoring nuclear reactor systems using neural networks and fuzzy logic," *Proc. Top. Mtg. Advances in Reactor Physics*, pp. 2-14, Charlston, South Carolina, March 1992.

[3] Z. Guo, and R. E. Uhrig, "Use of artificial neural networks to analyze nuclear power plant performance," *Nuclear Technology*, vol. 99, pp. 36-42, 1992

[4] I. E. Alguindigue, R. E. Uhrig, M. Cai and A. Trendy, "Discrimination of ex-core neutron noise signature using artificial neural networks," *Proceedings of the American Power Conference*, Chicago, IL, April 12-14, 1993.

[5] M. Roh, S. Cheon and S. Chang, "Thermal power prediction of nuclear power plant using neural network and parity space model," *IEEE Transactions on Nuclear Science,* vol. 38, No. 2, pp. 866-872, April, 1991.

[6] H. Kim and S. Lee, "Neural network model for estimating departure from nuclear boiling performance of a pressurized water reactor core," *Nuclear Technology*, vol. 101, pp. 111-122, 1993.

[7] H. G. Kim, S. H. Chang and B. H. Lee, "Pressurized water reactor core parameter prediction using an artificial neural network," *Nuclear Science and Engineering*, vol. 113, pp. 70-76, 1993.

[8] W. C. Jouse and J. G. Williams, "Neural control of temperature and pressure during PWR start-up," *Transaction of American Nuclear Society*, vol. 61, pp. 219-220, 1990.

[9] E. B. Bartlett and R. E. Uhrig, "Nuclear power plant status diagnostics using an artificial neural network," *Nuclear Technology*, vol. 97, pp. 272-281, 1992.

[10] Y. Ohga and H. Seki, "Abnormal event identification in nuclear power plants using a neural network and knowledge processing," *Nuclear Technology*, vol. 101, pp. 159-167, 1993.

[11] S. W. Cheon and S. H. Chang, "Application of neural networks to a connectionist expert system for transient identification in nuclear power plants," vol. 102, pp. 177-191, 1993.

[12] A. G. Parlos, J. Muthusami and A. F. Atiya, "Incipient fault detection and identification in process systems using accelerated neural network learning," *Nuclear Technology*, vol. 105, pp. 145-161, 1994.

[13] K. Kim, T. L. Aljundi and E. B. Bartlett, "Nuclear power plant fault-diagnostic using artificial neural networks. *Proc. Intelligent Engineering Systems Through Artificial Neural Networks*, vol. 2, pp. 751-756, ASME Press, New York, 1992.

[14] K. Kim, T. L. Aljundi and E. B. Bartlett, "Confirmation of artificial neural networks: nuclear power plant fault diagnostics," *Trans. of American Nuclear Society*, vol. 66, pp. 112-114, 1992.

[15] K. Kim and E. B. Bartlett, "Error prediction for a nuclear power plant fault-diagnostic advisor using neural networks," *Nuclear Technology*, in press, 1993.

[16] M. Stone, "Cross-validatory choice and assessment of statistical predictions," *Journal of Royal Statistical Society Series*, vol. B36, pp. 111-147, 1974.

[17] M. Stone, "Asymptotics for and against cross-validation, *Biometrica*, vol. 64, pp. 29-35, 1977.

[18] S. Geisser, "The predictive sample reuse method with applications," *Journal of the American Statistical Association*, vol. 70, pp. 320-328, 1975.

[19] K. Li, "From Stein's unbiased risk estimates to the method of generalized cross-validation," *The Annals of Statistics*, vol. 13, pp. 1352-1377, 1985.

[20] D. H. Wolpert, "Stacked Generalization," *Neural Networks*, vol. 5, 241-259, 1992.

[21] K. Kim, *Reliability Assessment of Nuclear Power Plant Fault-Diagnostic Systems Using Artificial Neural Networks*, Ph.D. Dissertation, Iowa State University, Ames, IA, 1994.

[22] H. S. Wilf, *Algorithms and Complexity*, Prentice Hall, Englewood Cliffs, New Jersey, 1986.

[23] J. S. Judd, *Neural Network Design and the Complexity of Learning*, The MIT Press, Cambridge, MA. 1990.

[24] D. Vest, C. Hunt and D. Berchenbriter, Data acquisition, personal discussion and correspondence with Duane Arnold Energy Center simulator complex employees, Iowa Electric Light and Power Company, Palo, Iowa, 1991-1993.

[25] D. E. Rumelhart, J. L. McClelland and the PDP research group, *Parallel Distributed Processing: Exploration in the Microstructure of Cognition*, Vol. 1 & 2, MIT Press, Cambridge, Massachusetts, 1986.

[26] L. P. Lippmann, "An introduction to computing with neural nets," *IEEE Acoustics Speech and Signal Processing Magazine*, vol. 4, pp. 4-22, 1987.

[27] R. Hecht-Nielsen, *Neurocomputing*, Addison-Wesley, Reading, MA, 1990.

[28] G. Cybenko, "Approximation by superposition of a sigmoidal function. *Mathematics of Control, Signals, and Systems*, vol. 2, pp. 303-31, 1989.

[29] D. H. Wolpert, "A mathematical theory of generalization: Part I and part II," *Complex Systems*, vol. 4, pp. 151-249, 1990.

[30] V. Kurkova, "Kolmogorov's theorem and multilayer neural networks," *Neural Networks*, vol. 5, pp. 501-506, 1992.

[31] C. Stanfill and D. Waltz, "Toward Memory-Based Reasoning," *Communications of the ACM*, vol. 29, pp. 1213-1228, 1986.

[32] T. Poggio and MIT AI Lab., MIT progress in understanding images. *Proceedings of the Image Understanding Workshop*, L. Bauman (Ed.), McLean, VA, pp. 111-129, 1988.

[33] A. Lapades and R. Farber, *Nonlinear signal processing using neural networks: prediction and system modeling*. Los Alamos National Laboratory Technical Report LA-UR-87-2662, 1987.

[34] K. S. Narendra and K. Parthasarathy, "Identification and Control of Dynamic Systems Using Neural Networks," *IEEE Trans. Neural Networks*, vol. 1, no. 1, pp.4-26, 1990.

[35] E. K. Blum and L. K. Li, "Approximation theory and feedforward networks," *Neural Networks*, vol. 4, pp. 511-515, 1991.

[36] E. B. Bartlett, "Dynamic node architecture learning: an information theoretic approach," *Neural Networks*, vol. 7, pp. 129-140, 1994.

[37] A. M. Hammit and E. B. Bartlett, "Determining functional relationships from trained neural networks," Submitted for publication to *Mathematical and Computer Modelling*, 1994.

[38] R. E. Uhrig, "Use of neural networks in nuclear power plant diagnostics," *Proc. Int. Conf. on Availability Improvements in Nuclear Power Plant*, p.310, Madrid, Spain. 1989.

[39] E. B. Bartlett and K. Kim, *Nuclear Power Plant Diagnostics with Artificial Neural Networks*, Final Phase 1 Report to U. S. Nuclear Regulatory Commission. Subcontracted with NETROLOGIC, 1992.

GENERAL SUMMARY

In this study, a validation and verification technique suitable for ANNs was developed and then applied to the NPP fault-diagnostic advisor systems. First, the advisor developed for the 10 transients of the San Onofre Nuclear Generating Station was capable of detecting and classifying the transients. The ANN error predictor also provides a figure of merit in the forms of error bound for the advisor. This advisor system demonstrate the feasibility of the error estimation method based on the concept of stacked generalization. The results of the proposed MBPC method show a considerable reduction in computation time without any degradation in the accuracy of the predicted error bound. Second, EESA, the new error-bound estimation scheme developed in this study, provides error bounds on an ANN's output or classification with computation advantages. The experiment results of the sine function mapping exhibit that the error bound estimated by EESA is much closer to the true error than that by the stacking procedure of Wolpert. It is also much smoother. In addition, EESA can resolve the complexity and difficulty of the stacking procedure hindering its implementation into complex, realistic problems. The results of the EESA implementation of the DAEC data demonstrate its capability to validate and verify the fault-diagnostic advisor developed for the 25 transient problem based on 33 simulated scenarios at their different severities. The performance test by adding noise to the system shows the relative robustness of the fault-diagnostic system. In general, high error bounds predicted by EESA indicate that the fault-diagnostic advisor needs more training data for a complete generalization. The EESA scheme and MBPC can be implemented to any system irrespective of ANN learning paradigm.

ADDITIONAL LITERATURE

Bartlett, E. B., and Kim, K. (1992). Nuclear Power Plant Diagnostics with Artificial Neural Networks, Final Phase 1 Report to U. S. Nuclear Regulatory Commission. Subcontracted with NETROLOGIC.

Bartlett, E. B., and Uhrig, R. E. (1992). "Nuclear Power Plant Status Diagnostics Using an Artificial Neural Network," *Nuclear Technology*, **97**, 272-281.

Blum, E. K., and Li, L. K. (1991). "Approximation Theory and Feedforward Networks," *Neural Networks*, **4**, 511-515.

Cheon, S. W., and Chang, S. H., (1993). "Application of Neural Networks to a Connectionist Expert System for Transient Identification in Nuclear Power Plants," *Nuclear Technology*, **102**, 177-191.

Hecht-Nielsen, R. (1990). *Neurocomputing*, Addison-Wesley, Reading, Mass.

Kim, K., and Bartlett, E. B. (1993). "Error Prediction for a Nuclear Power Plant Fault-Diagnostic Advisor using Neural Networks," *Nuclear Technology*, in press.

Kurkova, V. (1992). "Kolmogorov's Theorem and Multilayer Neural networks," *Neural Networks*, **5**, 501-506.

Lippmann, L. P. (1987). "An Introduction to Computing with Neural Nets," *IEEE Acoustics Speech and Signal Processing Magazine*, **4**, 4-22.

Ohga, Y., and Seki, H. (1993). "Abnormal Event Identification In Nuclear Power Plants Using A Neural Network And Knowledge Processing," *Nuclear Technology*, **101**, 159-167.

Parlos, A. G., Muthusami, J., and Atiya, A. F. (1994). "Incipient Fault Detection and Identification in Process Systems Using Accelerated Neural Network Learning," *Nuclear Technology*, **105**, 145-161.

Rumelhart, D. E., McClelland, J. L., and the PDP Research Group. (1986). *Parallel Distributed Processing: Exploration in the Microstructure of Cognition.* Vols. 1 & 2, MIT Press, Cambridge, Mass.

Wildberger, A. M. (1994). "Alleviating the Opacity of Neural Networks," To be presented at the IEEE World Congress on Computational Intelligence, June 26- July 2, 1994, Orlando, Fla.

APPENDIX: DESCRIPTION OF TRANSIENT SCENARIOS

DESCRIPTION OF TRANSIENT SCENARIOS

A brief description of the several transient scenarios simulated by the Iowa State University team at the Duane Arnold Energy Center (DAEC) simulator is given in this section.

MALFUNCTION AD05

Spurious automatic depressurization system (ADS) actuation
A. Logic A
B. Logic B
Generic. Logic Failure. 100% power.

This malfunction will cause the selected ADS channel to actuate spuriously from a channel logic failure. The effected valves will not respond to any other actuation signals, open or close, auto, or manual. The failed valves will cause the steam flow to increase and the reactor pressure will decrease. The reactor vessel water level will decrease, causing reactor scram on low level at 170". The suppression pool parameters will respond to the increased temperature, pressure and level will react to the steam regulating valve (SRV) discharge. The emergency core cooling system (ECCS) will activate automatically and provide the system with cooling as the plant condition degrades. The rate of depressurization and level decrease will be consistent with the mass and energy balances on the vessel.

Malfunction removal will restore the effected components to normal. Operator action may be required to restore the plant to normal.

Data files:

ad05.dat: Transient is inadvertent initiation of ADS (AD05A). IC24, 100% power, middle of cycle. This is for the first trend file.

MALFUNCTION CU10

Coolant leakage outside the primary containment.
Severity: 0 - 100% = 0 - 4" diameter pipe (single-ended shear).
Reactor Water Cleanup System (RWCS) expansion joint failure at 100% power.

This malfunction will cause a leak to occur at the cleanup system inlet expansion joint. The leak rate will be determined by the specified severity. A low-severity leak will cause the ambient temperature to increase and will actuate the leak detection system isolation and

annunciation at setpoint. As severity increases the leak detection system will be actuated by area temp/temp differentials. Prior to isolation, a brief decrease in pressure and flow will indicate mass loss on the inlet to the RWCS pumps. The pump discharge pressure will decrease proportional to leak severity and the cleanup system return temperature will decrease. When the reactor water cleanup system leak detection system activates, motor valves (MO-2700, 2701, 2740) will close, and the RWCU pumps will trip. The motor valve position indicating lights will indicate the valves are closed, and the RWCU pump motor breaker will indicate the breaker is open. The RWCU leak will cause the system pressure to decrease to atmospheric pressure. The system flow will decrease resulting in appropriate annunciation. The cleanup holding pumps will start automatically from the system low flow. System temperature will slowly decay to ambient, and the heat load on Reactor Building Closed Coolant Water (RBCCW) will decrease rapidly.

Malfunction removal will restore the effected components to normal. Operator action may be required to restore the plant to normal.

Data files:

cul0.dat: Accident is reactor water cleanup line break outside primary containment 100% break. IC24, 100% power, Middle of Cycle (MOC). Malfunction is YP:MCU10 at 100%. Decay heat is normal. No operator action.

cul0gp5.dat: Accident is reactor water cleanup line break outside primary containment 100% break. IC24, 100% power, Middle of Cycle (MOC). Malfunction is YP:MCU10 at 100%. Decay heat is normal. No operator action. Automatic group 5 isolation is overridden. Valves M02700, 2701, 2740 do not close feedwater pumps run out trip on delayed overload.

MALFUNCTION FW02

Malfunction is condensate pump trip.
A) Pump A
B) Pump B
Generic, breaker overcurrent device (50) failure, 100% power.

This malfunction will cause the selected main condensate pump breaker to trip from a faulty overcurrent device (50). The condensate pump breaker will indicate open, motor current will decrease, and annunciation from the trip will occur. When the condensate pump motor breaker trips, the pump will stop, and pump discharge pressure and flow will decrease. The corresponding reactor feedwater pump will trip and the recirculation system will run back low water level of 186" to 45% speed. Condensate header pressure will decrease, and flow will increase as the remaining condensate pump capacity is exceeded. If both condensate pumps are tripped, the reactor feedwater pumps will trip. The recirculation pumps will start to run back at 186" Reactor Pressure Vessel (RPV) water level to 45%

speed. The reactor will scram when level reaches 170". Malfunction removal will restore the effected components to normal. Operator action may be required to restore the plant to normal.

Data files:

fw02a.dat: Accident is trip of condensate pump A. No loss of power. When a condensate pump trips, the associated feedwater pump trips automatically. Reactor trips on low level. The turbine then trips on reverse power. IC24, 100% power, Middle of Cycle (MOC). Malfunction is YP:MFW02(A) the runback of recirculation pumps delays the reactor scram.

MALFUNCTION FW08

Feedwater heater tube leak.
A) Heater 1A C) Heater 2A E) Heater 3A G) Heater 4A
B) Heater 1B D) Heater 2B F) Heater 3B H) Heater 4B
Generic. Variable 0 - 100% = 0 - 4" diameter (equivalent to rupture of approx. 30 tubes); tube failure 100% power.

This malfunction will cause a tube failure in the selected feedwater heater at a rate specified by the severity. As the leak severity increases for the selected feedwater heater, water from the condensate system, for heaters #1 - #5, and water from the feedpump discharge, for heaters #6 will be induced into the shell side of the heater. The addition of mass will cause the mass within the heater to increase and the level control system will respond and modulate the drain and dump valves open. The cascading effect of the excess mass will impact the downline low pressure feedwater heaters and the level control systems. A maximum severity of multiple leaks in the #6 heater could cause insufficient feedwater flow to the reactor vessel and result in a reactor scram on low water level. A maximum severity or multiple leaks in the #1 - #5 heaters could result in a low suction pressure trip of the reactor feedpumps. A less severe leak will result in decreased feedwater heating and decrease in condenser vacuum. If the heater inleakage exceeds the normal drain and dump capacity the level will increase and actuate the high and hi-hi level annunciators. The level could backup into the turbine resulting in a turbine trip from high vibration, reactor scram and recirculation RPT breakers to open. The hi and hi-hi level alarms are bypassed if HS1393 in bypass and there is a turbine trip or a reactor scram.

Malfunction removal will restore the effected components to normal. Operator action may be required to restore the plant to normal.

Data files:

fw08-6.dat: 100% severity corresponding to 30 tubes breaking

MALFUNCTION FW09

Malfunction is reactor feedwater pump trip.
A) Pump A
B) Pump B
Generic. Spurious trip signal, 100% power.

This malfunction will cause the selected main feedwater pump to trip instantly from a spurious trip signal. The pump motor breaker will trip open and annunciation will activate. The pump pressure and flow will decrease and the recirculation valve will close, if open. The main feedwater pump trip will cause a partial loss of feedwater to the reactor, the level will decrease, and speed is runback to 45% at the recirculation pump. Reactor and turbine power are reduced accordingly. The feedwater control valves will modulate and maintain reactor water level in the control band at the reduced power level. The plant will stabilize at a new lower power. It is possible for low water level scram because of too high a power level or load line.

Malfunction removal will restore the affected components to normal. Operator action may be required to restore the plant to normal.

Data files:

fw09a.dat: Accident is reactor feedwater pump 'A' trip. IC24, 100% power, Middle of Cycle (MOC).

MALFUNCTION FW12

Feedwater regulator valve controller (FWRV) failure (auto).
A) FWRV A
B) FWRV B
C) Master controller
Generic. Variable 0 - 100% = 0 - 100% of valve position. Auto output signal failure. 100% power.

This malfunction will cause the selected feedwater regulator valve controller output to fail to the specified severity. The output will cause the regulator valve to modulate normally to the new position independent of the automatic control input signal. Placing the affected controller in the manual control mode will allow operator control. If the regulator valve position is decreased, the flow provided will decrease, if the unaffected feedwater regulator valve capacity permits, it will open and compensate for the failed valve control. If the failed valve closes or closes sufficiently to decrease the total system capacity the reactor water level will decrease. A reactor scram may result. If the output signal on the effected controller drops below 6 milliamps. The feedwater control valve lockout relay will actuate.

An amber alarm light and annunciation will respond. If the regulator valve position is increased, the flow provided will increase and the uneffected feedwater regulator valve will close to compensate for the failed control valve. The plant will remain stable in this condition. As flow is increased for either reactor feedwater pump to a value exceeding the design capacity, the motor current developed may exceed the overcurrent rating and the unit will trip on overcurrent. The master controller failure will cause the feedwater regulator valve controllers in auto to respond in unison, the overall effect will be similar to the above failures. Excessive flow will increase reactor water level and decreased flow will lower reactor water level. A reactor high water level of 211" will result in a trip of both feedwater pumps and the main turbine.

Malfunction removal will restore the effected components to normal. Operator action may be required to restore the plant to normal.

Data files:
Master feedwater controller failure. Fails both feedwater regulator valves. 100% power, IC24, middle of cycle. The following two simulations are for the first trend file:

fw12c0.dat: Feedwater regulator valves fail fully closed
fw12c1.dat: Feedwater regulator valves fail fully opened

MALFUNCTION FW17

Malfunction is main feedwater line break inside primary containment.
A. Feed line A
B. Feed line B
Generic. Variable 0-100% = 0-16" diameter double-ended shear weld failure on outlet of check valve, 100% power.

This malfunction will cause the selected feed line inside the primary containment to shear at the outlet of the check valve to the size specified by severity. This malfunction is unisolable from the reactor vessel through the selected feedwater line. At 100% severity, the rupture will cause a rapid depressurization of the reactor vessel and feedwater line. The reactor water level will initially increase resulting in a high-level trip of the main turbine, reactor feed pumps, High Pressure Coolant Injection (HPCI) and Reactor Core Isolation Cooling (RCIC). Low-Pressure Coolant Injection (LPCI) and Core Spray (CS) will initiate on the resulting containment pressure of 2 psig and inject into the reactor vessel when reactor pressure decreases below the shutoff head of the pumps. (Inject valves for LPCI and CS will not open until reactor pressure decreases below 400 PSIG). Drywell pressure and temperature will increase rapidly, and at 2 PSI group isolations 2,3,4,8,9 and reactor scram will occur. Suppression pool temperature and level will increase in response to the rupture severity. The reactor water level will decrease rapidly actuating reactor trip, and turbine

reactor water low, low-low, low-low-low isolation signals for groups 1,2,3,4,5,7,8, seal purge. The core spray, HPCI and LPCI systems will actuate and begin to flood the reactor with water. The unisoltated rupture will continue to cause mass loss from the reactor to the drywell and suppression pool. HPCI and RCIC will receive initiation signals on lo-lo reactor water level. If the reactor pressure is greater than 100 PSIG, these systems will initiate. Depending on which feedwater line is broken, HPCI or RCIC will inject to the reactor vessel. ('A' feedwater line break, RCIC injects to vessel, portion of HPCI bay inject and rest through break, and the opposite is true of 'B' feedwater line breaks). The reactor will cooldown in response to the Emergency Core Cooling System (ECCS),and the event will eventually stabilize. Reactor pressure and drywell pressure will equalize on large break in very short period of time.

This malfunction is unrecoverable, and the simulator will have to be reinitialized for malfunction removal.

Data files:

fwl7a.dat: Accident is main feed water line break. 100% single-ended shear loop A IC24, 100% power, MOC.

MALFUNCTION FW18

Malfunction is main feedwater line break outside primary containment. \\
A. Feed line A
B. Feed line B
Generic. Variable 0-100% = 0-16" diameter double-ended shear weld failure on outlet of feed reg. valve 100% power.

This malfunction will cause the selected feed line outside the primary containment to shear at the outlet of the feedwater regulator valve to the size specified by severity. At 100% severity, the rupture will cause the feedwater header pressure to decrease rapidly to less than reactor pressure. Header flow will increase rapidly to maximum, and the feedwater pumps capacity will be exceeded and trip on low suction pressure of 250 PSIG. Initially the feedwater regulator valves will modulate open from steam/feedwater mismatch, then open when the decreasing reactor water level overrides control. A reactor scram will occur when reactor water level decreases from lack of feedwater, the low water level causes High Pressure Coolant Injection (HPCI), and Reactor Core Isolation Cooling (RCIC) actuation and begin to flood the reactor with water and eventually recover the level. Group isolations will occur at the respective setpoints. The reactor will cool down in response to the Emergency Core Coolant System (ECCS), and the event will eventually stabilize. This malfunction is unrecoverable, and the simulator will have to be reinitialized for malfunction removal.

Data files:

fwl8a.dat: Accident is main feedwater line break outside primary containment 100\% break.

MALFUNCTION IA01

Loss of instrument air
Variable 0 - 100% = 0 - 200% of capacity (CFM). 100% capacity = 3000 CFM. Air receiver leak 100% power.

This malfunction will cause the instrument air system to leak from the air receiver at a rate specified by severity. At severities less than 100% the pressure will decrease to the auto start setpoint of the standby compressors which will start and recharge the system. At severities greater than 100% the system pressure will decrease with all three compressors running, severity will determine the rate of decrease. The following automatic functions will occur at setpoint:

1. 87 PSIG - service air low press ann.
2. 82 PSIG - CV3032 isolates service air hdr.
3. 85 PSIG - inst air dryer disch. press low ann.
4. 80 PSIG - CV3034, CV3035, CV3039 isolate appropriate I.A. hdrs
5. 60 PSIG - breathing air low press ann.

Each isolated air header pressure will decrease dependent on header air usage and individual components will go to the fail position or mode. The plant is expected to trip and will stabilize in a post shutdown condition.

Malfunction removal will restore the effected components to normal. Operator action may be required to restore the plant to normal.

Data files:

ia01.dat: Transient is complete loss of instrumentation air (IA01). 100% severity. IC24, 100% power, MOC. This is for the first trend file.

MALFUNCTION MC01

Malfunction is main circulating water pump trip.
A. Pump A, LP4A
B. Pump B, LP4B
Generic. Upper motor bearing failure, 100% power.

This malfunction will cause the selected main circulating water-pump motor upper bearing to fail, resulting in a motor breaker trip on overcurrent. The circulating water-pump upper motor bearing will fail causing the motor speed or current to fluctuate. After approximately one minute the motor bearing will seize and cause a very high current to be drawn by the motor, and the supply breaker will trip on overcurrent. As the circulating water pump discharges pressure, flow will decrease, and the pump discharge valve will close. The cooling tower basin level will increase slightly then return to normal as the system mass rebalances. With a circulating water pump tripped the circulating water temperatures will increase across the condensers. Condenser vacuum will decrease, and annunciation and a turbine trip will result, causing a reactor scram and Reactor Pump Trip (RPT). The plant protection system will respond appropriately to the turbine trip, and the plant will stabilize in a post trip condition with Electro-hydraulic Control (EHC) maintaining reactor pressure with the bypass valves.

Malfunction removal will restore the affected components to normal. Operator action may be required to restore the plant to normal.

Data file:

mc0la.dat: Accident is main circulation water pump "a" trip. No loss of power IC24, 100% power, Middle of Cycle (MOC). Malfunction is YP:MMC0l(A).

MALFUNCTION MC04

Main condenser air inleakage.
A) High pressure condenser
B) Low pressure condenser
Generic. Variable 0 - 100% = 0 - 1000 SCFM at 29" Hg. Condenser boot seal failure. 100% power.

This malfunction will cause the selected condenser to have air inleakage at a CFM rate specified by severity. At low severities the air ejector system will compensate for the air inleakage, however as severity is increased the selected condenser will lead a total vacuum decrease by both condensers. As the condenser pressure decreases the following functions occur:

1) 5.0" HgAbs - Condenser low vacuum annunciation
2) 5.0" HgAbs - Turbine 1B/1C low vacuum annunciation
3) 7.5" HgAbs - Turbine trip actuates
4) 19" HgAbs - Group 1 isolation signal
5) 22" HgAbs - Bypass valves are closed

The off-gas system will be affected by this malfunction. The pressure and flow will increase and as severity increases, the loop seals will isolate on high pressure. The flow will alarm. The recombiner temperatures will decrease depending on the malfunction. Offgas should stabilize after a short period of time.

Malfunction removal will restore the effected components to normal. Operator action may be required to restore the plant to normal.

Data files:
Main condenser air inleakage. IC24, 100% power, middle of cycle.
mc04a.dat: 100% severity
mc04a_2.dat: 60% severity
mc04a_3.dat: 30% severity

MALFUNCTION MS02

Steam leak inside the primary containment.
Variable 0 - 100% = 0 - 4" diameter single ended shear. Caused by RCIC steam line weld failure at elbow instrument tap (unisolable). 100% power.

This malfunction will cause a main steam leak at RCIC line elbow instrument tap at a rate specified by severity. Very small severities will cause local heating inside the drywell, a very slight pressure increase, and an increase in leakage to the drywell floor drain system. The main steam flow will increase and Reactor pressure will decrease. The turbine Electro-Hydraulic Control (EHC) system will detect the pressure decrease and respond to maintain pressure. With the decreased steam flow the feed flow will decrease causing the reactor vessel water level to decrease until the level dominates and stabilizes the level. The drywell pressure and temp will respond quickly to the leak and the high drywell pressure trip at 2 psig. The HPCI, LPCI, CS and DG's will start, group 2, 3, 4, 5 isolations will activate. If the rx pressure decreases to 850 psig, group 1 isolation will occur and isolate the turbine bypass system. The reactor will continue to blow down and the reactor pressure and level will decrease consistent with the severity. Reactor pressure and temperature will decrease rapidly. The torus level and temperature will increase in response to the rupture.

Malfunction removal will restore the effected components to normal. Operator action may be required to restore the plant to normal.

Data file:
ms02_2.dat: RCIC line break inside primary containment. The simulation was a 60% single ended shear in a 4" dia pipe. Initial condition is IC24, 100% power, Middle of Cycle (MOC). 60% severity.

MALFUNCTION MS04

Malfunction is Main Steam Line (MSL) rupture outside primary containment.
A. Steam line A
B. Steam line B
C. Steam line C
D. Steam line D
Generic. Variable 0 - 100% = 0 - 20" diameter double-ended shear, piping failure at ms common header, 100% power.

This malfunction will cause the selected main steam line to rupture outside the containment at the turbine inlet header at a rate specified by severity. At lower severities, the main steam flow will increase, and reactor pressure will decrease. The turbine bypass and control valves will modulate close, if open, in an attempt to increase steam pressure to control the increased demand. The hot well level control system will begin to makeup from the condensate storage tank to maintain the hotwell level in the normal control band, compensating for the system mass loss. A Primary Containment Isolation System (PCIS) group I isolation is possible on steam line high temp (200 DEG F), and probability increases with severity. At 100% severity, the PCIS group I isolation will be initiated on steam line low-pressure (850 PSIG in the run mode) with the steam line flow (140%) as a backup. The reactor will scram on MSIV closure. Because of the rapid steaming rate, the reactor water level will rapidly increase causing the main turbine and both reactor feed pumps, HPCI and RCIC, to trip. As the MSIVs close, steam flow through the break will cease, voids will collapse, and reactor water level will stabilize at some new lower level. Emergency Core Cooling System (ECCS) will respond to maintain adequate core cooling. The pressure rise in the turbine building will cause the blowout panels to function, releasing the steam cloud to the environment.

Malfunction removal will restore the affected components to normal. Operator action may be required to restore the plant to normal.

Data file:

ms04a.dat: Accident is main steam line header double ended shear. 100%. (20" line). Outside primary containment. IC24, 100% power, Middle of Cycle (MOC).

MALFUNCTION MS14

Loss of extraction steam to feedwater heater
A) Heater 1A
B) Heater 2A
C) Heater 3A

D) Heater 4A
E) Heater 5A
F) Heater 6A
G) Heater 1B
H) Heater 2B
I) Heater 3B
J) Heater 4B
K) Heater 5B
L) Heater 6B
Generic. Extraction line restriction, 100% power.

This malfunction will cause the selected feedwater heater to lose extraction steam. The loss of extraction steam will cause the selected heater level to decrease and the associated heat gain across the heater will be lost. The resultant decrease in feedwater temperature will cause a power increase for the resultant load. The extent of power increase will be based on the heater selected, and/or the number of heaters selected. Worst case would produce a reactor scram on high flux. Less severe failures will produce possible long term effects for fuel failure considerations and administrative requirements. The reduced drain flow to the next heater in the drain line will cause its level to decrease and the heater level controller will modulate to compensate and maintain the setpoint level. The reduced flow will cause a cascading effect for the remaining heaters down line. Once the mass transient is over, the drain heaters individual level control system will compensate for the loss of extraction steam and stabilize transient condition.

Malfunction removal will restore the effected components to normal. Operator action may be required to restore the plant to normal.

Data files:

ms14-6.dat: Loss of feedwater heating to both feedwater heaters 6A & 6B.
IC24, 100% power, middle of cycle. No associated severity.

MALFUNCTION RD13

Loss of air pressure to control rod drive (CRD) hydraulic control units (HCUs).
Variable 0 - 100% = 0 - 1.5" diameter pipe break. Air header piping failure.
100% power.

This malfunction will cause the loss of air pressure to the CRD HCU'S at a rate consistent with the piping failure specified by severity. Loss of air pressure will cause the flow control valves to fail closed eliminating the supply from the CRD pumps to the drive, exhaust and cooling water headers. The scram discharge volume will be isolated when CV'S 1867A/B and 1859A/B fail closed. Manipulation of the rod control system will not be

available, however the charging header will remain pressurized. The drive/exhaust valves, CV1849,1850 are fail open valves. If they loose air pressure the charging header pressure will insert the control rods.

Malfunction removal will restore the effected components to normal. Operator action may be required to restore the plant to normal.

Data files:

rd13.dat: Transient is loss of air to HCU (RD13). 100% severity. IC24, 100% power, MOC. This is for the first trend file.

rd13_2.dat: Transient is loss of air to HCU (RD13). 60% severity. IC24, 100% power, MOC. This is for the first trend file.

MALFUNCTION RP05

Malfunction RPS scram circuit failure (ATWS).
A. Auto-scram failure
B. Manual-scram failure
C. ARI failure
D. RPS fuse removal failure
E. All individual rod-scram switches fail
F. Hydraulic lock-scram discharge volume
Discrete, RPS scram circuit internal short circuit in wiring (A,B,C,D,E) scram discharge volume blockage (F), 100% power.

This malfunction will cause the selected RPS scram circuit to fail to cause a reactor scram when actuated. (A,B,C,D,E) selection of the hydraulic lock malfunction will reduce the scram discharge volume to simulate flow blockage. If the auto-scram is selected for failure, the plant will respond to the effects of the condition that generated the scram signal. The annunciators and indications will respond to auto-scram inputs as they are generated. However, the plant will remain operating until a protection feature or injection of sodium pentaborate causes the plant to shutdown. The reactor has the manual-scram capability functional, and the operator can utilize this mode as desired. With an active auto-scram, the plant will scram as required by logic whenever the appropriate condition exists. A failure of ARI to cause a scram will also cause a failure of the RPT breakers to trip on lo-lo reactor water level, high reactor pressure, or manual initiation of ARI. The effects of the manual-scram feature failures would be the response failure of the function to respond when activated manually. RPS fuse removal failure simulates a failure of the RPS fuse removal to work. Failure of the rod-scram switches simulates a failure of all 89 scram switches to work. The hydraulic lock malfunction reduces the volume and will allow the rods to partially insert, with each scram signal/reset applied. Insertion of all (6) generic failures will result in a "ATWS" condition.

Malfunction removal will restore the affected components to normal. Operator action may be required to restore the plant to normal.

Data files:

rp05tc01.dat: Accident is trip of main turbine together with failure to scram (ATWS). No operator action. IC24, 100% power, Middle of Cycle (MOC). Malfunction is YP:MTC01 (turbine trip) followed by YP:MRP05(A) (failure to automatically scram). Scram will be delayed and slow. Scram is from alternate rod insert (ARI). Recirculation pumps also trip on ARI. ARI is triggered at 119" vessel level or 1140 PSIG vessel pressure. Recirculation pump trips at turbine control valves fast closure or stop valves less than 90% open.

rp5actcl.dat: Accident is trip of main turbine together with failure to scram (ATWS), and Alternate Rod Insert (ARI). No operator action. IC24, 100% power, Middle of Cycle (MOC). Malfunction is YP:MTC01 (turbine trip) followed by YP:MRP05(A) (failure to automatically scram) and YP:MRP05(C) (failure of ARI). Recirculation pump trips on turbine control valves fast closure or stop valves less than 90% open.

MALFUNCTION RR05

Recirculation pump shaft seizure
A) Pump A
B) Pump B
Generic. Internal pump failure. 100% power.

This malfunction will cause the selected recirculation pump to seize mechanically and cause locked rotor current to develop for the motor. The selected recirculation pump internal total failure will be preceded by about 30 seconds of erratic speed, flow, current and excessive vibration as the failure develops into a totally seized pump. The recirculation M-G supplying power to the failing recirculation pump will have excessive generator current, which will result in a motor-generator lockout relay trip. The lockout actuation will trip open the generator field breaker, interrupting power generation for the seized recirculation pump motor. The recirculation pump trip will reduce the loop flow to minimum, core total flow and discharge pressure will decrease. With less core discharge pressure, the unaffected loop flow will increase slightly. Because the recirculation system total flow and pressure decrease, increased core voiding will reduce core power and cause a rapid increase in reactor vessel level. As reactor power decreases, the turbine generator power will decrease, the plant will stabilize at reduced power and vessel level will return to normal.

Malfunction removal will restore the effected components to normal. Operator action may be required to restore the plant to normal.

Data files:

rr05.dat: Recirculation pump shaft seizure. IC24, 100% power, middle of cycle.

MALFUNCTION RR10

Malfunction recirculation pump speed feedback signal failure.
A. Pump A
B. Pump B
Generic. Variable, 0 - 100% = 0 - 100% of feedback signal, speed control circuit failure, 50% power.

This malfunction will cause the selected recirculation pump speed-control feedback circuit to fail to the specified severity. The pump speed indicator will fail to the specified severity. With the tacho-generator signal failing below the speed demand/manual pot position signal, the recirculation pump actual speed will increase, and the scoop tube will increase to maximum or auto lock if auto-lock conditions are met. With the tacho-generator signal failing above the speed demand/manual pot position signal, the recirculation actual speed will decrease to minimum. The resulting effect on the plant will be the increase in power for an increased recirculation flow and a decrease in power for a decreased recirculation flow. Turbine generator power and control valve positions will respond as appropriate. Annunciator response to flow limits and control failures will actuate at setpoint. Reactor water level will respond to the opposite of the recirculation speed initially until feedflow and steam flow can get matched at the proper water level.

Malfunction removal will restore the affected components to normal. Operator action may be required to restore the plant to normal.

Data file:

rr10.dat: Accident is recirculation pump speed feedback signal failure caused by speed circuit control failure IC24, 100% power, Middle of Cycle (MOC).

MALFUNCTION RR15

Malfunction is recirculation loop rupture (Design basis Loss of Coolant Accident (LOCA) at 100%).
A. Loop A
B. Loop B

Generic, variable, 0 - 100% = 0 - 22" diameter double-ended shear piping failure at recirc. pump suction, 100% power.

This malfunction will cause the selected recirculation loop, inside the primary containment, to shear at the recirculation pump suction to the size specified by severity. At 100\% severity, the rupture will cause the recirculation loop and reactor pressure to decrease rapidly. The affected loop recirculation pump will cavitate and flow will be lost. Reactor water level will decrease rapidly as the reactor blows down through the rupture into the containment. The reactor water level decrease will actuate reactor scram, and reactor water level low, low-low, low-low-low isolation signals for groups 1, 2, 3, 4, 5, 7, 8, seal purge. The Core Spray (CS), High-Pressure Coolant Injection (HPCI), Low-Pressure Coolant Injection (LPCI), DG, and ADS systems will actuate and begin to flood the reactor with water. The RR pump discharge valves will close on the non-broken loop on the LPCI loop select signal. Reactor feed pumps will trip on overcurrent. At 100% severity, the HPCI and RCIC will receive initiation signals. However, the reactor pressure will decrease so fast that they will trip and isolate on low pressure before they will have any noticeable effect. Drywell pressure and temperature will increase rapidly and at 2 PSI group isolations 2,3,4,8,9 will occur. Suppression pool temperature and level will increase in response to the rupture severity. The reactor will cooldown in response to the Emergency Core Coolant System (ECCS), and the event will eventually stabilize. This malfunction is unrecoverable, and the simulator will have to be reinitialized for malfunction removal.

Data files:

rrl5a_2.dat: Accident is recirculation loop rupture. 60% double-ended shear - loop a IC24, 100% power, Middle of Cycle (MOC).

rrl5a_3.dat: Accident is recirculation loop rupture. 30% double-ended shear - loop a IC24, 100% power, Middle of Cycle (MOC).

MALFUNCTION RR30

Malfunction is coolant leakage inside primary containment.
Variable (exponential) 0 - 100% = 0 -52" diameter pipe (double-ended shear) reactor vessel bottom drain weld failure, 100% power.

This malfunction will cause reactor coolant to leak from the reactor vessel bottom drain failed weld at a rate specified by severity. As severity increases the mass loss from the reactor will easily be made up for by the hotwell level control system. In fact, at 100% severity the effects on reactor level/hotwell level will be very small. The most effective display of mass loss will be at hot standby. At 100% severity, drywell pressure, temperature, and activity will increase. At 2 PSI, group isolations 2,3,4,5,8 will occur. Suppression pool temperature and level will increase in response to the rupture severity. The reactor scram

will result from the 2 PSIG drywell pressure, and a turbine trip will result from reserve power. The shutdown plant will cooldown in response to the Emergency Core Cooling (ECC) and will stabilize. The long term effect of the leak will be the transfer of the Condensate Storage Tanks (CST) mass to the suppression pool via the leak in the reactor vessel. At small severities where the drywell pressure remains below 2 PSIG, the floor drain equipment system will see a high leak (in excess of the 5 GPM tech spec. limit). The drywell cooler heat load will increase as seen on the cooler temperatures on lC25.

Malfunction removal will restore the affected components to normal. Operator action may be required to restore the plant to normal.

Data file:

rr30.dat: Accident is reactor bottom head drain 100% single-ended shear (2" line). IC24, 100% power, Middle of Cycle (MOC).

MALFUNCTION RX01

Malfunction is fuel cladding failure.
Variable, exponential, 0 -100% = 0 - 30% fuel clad damage, fuel cladding degradation, 100% power.

This malfunction will cause the fuel cladding to fail to a value specified by severity. As the fuel failure increases, the amount of activity in the reactor recirculation and main steam system will increase. This activity will propagate throughout the plant and the radiation monitoring system will detect, indicate, and alarm as the activity increases. At low severities, offgas post-treat radiation monitors will cause offgas to isolate (without a group isolation) resulting in a loss of condenser vacuum, main turbine trips, and reactor scram. As the severity increases, the main steam line radiation monitors will cause main steam line isolation and reactor scram at setpoint. As the normal power dependent background radiation levels decrease, the additional radiation levels will be more evident on area and process monitors. At high severities the before mentioned will occur faster with more dramatic increases. Various system trips and isolations will occur, protecting the environment from excessive discharges. The sequence of the fuel failure indication will be as follows:

Offgas pretreat and post-treat radiation monitors increase
Offgas stack release will start to increase
Offgas system isolates on post-treat hi-hi radiation level
Main steam line radiation monitors respond:
a. MSL high radiation alarm
b. Group I isolation
c. Reactor scram

Drywell monitors increase Torus radiation monitors increase from relief valve discharge or HPCI and/or RCIC exhaust. Reactor building area radiation increases from Emergency Core Cooling System (ECCS) system operation. (HPCI, RCIC, LPCI, CS). NOTE: Malfunction severity will cause some of the above items to be "passed over" or will result in a delayed response.

Data file:

rx0l.dat: Accident is 30% fuel clad failure. Causes high radiation alarm to go off IC24, 100% power, Middle of Cycle (MOC).

IC-24: FULL POWER OPERATIONS (ANSI PARAMETERS)

A) Moderator temperature = saturated conditions
B) Reactor pressure = power dependent
C) Reactor power level = 100% power
D) Reactivity = critical
E) Xenon condition = 100% equilibrium
F) Core life = beginning of life

This IC is set up to meet the ANSI criteria for 100% power.
This IC is similar to IC-14, except the core is at middle of life (MOL).

ic14scra.dat: Accident is spurious scram. No operator action. IC14, 100% power, BOC. Malfunction is YP:MRP03.